Designing a Thermoresponsive Ocular Drug Delivery System for Rare Corneal Disease Treatment

by

Jorge Jimenez

Bachelor's of Science in Biomedical Engineering, Arizona State University, 2016

Submitted to the Graduate Faculty of the

Swanson School of Engineering in partial fulfillment

of the requirements for the degree of

Doctor of Philosophy

University of Pittsburgh

2021

UNIVERSITY OF PITTSBURGH

SWANSON SCHOOL OF ENGINEERING

This dissertation was presented

by

Jorge Jimenez

It was defended on

November 3, 2021

and approved by

Kira Lathrop, MAMS, Assistant Professor, Department of Ophthalmology and Bioengineering

Steven Little, PhD, Chair, Department of Chemical and Petroleum Engineering and Bioengineering

Ken K. Nischal, MD, FAAP, FRCOphth, Quality Vice Chair, Department of Ophthalmology

Shilpa Sant, PhD, Associate Professor, Department of Pharmaceutical Sciences and Bioengineering

Dissertation Director: Morgan V. DiLeo, Assistant Professor, Departments of Ophthalmology, Bioengineering, Chemical Engineering and Clinical and Translational Sciences

Copyright © by Jorge Jimenez

2021

Designing a Thermoresponsive Ocular Drug Delivery System for Corneal Rare Disease Treatment

Jorge Jimenez, PhD

University of Pittsburgh, 2021

Cystinosis is a rare, metabolic, genetic disease with less than 2,000 patients in the U.S. Intralysosomal accumulation of cystine leads to system-wide organ and tissue damage in patients. In the eye, cystine accumulates in all ocular tissues and is noticeably present in the cornea as hyperreflective, spindle structured crystals. The crystals cause light sensitivity and impair vision. Untreated, progressive accumulation of crystals leads to foreign body sensation and corneal erosion, further impacting ocular health. These crystals are treated with eyedrops containing the small molecule, cysteamine. Cysteamine therapeutic levels are reached when administered 6 to 12 times daily and used within their 1-week shelf-life. The frequency of administration and poor drug stability add burden to lives of patients, particularly when considering the multifaceted complications arising from a systemic, rare disease.

I hypothesized cysteamine encapsulated into spray-dried poly(lactic-co-glycolic acid) (PLGA) microspheres embedded within a thermoresponsive gel (SD-CMS/Gel) will reduce the dosing frequency and improve drug stability. This delivery system can be topically administered at room temperature (approximately 25°C) in its liquid phase and retained at ocular surface temperatures (32-34°C) as it undergoes a solution-gel transition. In this thesis, I developed and evaluated this topical drug delivery system using in vitro and in vivo methods. Spray-dried encapsulation of cysteamine was performed and evaluated in vitro for drug release, stability, drug permeation, and ocular irritation. Cysteamine ocular pharmacokinetics and biodistribution were

evaluated in rabbit model. Therapeutic efficacy of our formulation was investigated in a genetic knockout mouse model of cystinosis by measuring corneal cystine crystal reduction using optical coherence tomography (OCT).

The data suggest encapsulated cysteamine improves stability to 7-weeks when compared to 1-week aqueous cysteamine eyedrops. One drop of SD-CMS/Gel delivered cysteamine to ocular tissues for 12 hours in vivo compared to 12 drops of traditional eyedrops, providing the first insights into in vivo cysteamine ocular pharmacokinetics. Studies towards efficacy resulted in our ability to measure cystine crystals with longitudinal OCT and informed the translation of our formulation to the mouse eye. In total, the dissertation presents preclinical studies towards a novel drug delivery system for rare corneal disease.

.

Table of Contents

List of Tables

List of Figures

Preface

I have the upmost gratitude for the support I have received from my family, friends, mentors, and Pittsburgh community members. I was recruited to the University of Pittsburgh through the National Science Foundation Alliance for Graduate Education and the Professoriate, Pitt STRIVE, who I thank for awarding me the K. Leroy Irvis Fellowship and introducing me to my advisor, Dr. Morgan DiLeo. Dr. DiLeo has provided the necessary training to become an independent scientist while supporting my career development enthusiastically.

My scientific training would not have been possible without her dedication to my growth. In doing so, we gained support from the National Institutes of Health T32 Interdisciplinary Visual Sciences Training Program and Cystinosis Research Foundation. Through these agencies, we were connected with the cystinosis community in Pittsburgh and I thank the Hart family for their dedication to improving the life of their son, who has cystinosis. I am grateful for Dr. DiLeo's dedication to this community and for fostering a collaborative lab experience.

I would like to thank the past and present DiLeo Ophthalmic Biomaterials Lab. Dr. Liza Bruk for being the first graduate student in the lab, an amazing friend, expert otic drug delivery scientist, and best guardian to Mason, a best dog companion. Thank you to Dr. Mike Washington for supporting me in all our chemistry endeavors and for always saying "yes" to eating spicy chicken sandwiches. To Jayde Resnick, I could not have raised our mouse colony without you. You are the premier mouse queen and rabbit handler. To our fellow lab neighbors, Dr. Lindsay Leach, Dr. Esin Ozturk, Dr. Leah Byrne, Dr. Yuanyuan Chen – it's been a great pleasure to work alongside and collaborate with you.

To my friends and mentors in the field of engineering, I thank you. I thank Yvette Moore, Dr Sosenna Wood, and Dr. Deanna Easley for embracing my authentic self and supporting me from the first day I landed in Pittsburgh. Dr. April Dukes for being a great mentor and supporting my training in scholarly teaching. To Dr. Emily Ackerman for being my favorite person to trade music and discuss equitable science with. Nick Card for being a great running pal and helping me with Matlab code. To Dr. Yoojin Lee for baking and cooking amazing food for me. To Dr. Chris Reyes for being an amazing roommate and taco enthusiast. To all former and present Bioengineering PhD students and friends: Dr. Danielle Minteer, Dr. Rex Tien, Dr. Matt Sunderman, Dr. Garett Jeffries, Dr. Jessi Mischel, Dr. Erinn Grigsby, Dr. Erika Pliner, Patrick Cody – thank you for all the feedback on writing, generating ideas, practicing presentations, and dancing.

I would like to thank the Emerging Latinx Community reading and publishing group, specifically Dr. Patricia Documet, Dr. Sharon Ross, Dr. Robin Mejia, Dr. Jorge Delgado, and Dr. Camilo Ruiz. You've given me the context and language to communicate my experiences in the U.S. healthcare and education systems. Thank you for introducing me to your colleagues at Casa San Jose, the local Latino immigrant resource center. I am proud to have worked with Casa San Jose on an education outreach project with my dear friend, Marisol Villela Balderrama. Marisol, thank you for embarking on the journey with me and for giving me the confidence to continue practicing my Spanish.

Thank you to all my childhood friends from Arizona and my Arizona State family: Alina Cordoba, Brianna Udave, Megan Clark, Darien Cornett, Alexandria Lam, Esteban Barboza, Maria Jose Quezada, Joseph Del Rosario, Carlos Renteria, Elizabeth Lopez, Jai Hebel, Antonio

Anderson, and Zachary Young. Thank you for always calling, sending music, and supporting me from a distance.

To all my Bloomfield and local Pittsburgh family, I couldn't have made it through the pandemic without neighborly support. Connor Berndt for being a supportive friend, caring nurse, and healthcare advocate for our community. Emma Vescio for gifting me precious literature and encouraging me to rest intentionally. Stephanie Tsong for extending their love of disco and community building with me. Cody Peters, Kalya Spridik, Ava Bear, and Reginald "Reggie" Bear for being the best next-door neighbors and animal buddies. Aaron Reffett, thank you for taking care of me on my toughest days, sharing fantastic meals, and picking up after my chaos.

Lastly, I dedicate this work in its entirely to my parents, Ana Francisco Pascual Jimenez and Jaime Pascual Jimenez. They immigrated to the U.S. in the 1980's from Guatemala and raised my siblings and I in a Southwestern Arizona farming community. They gave 20 years of physical labor to the U.S. to support our family. After 40 years in the U.S., they became U.S. citizens in 2021. My older sister, Maria Elena Jimenez, and older brothers, Sergio Francisco Jimenez, Jaime Jr. Jimenez, and Hector Pasqual Jimenez, and I have greatly benefited from their love and support. I am the first in our generation to earn engineering degrees, which was not possible without each of their support. Looking towards the future, I wish to pass down all my knowledge to my nieces, Emma Isabella Jimenez, Emily Carmen Jimenez, Aliyana Marie McDonel, and Jasmine Remi McDonel. They will continue to accomplish greatness beyond our ancestors' wildest dreams. Gracias mamá y papa, nosotros lo hacemos juntos.

1.0 Introduction

Portions of the dissertation include reference to, image reproduction, and modified text from publications where I am the first author. Section 1.0 Introduction is associated with a publication in Drug Discovery Today, 24(8):1564-1574, Jimenez, J., Sakthivel, M., Nischal K. K., Fedorchak, M.V., "Drug delivery systems and novel formulations to improv improve treatment of rare corneal disease", pg.1564-1574, Copyright Elsevier (2019) [1]. Section 2.0 Specific Aim 1 is associated with a research article from Jimenez et al 2021, "A sustained release cysteamine microsphere/thermoresponsive gel eyedrop for corneal cystinosis improves drug stability", published 2021, Copyright Springer Nature [2].

A wide variety of approaches can be employed to address issues of drug delivery in almost every disease and physiological system. This includes reformulation of an existing drug into a form that is safer, more effective or compatible for patient compliance. Reformulation can include adjustments to the chemical composition of the drug itself or packaging the compound into a carrier to control the rate of drug release [3]. The discovery of new drugs or alternative treatments, such as cell or gene therapy, can also offer hope for improved treatment options for serious conditions. Often, investigational studies for such alternatives are driven by the potential market and the opportunity for disruption of current standards of care.

Ocular disease treatment is of particular interest because of the high incidences of many chronic conditions such as glaucoma and age-related macular degeneration (AMD); and the correspondingly large markets for associated therapeutics. Many first-generation ophthalmic drugs are good candidates for reformulation to improve patient adherence with eyedrop administration, increase tolerability through dose sparing or decrease the cost of ongoing treatment. As one

example, the effective off-label use of bevacizumab for AMD – and the later FDA approval of its ophthalmic counterparts, Lucentis® and Eylea® – has led to a surge of interest in improved retinal drug delivery [4]. Beyond AMD, controlled-release strategies are employed to develop next-generation glaucoma therapeutics with the goal of bypassing the anatomical barriers to effective ocular drug delivery traditionally associated with eyedrop administration (Fig. 1). Compared with a widely studied disease affecting the anterior segment like glaucoma, and despite the similarity in location and possible routes of drug administration, far less research has been done in the area of rare ocular diseases. A rare or orphan disease is defined by the FDA as a disease or disorder affecting fewer than 200, 000 people in the U.S.; or affecting more than 200, 000 but for which the costs of developing and marketing a therapeutic compound are not expected to be recoverable (adjusted to 2,000 individuals in the EU) [5].

The dissertation research area encompasses drug delivery strategies used for ocular drug delivery, specifically methods to overcome the barriers (anatomical and physiological) to drug delivery in the cornea. The primary focus of the dissertation is to develop a novel drug delivery system for cysteamine delivery to treat corneal manifestations of the rare corneal disease, cystinosis. An overview of rare corneal diseases is presented to inform the motivation and importance on developing therapies for underappreciated diseases and their communities. For example, approved orphan drugs are discussed to highlight state-of-the-art products along with experimental therapies in development. Along with discussing therapies, key aspects of translational research are documented to align the scientific approach that composes the entirety of the present dissertation.

1.1 Ocular Drug Delivery

Engineering effective therapeutics requires a deep understanding of the structure and function of target tissues to develop strategies to provide, or deliver, effective drug levels. The eye is a complex organ composed of three fluid chambers: anterior chamber (between the cornea and iris), posterior chamber (between iris, zonule fibers and lens) and the vitreous chamber (between the lens and the retina). Each tissue is responsible for regulating fluid homeostasis, maintaining normal intraocular pressure, and allowing the transmittance of light from the front of the eye (anterior segment) to back of the eye (posterior segment). The cornea is a transparent tissue that refracts light to the lens and retina. Light refraction reaches the retina and stimulates neurons to provide input signals to the brain to produce visual function. As the outermost tissue central in the eye responsible for two-thirds of the refractive power required for light transmittance, diseases of the cornea can affect vision in many ways [6]. Any damage (e.g., scratches, swelling, scarring, or compression) or changes in morphology, as seen in keratoconus, a condition resulting in the cornea's dome-shaped surface gradually bulging outward into a cone shape, will bend the light irregularly and impact retinal response after light transmittance. Typically, corrective lenses (e.g. glasses or contact lenses) will be prescribed for progressive morphological changes throughout the patient's lifetime. To treat an injury, like corneal wounds, a person may be prescribed corneal bandages [7], topical eyedrops [8] and in severe cases, undergo surgery for a corneal transplant [9]. Similarly, genetic diseases of the eye progress over a person's lifetime impacting vision and may require a multifaceted treatment approach, including pharmacological therapies delivered topically, from an eyedrop, and systemically. In the context of pharmacology, the structure and function of tissues impacts the absorption, distribution, metabolism, excretion (ADME) of a pharmaceutical compound. ADME describes the phenomena in which an organism processes a

pharmaceutical compound or therapeutic (i.e., small molecules, biologics, cells, genes). These therapeutics may be delivered in various forms (e.g., eyedrops, polymeric devices, injections) based on the pharmacokinetic profile of the active pharmaceutical ingredient (API) dictated by ADME properties. The dosage, size and frequency of administration, of a therapy is directly associated with the presentation of the drug at therapeutic levels. That is, specific drug ranges (e.g., concentrations of drug in the blood or biological fluid) that is required for the drug to be effective (i.e., produce an action). Many of these therapies and their delivery systems are designed to provide a therapeutic effect while minimizing adverse effects and toxicity. This careful balance between effective drug concentrations and low toxicity is accomplished by studying ADME processes and the anatomical and physiological barriers to drug delivery. For ocular drug delivery, specifically the cornea, the natural barriers to delivery include ocular surface layers, tear production and drainage (lacrimal glands and duct), the corneal layers, and anterior segment fluid exchange.

1.1.1 Anatomical and Physiological Barriers to Corneal Drug Delivery

A representative image in Figure 1 presents the anatomical features of the cornea and the associated barriers to topical drug delivery that are considered in this dissertation. Among these barriers are the physiological components of tears and the cornea. Tears are produced by lacrimal glands in the upper eyelid of the human eye. Tears are essential to lubricate the eye and spread across the ocular surface and contribute to tear film components, and excess tears are blinked away into lacrimal drainage ducts located in both upper and lower eyelids [10,11]. The tear film consists of a lipid layer, aqueous layer and a mucous layer, all of which contribute to lubrication and repair of the corneal epithelium after epithelial cells are lost from blinking [10]. The differences in hydrophilicity (hydrophobic lipid layer versus hydrophilic aqueous layer) impact the diffusion and

absorption of a drug based on its biochemical property. It is likely that a hydrophilic drug would diffuse readily through the lipid layer, but may not diffuse through an aqueous layer – making it challenging for the drug to reach the target tissue (e.g., cornea). The mucous layer may also have this effect as it contains secreted mucins, electrolytes and water, which all have various chemical ionic charges that contribute to drug diffusions. Although each tear film layer component has its own biochemical property that could interfere with drug delivery, tear turnover rate (1 ml/min) significantly impairs topical drug delivery to approximately 10–20% bioavailability [11,12]. Furthermore, the corneal epithelium itself is a barrier to drug penetration when drug is not lost to convective mechanisms on the ocular surface.

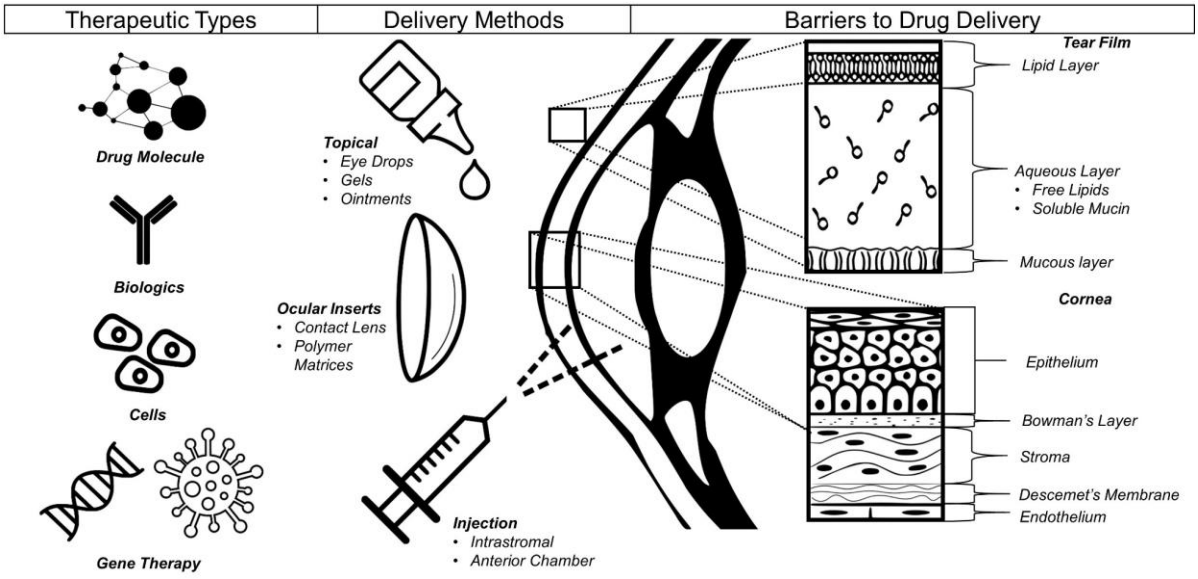

Figure 1 Corneal drug delivery systems and barriers to drug delivery. Image modified from Jimenez et al 2019.

Drug diffusion through the cornea is dependent on the layers of the cornea and the physiochemical properties of the therapeutic substance. The cornea is composed of five distinct layers: epithelium, Bowman's layer, stroma, Descemet's membrane and endothelium. Bowman's

layer and Descemet's membrane act as transitional, acellular interface between the cell layers of the cornea [13] and, as such, do not contribute substantially to permeability rates of drugs through the cornea. The epithelium is the outermost layer of the eye that limits transcorneal diffusion of foreign body substances and protects the eye. In particular, the epithelium prevents hydrophilic drugs from absorbing easily owing to its lipoidal properties [14]. The corneal stroma, by contrast, contributes up to 90% of the total cornea thickness and is a diffusional barrier to highly lipophilic drugs. The endothelium does not offer a significant barrier to transcorneal permeability based on hydrophilicity. However, the molecular weight of a given therapeutic agent can be significant factor in diffusion due to intracellular junctions that can prevent free passage of macromolecules between the stroma and anterior chamber [13]. Despite the significant challenges to topical administration of ophthalmic drugs, this route is generally preferred over systemic administration.

Systemic drug forms of drug administration, including oral and intravenous routes, are indeed useful in treating genetic diseases described in this dissertation but suffer limitations in treating the ocular manifestations or their symptoms. The anatomical and physiological barriers of the body lead to poor drug distribution to the eye. Orally administered drugs, for example, must pass through the gastrointestinal tract before absorption into the bloodstream [15]. Distribution to various organs and tissues, most notably the liver, severely reduces the amount of drug available to the eye. The relatively small amount of drug that is bioavailable must pass through indirect, selective permeability barriers to reach the cornea because it is an avascular tissue. These include the anteriorly located blood–aqueous barrier and posterior blood– retinal barrier, which selectively allow the passage of fluids and biochemicals. The blood–aqueous barrier consists of tight junctions in the nonpigmented epithelial layer of the ciliary body and endothelial cells of the iris blood vessels that limit diffusion in the paracellular space [16]. The blood–retinal barrier is located in

the retinal pigment epithelial cell layer and uses similar tight junctions to restrict solute permeability from the highly vascular choroid to the subretinal space [17]. For these reasons, systemic drug delivery for corneal delivery and other parts of the eye remains impractical – leading to the overall consensus that topical delivery of ophthalmic compounds is the most favorable in clinical practice.

1.1.2 Corneal Drug Delivery Systems and Clinical Considerations

Many of the challenges associated with topical ocular drug delivery can be overcome with various types of novel drug delivery systems (DDS) [18]. A pharmacological compound may be incorporated into a DDS by various methods including, but not limited to, chemically modifying the compound into a prodrug [19], encapsulating into a nanocarrier [20], or mixing into a suspension of inactive ingredients that promote enhanced tissue permeability [21]. Additionally, DDS also encompasses delivery with physical techniques that bypasses the aforementioned anatomical barriers [13]. like ultrasound-based methods (i.e, iontophoresis) [22], syringe injections, and bioabsorbable polymeric materials like microneedle arrays [23]. Any strategy that prolongs drug residence time on the cornea has the potential to decrease the dosing frequency and improve patient adherence, which for chronic conditions in particular can be low [24]. Increased bioavailability, the proportion of a drug that is able to have an active effect, on the ocular surface can also lead to a reduction in the amount of drug required per dose, which can then improve the tolerability or toxicity profile of certain medications. Other translational considerations, like protection of the therapeutic payload, storage, shelf-life or cost-effectiveness, can make DDS an attractive option for reformulating a given compound or investigating new treatments. A DDS that

is designed to prolong action and maintain therapeutics drug levels without hazardous peaks in drug concentration is the fundamental concept of controlled release.

Controlled release DDS extend the drug presentation of a drug compound from a payload for a matter of hours to months often from one single dose [25]. The chemical and physical properties of materials that compose the DDS dictate the length of time and the amount of drug release (mass) from the system. A classical method in controlled release is using biodegradable polymers which are materials (plant and animal derived or synthetic) that are slowly degraded via biological process (hydrolysis) and have biocompatible degradation products [26]. One example is the use of gelatin, composed of animal protein derived from collage, to deliver cellular compounds to the ocular surface for corneal wound healing [27]. Controlled release takes into the account ADME properties as parameters to meticulous engineer the correct therapeutic dosage as approved by medical product agencies like the Food and Drug Administration (FDA). As therapies specific for corneal disease are described in subsequent sections, the discussion of controlled release and its clinical impact will be reinforced with cases studies of approved therapies and experimental drug studies.

1.2 Rare Corneal Diseases and Clinical Treatment Approaches

It is within the context of the previously described anatomical barriers and the numerous techniques being employed for improved treatment of other ocular diseases that new therapeutic strategies for rare or orphan disorders affecting the cornea (either primarily or secondary to the underlying pathophysiology) are explored in this dissertation. There are many resources available to inform clinicians and researchers on rare genetic diseases. The Genetic and Rare Disease

Information Center (GARD) as part of the NIH National Center for Advancing Translational Sciences database [28] lists rare diseases and provides supplemental resources for diagnostics, treatment and resources for patient groups and their research foundations. Of these resources, the National Organization for Rare Disease (NORD) [29] and Orphanet [30] were used to screen for rare diseases with corneal effects and understand the current available therapies. This widely varied and extensive list includes developmental, metabolic, connective tissue, dermatological and other diseases. Many of these diseases also demonstrate multiple ocular manifestations but all share the commonality of affecting the cornea in some way. The Online Mendelian Inheritance in Man (OMIM) number, when applicable, is included to distinguish inherited from non-inherited diseases in this table. Although many of the strategies discussed below have widespread applicability, the genetic basis (or lack thereof) for a given disease must be considered when investigating new treatment options. This dissertation is stratified based on the type of drug available for treating corneal symptoms: no drug (or investigational drugs only), orphan designated drug(s) or nonorphan drug(s). Table 1 provides a summary of the specific diseases discussed in this review. Further, the research approach for translating new drugs and DDS for rare diseases is discussed to frame the scientific strategies that dictate the entirely of this dissertation.

Table 1 Summary of rare diseases highlighed with key elements from rare disease resources and relevent orphan drugs

Disease	OMIM no.	Gene	Defective Protein	Incidence	Orphan Drugs
Mucolipidosis type IV	252650	*MCOLN1*	Mucolipin-1	1 in 40,000; 70% of cases in Ashkenazi Jewish population	N/A
Familial LCAT deficiency Fish-eye disease	245900 136120	*LCAT*	Lecithin-cholesterol acyltransferase	Familial: at least 70 repeated cases70 repeated cases Fish-eye: at least 30 reported cases	N/A
Galactosialidosis	256540	*CTSA*	Protective protein/cathepsin A	At least 100 reported cases	N/A
Mucopolysaccharidosis type I Scheie syndrome Hurler–Scheie syndrome	607014 607016 607015	*IDUA*	α-l-iduronidase	1.07 in 100,000	Aldurazyme®

Table 1 (continued)

Mucopolysaccharidosis type IVA Morquio syndrome IVB	253000 253010	*GALNS*	*N*-acetylgalactosamine-6-s	MPS IVA: 1 in 270,000 MPS IVB: <1 in 1,000,000	Vizim®
Fabry's disease	301500	*GLA*	α-Galactosidase A	1 in 40,000 to 1 in 117,00	Fabrazyme®
Cystinosis Nephropathic Adult non-nephropathic Late-onset juvenile or adolescent nephropathic cystinosis	219800 219750 219900	*CTNS*	Cystinosin	1 in 100, 000 to 200,000	Cystaran™ Cystadrops® Cystagon® Procysbi®
Vernal keratoconjunctivitis	N/A	N/A	N/A	3.2 in 10,000 0.8 in 10,000 with corneal complications	Verkazia®

1.2.1 Rare Corneal Diseases for Which No Approved Treatment Exists

Often, corneal transplantation is the only option when a patient is a candidate and their disease has progressed beyond treatment. Although 45,000 (USA) [31] and nearly 185,000 (globally) [32] corneal transplants are performed each year, corneal transplant is often not a permanent solution. A common transplantation technique includes allografted corneas – a cornea received from a freshly acquired human donor cornea. An estimated 10% of allografted corneas are rejected after transplantation in avascular, noninflamed host beds (deemed 'low risk' transplantations) [33]. In pediatric corneal transplants, rejection rates are higher and reversibility of graft rejection after treatment is significantly lower than in adults [34]. Immunosuppression therapies can be used to improve outcomes after transplantation, which includes the use of cyclosporin and tacrolimus, and additional long-term studies are ongoing in this area [35]. For example, the use of topical immunosuppression in low- versus high-risk corneal transplantations results in 5-year graft survival rates of 90% and 35% survival rates, respectively [33]. The complexities of allotransplantation combined with ease of access to the cornea makes it a strong candidate for alternative therapeutic options including novel drug discovery [36], gene therapy approaches [37] and cell therapy [38]. Similarly, a recently published review by Moore et al. highlights the potential for genome editing to significantly impact the treatment of corneal dystrophies — a broad and poorly understood category of rare corneal disease discussed in more detail in section 1.2.4 corneal dystrophies [39].

One notable disease in this subcategory, mucolipidosis, is a group of lysosomal storage disorders that are characterized by the accumulation of gangliosides, phospholipids and acidic mucopolysaccharides in all tissues [40,41]. Variations in mutations lead to different types and

severities of the disease. Of the mucolipidosis diseases, mucolipidosis type IV (ML IV) is strongly associated with severe visual complications [40,42]. Patients with this type of disease experience severe vision loss and blindness by their teenage years. Corneal clouding is bilateral, symmetric and diffuses throughout the cornea [40,43]; and is thought to be caused by accumulation of phospholipids, mucopolysaccharides and gangliosides in the epithelial cells of the cornea [44]. Surgical treatment options for ML IV include conjunctival transplantation, which temporarily resolves opacification through removal of the epithelium [45]. In addition to surgical approaches, several ongoing clinical trials are focused on identifying biomarkers and understanding and documenting the natural history and progression of ML IV patients [46]. Recent studies have also proposed ML IV models in Caenorhabditis elegans and zebrafish that could further elucidate lysosomal defects and cell death [47,487]. These models may provide tools to determine a specific pathway and identify novel drug targets. Treatment of ML IV may benefit from following a similar path to ML II, in which adeno-associated virus serotype 8 (AAV8)-mediated expression of the mutated gene has shown an ability to attenuate deleterious effects of the disease in bones [49].

Indeed, success of other gene therapy models in the cornea would suggest that viral vector incorporation could be straightforwardly tested in appropriate animal models [50]. As one example, corneal fibrosis (a common cause of corneal haziness associated with many of the diseases discussed herein) was treated in an *in vivo* rabbit model and *in vitro* human models using a topical application of combination gene therapy [51]. Corneal fibrosis occurs owing to disorganized extracellular matrix components from myofibroblasts along with decreased expression of corneal crystallin, which are biological processes required for corneal structure and transparency. This particular treatment used gold nanoparticles conjugated to plasmids expressing bone morphogenic protein 7 (BMP7) and hepatocyte growth factor (HGF). The treatment was well

tolerated and restored transparency of the cornea *in vivo*. The authors concluded that this effect was mediated by promoting apoptosis in established myofibroblasts via multiple signaling pathways. Although the specific mechanisms underlying injury versus ML-IV-induced corneal haziness are distinct, recent evidence suggests they are associated with the transient receptor potential channel superfamily [52]. Additional research in this area could lead to novel therapies targeting the specific channelopathies in chronic disease.

Familial lecithin cholesterol acyltransferase (LCAT) deficiency is another rare inherited disease affecting the cornea via accumulation of unesterified cholesterol, triglycerides and phospholipids. Corneal opacity occurs as a result of increased lipid deposits in the stroma, which could in turn result in visual impairment [53,54]. Fish-eye disease, the partial familial LCAT deficiency, results in severe visual impairment [55,56]. This is a result of diffuse haziness of the corneal stroma, with more-pronounced opacity near the limbus, often arranged in diffuse, grayish, circular bands [57, 58]. Severely reduced vision has been treated with corneal transplantation [57]. In addition to treatment with statins and angiotensin receptor blockers [59,60] recent first-in-human clinical studies have investigated novel enzyme replacement therapy with recombinant human LCAT (rhLCAT) [62]. These trials have shown promising results regarding renal function and plasma lipid/LCAT levels and acceptable safety after intravenous (IV) infusion [62]. Although it is unlikely that IV infusion would affect corneal symptoms, successful translation of rhLCAT therapy could represent a significant step toward development of an ocular formulation.

Galactosialidosis (GS) is a lysosomal storage disease involving cathepsin A – a protein that protects neuraminidase (sialidase) and beta-galactosidase. Deficiency of these two enzymes causes accumulation of sialyloligosaccharides in lysosomes [63,64]. Systemically this can be excreted in body fluids and impacts cardiac function, skeletal growth and neurological disorder.

The ocular effects are cherry-red spots of the macula and mild corneal clouding [65,66]. Corneal clouding occurs in early infantile GS, late infantile GS and juvenile and adult forms, with early infantile GS having the most severe corneal effects [67]. These patients die within the first year of life because of suspected kidney and heart failures [66] contributing to a lack of information and research on the management of ocular effects beyond the use of corneal clouding as a diagnostic measure. There are no treatments for GS and treatment is symptomatic and supportive. Animal models of GS involve murine models [68, 69] and some preclinical therapies of bone-marrow-mediated *ex vivo* gene therapy [70] and recombinant AAV *in vivo* gene therapy [71]. Like LCAT deficiency, the possibility exists that successful systemic treatment might be augmented by a cornea-specific treatment or one for the macular spotting primarily responsible for vision loss. Ocular gene therapy has recently become a more viable option because of the late 2017 approval of Luxturna® (Spark Therapeutics, Inc.) – the first ever direct gene therapy product approved in the USA [72] that targets an inherited form of vision loss caused by retinal dystrophy.

The aforementioned diseases represent a subset of rare diseases associated with corneal pathologies that are potential candidates for investigational therapies. Such alternatives could move current treatments from symptom management to actual treatment of the underlying mechanisms causing dysfunction or damage to the cornea.

1.2.2 Rare Corneal Diseases with Approved Orphan-Designated Drugs

This category of rare corneal diseases includes examples for which there are approved orphan drug products specifically formulated for ophthalmic use and those for which an ophthalmic version is not (yet) available. When effective drugs are available, reformulation for ophthalmic use is an attractive option. This might include repackaging into a novel drug delivery

system, such as sustained- or controlled-release nanocarriers, to avoid or minimize the anatomical barriers to drug absorption mentioned previously.

One such disease with an approved and orphan-designated pharmacologic treatment is mucopolysaccharidosis (MPS), a rare metabolic disease that affects an enzyme involved in the degradation of glycosaminoglycans (GAGs). Accumulation of GAGs occurs in various tissues [73, 74], with the degree of enzyme deficiency and type of enzyme giving rise to many subcategories of MPS [75]. The corneal effects of MPS include corneal clouding and accumulation of GAGs in the corneal stroma as seen in Figure 2. Corneal clouding occurs in all individuals with MPS I, VI and VII and occurs mildly in MPS II and IV; and progression can lead to severe visual impairment (Figure 2 representative image) [75, 76]. Although deep anterior lamellar keratoplasty (DALK) has proven to be a successful surgical method of treating severely cloudy corneas in cases of MPS, not all health centers can perform these procedures and a therapy to clear these cloudy corneas without surgery would be extremely beneficial. This is particularly important because outcomes with penetrating keratoplasty tend to be less favorable than with DALK [77]. There are several therapies currently approved and within investigational clinical trials. In particular, enzyme replacement therapy with alpha-liduronidase (IDUA, Aldurazyme1) [78, 79] and hematopoietic stem cell transplantation (HSCT) have extended the life of MPS I patients [80, 81], with limited effect on preventing progressive corneal clouding via systemic administration. Despite systemic HSCT having limited effect on preventing progressive corneal clouding, the translation of novel HSCT technologies to animal models is promising for ocular delivery routes. Intrastromal mesenchymal stem cell transplantation has also shown promise in treating corneal clouding in an MPS VII mouse model. In addition to these therapies, preclinical studies for CNS targeting using AAV vectors containing IDUA have been carried out in animal models of MPS I [82, 83],

including topical ocular administration [84, 85] and via intrastromal injection [86]. Topical administration of AAV6, AAV8 and AAV9 were successful in *in vivo* mouse cornea and *ex vivo* donor human cornea [84]. One current limitation is that debridement of the corneal epithelium was necessary to achieve high levels of intracorneal transduction. Transduction of AAV8G9 in human corneal stromal cell types resulted in the production of IDUA (> ten-fold) after intrastromal injection [86]. Application of AAV in human corneas of MPS I has been demonstrated as well. It was shown that low levels of IDUA efficiently restored wild-type IDUA function in the corneas of MPS I patients [87]. IDUA was overproduced in the human corneal stroma with widespread distribution in multiple cell types, which included cells that naturally produce IDUA [87]. This provides initial validation for ocular gene therapy for MPS I. Further, many controlled-release systems have shown promise for improving the stability and pharmacokinetic profile of biomacromolecules [88, 89], which could enable ocular delivery of other forms of treatment for MPS I as well.

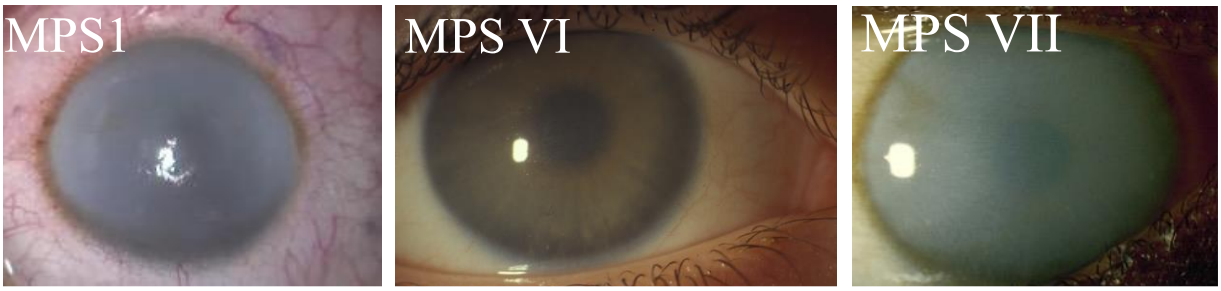

Figure 2 Corneal abnormaltites in mucopolysaccharidosis. Images reproduced from Jimenez et al 2019.

Similar to MPS I, enzyme replacement therapy has been offered since 2001 (EU) and 2003 (U.S.) to treat Fabry disease, a rare metabolic disorder wherein the deficiency of a-galactosidase A leads to depositions of glycosphingolipids in tissues. In ocular structures this accumulation leads

to conjunctival vascular abnormalities, corneal opacities (cornea verticillata), lens opacities, cataracts and retinal vascular abnormalities [90, 91]. Representative images from clinical photographs in Figure 3 were obtained from clinical collaborations and offer insight to corneal abnormalities. Corneal verticillata are whorl-like deposits of lipids in corneal epithelium that are diagnostic for Fabry disease (either female carrier or affected male) but do not impair vision. However, tearing of eyes (lacrimation) and increased corneal sensitivity have been reported in these patients, with artificial tears being prescribed as needed [92, 93]. Since the advent of enzyme replacement therapy, the long-term prevention of renal, cardiac and CNS dysfunction remains to be further established [94]; however, there has been some evidence of reduction of neuropathic pain [95] along with significant improvement in glomerular histology and increase in mean creatinine clearance [96]. Enzyme-replacement-therapy treated patients exhibiting corneal verticillata, conjunctival vessel tortuosity or cataracts have been studied to investigate the correlation between disease severity and ocular findings [97]. These results suggest that appropriately designed systemic pharmacotherapy can, in some cases, positively impact ocular manifestations. Continued longitudinal analysis of ocular results could further elucidate the benefit to the lacrimal system and retinal vasculature.

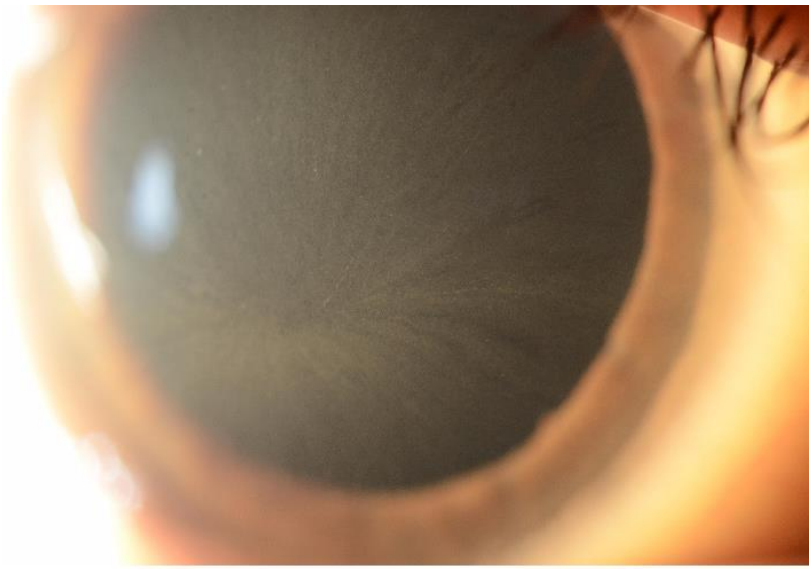

Figure 3 Fabry's disease with corneal verticillate. Image reproduced from Jimenez et al 2019

Perhaps the best example of orphan drug reformulation is that of cysteamine for the treatment of cystinosis. Cystinosis is a rare autosomal-recessive disease where the protein cystinosin is defective or absent [98, 99] resulting in intracellular cystine accumulation in all tissues of the body. The orally administered drug cysteamine (Cystagon®; and its sustained-release counterpart Procysbi®) is effective in removing cystine from many tissues in the body but has no effect on the cornea. Cystine accumulation in the cornea appears as needle-like structures that cause severe light sensitivity, blepharospasm (involuntary closure of eyelids) and significant foreign body sensation (Figure 4) [99, 100]. A clinical trial initiated in 1986 and sponsored by the National Eye Institute tested whether cysteamine eyedrops could remove cystine crystal accumulation from the eyes [101]. The final formulation was approved by the FDA in 2012 as a 0.44% cysteamine ophthalmic solution (Cystaran™, equivalent to 0.55% cysteamine hydrochloride in the European Union). Topical cysteamine has been proven to be safe and effective in dissolving cystine corneal crystals but requires extremely frequent administration — up to once

per waking hour — to achieve clinically relevant results [102]. Cysteamine is also highly susceptible to oxidative degradation, therefore requiring that the eyedrops are frozen until opening, stored in the refrigerator and disposed of within 1 week [102]. The high drug concentration and resulting ocular irritation combined with burdensome dosing and storage requirements makes cysteamine a good candidate for reformulation into an encapsulated form that increases bioavailability and drug stability.

Controlled-release technologies using viscous gels or hydrogels [103, 104], prodrugs [105] and loaded contact lenses [106] have been explored using *in vitro* studies. A dissolvable polymer nanowafer has shown reduction of corneal cystine crystals in a rodent model of cystinosis [107]. Recent efforts in translating clinical trial study results into EU orphan drug approval have been successful with the introduction of Cystadrops® in 2017– carmellose sodium gel formulation with cysteamine [108, 109]. The recommended dosing for Cystadrops® is four-times daily, representing a significant reduction in administration frequency over Cystaran™ (up to 12-times daily); however, patients still report pain upon instillation and an increase in mean intraocular pressure after 12 months [108]. The local side-effect of pain is inherent to similar cysteamine concentrations, suggesting patients favor a viscous gel formulation over traditional cysteamine eyedrops if local pain is still exhibited. Beyond pharmacologic approaches, current clinical studies seek to address the genetic mutation underlying cystine accumulation in cystinosis as an alternative to lifelong cysteamine administration. Hematopoietic stem and progenitor cell transplantation have been explored in rodent models to establish the therapeutic effect of transport of cystinosin to diseased cells, which have shown clearance of corneal cystine crystals [110]. Interestingly, these studies did in fact demonstrate stem cell localization in the cornea and rescue of ocular defects, including a reduction in corneal cystine crystals and restoration of normal corneal thickness [202].

The need, if any, for supplementary therapy with cysteamine eyedrops to support stem cell transplantation will not be fully understood until future evaluation of clinical results. To this end, the first report of human hematopoietic stem cell transplantation was published in July 2018 [111].

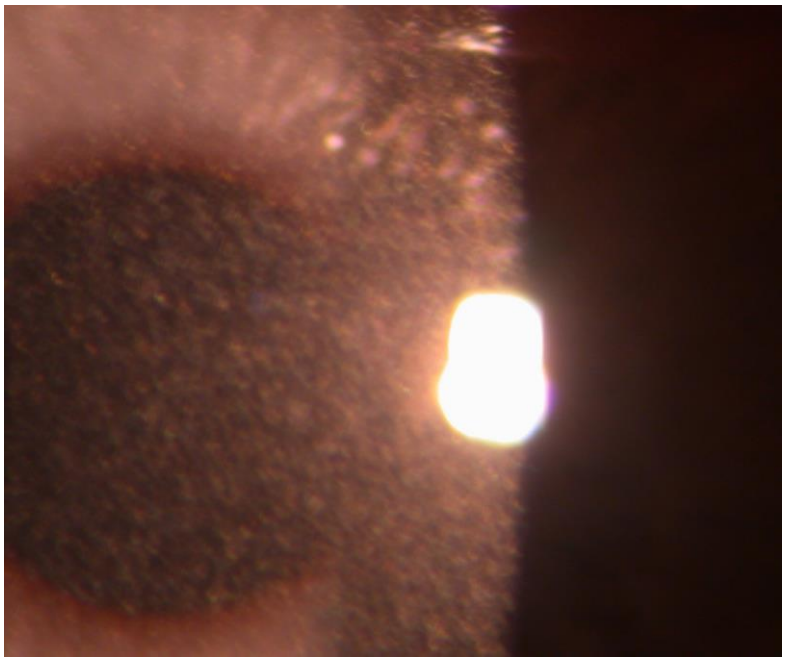

Figure 4. Corneal cystine crystals in cystinosis. Image reproduced from Jimenez et al 2019.

1.2.3 Rare Corneal Diseases Treated with Non-Orphan-Designated Drugs

Often the ocular symptoms associated with rare diseases, particularly intracellular diseases affecting multiple systems or tissues, are managed using supportive pharmacotherapy with common, FDA-approved drugs. These drugs, including anti-inflammatory and immunosuppressive agents, have broad applicability as ophthalmic therapeutics. Still, they are subject to all of the aforementioned barriers to effective intraocular absorption in and around the cornea. Significant work has been done in reformulating these classes of drugs into controlled- or sustained release formulations. Thus, the investigation of novel drug delivery systems for these

more common pharmaceutical agents is one that might offer substantial benefit to patients with diseases in this subcategory.

One example of approved, reformulated steroids is the Ozurdex® implant, used to treat macular edema and noninfectious uveitis [112]. This rod-shaped intravitreal implant is administered every 6 months at a maximum, during which time it slowly degrades and releases dexamethasone. Although not specifically used in a topical administration, this example is noteworthy because similar degradable materials can be used for ocular surface or anterior chamber indications. Indeed, investigational techniques have attempted to locally and sustainably deliver corticosteroids for such purposes as managing post-cataract surgery inflammation, inflammatory eye diseases or injury. This includes a depot placed in the canaliculus [113], polymeric nanoparticles [114], and drug-loaded contact lenses [115,116], and nanowafers [117].

The treatment of vernal keratoconjunctivitis (VKC) highlights many of the topics discussed in this dissertation introduction —with non-orphan drug use and a recently approved orphan drug product to manage the variety of symptoms associated with the disease. VKC is a chronic allergic condition that affects the ocular surface, thought to be IgE and T-cell-mediated and typically leading to chronic inflammation [118, 119]. The disease is characterized by papillary conjunctivitis in the upper eyelids, which can progress to giant papillae and development of gelatinous nodules in the limbus area of the cornea. Papillary conjunctivitis is the irritation of the thin, translucent lining of the eye and the under surface of the eyelids. It is often caused by bacteria, viruses and, in this case, allergies. Although VKC is often self-limiting, severe cases can lead to corneal shield ulcers and cataracts. Additionally, patients experience light sensitivity, blepharospasm, redness and thick mucus discharge [120-122]. Treatment is generally focused on relieving specific symptoms. This includes the use of mast cell stabilizers (such as sodium cromoglicate, nedocromil,

lodoxamide, pemirolast) and antihistamines (such as levocabastine and emedastine). Severe forms of VKC can be treated using nonsteroidal anti-inflammatory eyedrops including indomethacins 1%, ketorolac 0.5% and diclofenac 0.1% [123-125]. In addition, immunosuppressive agents such as topical cyclosporine and tacrolimus have been used as an alternative treatment when corticosteroid-induced ocular hypertension or other side-effects are of particular concern [136-128]. Recently, a cationic nanoemulsion of cyclosporine (Verkazia®) was approved by the European Commission (EC) and European Medicinal Agency (EMA) and granted orphan drug designation in 2018 with the intended purpose of increasing residence time on the ocular surface through electrostatic attraction with a negatively charged mucosal layer [129].

1.2.4 Corneal Dystrophies and Therapies

At the intersection of genetic corneal diseases and poorly understood, rare conditions, we categorize a group of progressive eye disorders called corneal dystrophies. The high number of corneal dystrophies and wide range of treatment options make this a unique category in a review of rare corneal diseases. The severity of visual effects resulting from corneal dystrophies ranges from asymptomatic to significant vision impairment (Figure 5 and Figure 6). In many patients, the cornea can become cloudy with accumulation of material leading to photophobia, recurrent corneal erosion and foreign body sensation [130, 131]. Corneal dystrophies are often bilateral, symmetric and not related to environmental or systemic factors. In the past decade, there have been large efforts by clinicians and researchers to categorize types of corneal dystrophies. The International Committee for Classification of Corneal Dystrophies (IC3D) has been responsible for defining each one based on genetics, corneal layers and clinical outcomes [131]. The IC3D has expressed many challenges in distinguishing types and approaches to treat each type; there is currently no

standard treatment for corneal dystrophies owing to the vast differences among them. Some similarities in possible treatment can be found by categorizing according to which layers of the cornea are affected. If the endothelium (the innermost layer adjacent to aqueous humor) is affected an endothelial keratoplasty or transplant might be considered. Anterior stromal dystrophies, by contrast, can be treated by superficial keratectomy. Dystrophies of the epithelium can be treated conservatively with bandage contact lenses; lubricating eye drops or even alcohol delamination – an approved treatment for corneal epithelium removal for recurrent corneal erosions [131]

Limbal stem cell deficiency (LSCD), although not categorized as a corneal dystrophy, has been granted orphan designation and is currently being treated with a recently approved product called Holoclar®. Holoclar® was the first stem-cell-based medicinal product approved in the western countries [132]. It uses a disc made of limbal stem cells expanded in culture after taking a biopsy from a small section of healthy limbus [133]. This is particularly useful in cases where bilateral LSCD is present (precluding autologous transplant), as is common in several corneal dystrophies in which damage to the limbus occurs. Another complication of LSCD and other forms of trauma to the cornea is persistent corneal epithelial defect, for which EyeVance Pharmaceuticals' Nexagon® has recently received orphan designation. This treatment modality, an antisense oligonucleotide that downregulates expression of the gap junction protein Connexin 43, has shown promising results in wound healing for burns and trauma [134, 135] and will soon begin its clinical evaluation. Further studies will elucidate the role of treatments like Holoclar® and Nexagon® in improving outcomes for the widespread forms of corneal dystrophies, specifically those associated with epithelial dysfunction [136]. Beyond these specific methods, and similar to the other rare corneal diseases highlighted herein, reformulation techniques to improve key

properties like stability, biocompatibility and efficacy of conventional treatments have the potential to significantly enhance the quality of life for patients with corneal dystrophies.

Figure 5 Granular-lattice corneal dystrophy. Image reproduced from Jimenez et al 2019.

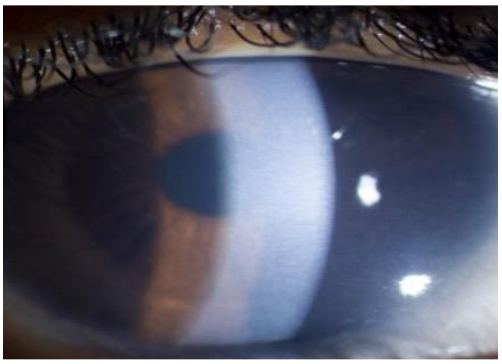

Figure 6 Congential hereditary endothelial dystrophy. Image reproduced from Jimenez et al 2019.

1.3 Specific Aims and Hypothesis for Eyedrop Reformulation in Cystinosis

As previously noted in section 1.2.22 *Rare corneal disease with approved orphan-designated drugs*, a prime candidate for eyedrop reformulation into a controlled release DDS is cysteamine eyedrops for cystinosis. Cystinosis is a rare, autosomal recessive disease that effects approximately 2000 people in the US and is categorized as an orphan disease by the FDA.

Nephropathic cystinosis, the most severe case, results in high accumulation of cystine in the cells of multiple organs. In the eyes, accumulation of cystine in the cornea results in highly reflective crystals that cause photophobia, corneal erosion, and foreign body sensation. Currently, two cysteamine formulations are approved by the FDA to treat corneal cystine crystals. From October 2012 to August 2020, Cystaran™ (0.44% cysteamine hydrochloride, Leadiant Biosciences Inc.) was the only FDA approved cysteamine eyedrop prescribed at 6-12 hourly eyedrops (every waking hour) with a shelf-life of 1-week (after opening and stored between 2°C-25°C). In August 25th, 2020, a new gel formulation, Cystadrops® (Recordati Rare Diseases Inc.), was FDA-approved at 4 hourly eyedrops with a similar shelf-life after opening for 1-week when stored at or below 25 °C, but above freezing temperatures. The frequency of administration of ranging from 6-12 eyedrops for cysteamine eyedrops and 4 times daily for viscous cysteamine. The one-week shelf life makes the current eyedrop formulations inconvenient and incompatible with effective treatment and compliance. Furthermore, various concentrations of cysteamine are required due to the poor bioavailability inherent to eyedrops and the high instability of cysteamine, which is readily oxidized into its inactive form, cystamine. An ideal alternative to current cysteamine eye drops would deliver the drug more efficiently over time to intraocular tissues, therefore reducing the number of doses and potentially lowering the concentration of drug needed per dose. Unfortunately, there is no current cysteamine eye drop therapy that combine timed release ocular drug delivery in a familiar and comfortable format.

The objective of this dissertation is to develop a topical controlled release DDS of cysteamine for the treatment of ocular cystine crystals in cystinosis. The dissertation describes the development of a topical, thermoresponsive gel depot containing drug-loaded poly(lactic-co-glycolic acid) (PLGA) microspheres (MS). The cysteamine loaded PLGA MS (CMS) is mixed

into the gel; the combination of these materials offers extended cysteamine release from a DDS that can be topically placed in the lower eyelid space. The DDS is administered as liquid (solution) at room temperatures (25°C) and transitions into an opaque gel upon solution-gel (solgel) transition at ocular surface temperatures (32-34°C). The gel depot after solgel transition takes the shape of the lower eyelid and can be retained for over 24 hours to 30 days, as previously show in large animal models [137, 138]. Previous studies also support the use of the DDS mitigate ocular drug delivery barriers by increasing residency time, extending drug release in vivo, and lowering drug concentrations required for effective treatment. In addition, the literature on the mechanism of cysteamine oxidation (pH dependence) in aqueous solutions favors cysteamine delivery from our CMS/gel DDS system that may limit oxidation in an encapsulated environment. For these reasons, this dissertation hypothesizes that the issues of oxidative instability, frequent dosing, and low bioavailability of cysteamine will be lessened using encapsulated cysteamine and the combination DDS.

To test this central hypothesis, the dissertation examined the following specific aims:

1) development and testing of cysteamine loaded MS/gel to characterize clinically relevant drug levels, physical properties, and stability.
2) to study cysteamine pharmacokinetics and biodistribution in an ophthalmic rabbit model.
3) to study efficacy in the CTNS (-/-) murine model, a knockout model of cystinosis.

1.3.1 Specific Aim 1

Specific Aim 1: to develop and test cysteamine loaded MS/gel for clinically relevant drug levels, physical properties, and stability.

Hypothesis: cysteamine encapsulation in PLGA MS will improve drug stability and retain physical and chemical properties within a thermoresponsive gel for topical application to the eye.

The objectives of Specific Aim 1 were to:

1) Optimize cysteamine encapsulation in PLGA MS for 1 week at drug concentrations similar to existing therapeutic eyedrops
2) Characterize materials and verify compatibility with thermoresponsive gel
3) Develop a stability assay and compare shelf-life stability of encapsulated cysteamine to cysteamine eyedrops
4) Examine ocular irritation of materials with in *in vitro*/*ex vivo* models and compare to traditional eyedrops
5) Quantify in *vitro* drug permeation through the cornea in a diffusion chamber setup
6) Topically administer delivery system and evaluate preliminary safety and retention in *vivo*

1.3.2 Specific Aim 2

Specific Aim 2: to study cysteamine pharmacokinetics and biodistribution in a rabbit model.

Hypothesis: Encapsulated cysteamine combined into a topical thermoresponsive gel will deliver cysteamine at drug levels similar to multiple doses of traditional eyedrops *in vivo*. Results of *ex vivo* and *in vitro* ocular irritation assays in Specific Aim 1 justified additional safety and eyedrop tolerability of candidate formulations during *in vivo* studies.

The objectives of Specific Aim 2 were to:

1) Quantify *in vivo* cysteamine concentrations in ocular tissues including the cornea, aqueous humor, vitreous humor
2) Quantify in vivo cysteamine concentrations in systemic tissues including plasma
3) Compare cysteamine eyedrops and encapsulated cysteamine/gel drug profiles over the time course of prescribed treatment
4) Clinically score tolerability during instillation of eyedrop formulations

1.3.3 Specific Aim 3

Specific Aim 3: to study efficacy in the CTNS (-/-) murine model, a knockout model of cystinosis

Hypothesis: Cysteamine delivered from encapsulated cysteamine/gel is stable and will treat corneal cystine crystals confirmed by longitudinal *in vivo* corneal imaging analysis.

The objectives of Specific Aim 3 were to:

1) Breed and maintain a colony of CTNS (-/-) knockout mice.
2) Develop corneal imaging strategies and quantify corneal properties and corneal cystine crystal pixel intensities.
3) Administer and retain encapsulated cysteamine/gel in the mouse eye.
4) Compare efficacy of cysteamine/gel to cysteamine eyedrops.

1.4 Translational Impact of Specific Aims

As presented in the review of relevant literature, the following statements comprise the scientific premise and impact of dissertation studies:

1) There are well-defined clinical needs for improved treatment for corneal cystine crystals in cystinosis.
2) Current approved and investigative technologies have not fully addressed the myriad issues with cysteamine ocular delivery.
3) Controlled release technology may offer an alternative to current treatment strategies.

The engineered drug delivery system is unique in that it will require only a single drop for the dosage and will provide therapeutic levels of cysteamine to the cornea in a stable and safe method. As previously discussed, the poor aqueous stability of cysteamine is a large inherit issue to this small molecule. Oxidation rates of cysteamine to its inactive counterpart, cystamine, have been studied to occur in higher pH solutions (pH 7.4 vs pH 4.3) [139]. By encapsulating cysteamine, we avoid the issues of pH prior to the introduction of CMS to the liquid phase of our gel. Upon administration and rapid transition, cysteamine will diffuse through the polymer matrix with a pH dictated by the surrounding ocular environment (pH 7.0-7.3) [140] This single-drop treatment will continuously provide therapeutic amounts of active drug to the ocular surface, as opposed to the daily 6-12 drops Cystaran™, which in turn may reduce concerns with patient noncompliance and minimize drug concentrations. Quality of life may be dramatically improved, as only a single drop will be needed for treatment, and side effects (pain) may be mitigated. The distinctive, simple removal of the non-degradable gel may also be attractive as it will further reduce concern of long-term adverse side effects due to lingering material or degradation products.

Furthermore, much of the research in this area did not take advantage of biodegradable microspheres as a method to improve stability and extend release, giving our novel and patent-pending system a significant advantage as it will provide sustained drug release in a more reliable and stable manner

The results of these studies demonstrate the preclinical potential of a novel controlled release cysteamine delivery system for cystinosis. Future studies will further explore the translational capabilities of our technology through scale-up manufacturing and sterilization testing. Ultimately, these models developed in this dissertation represent preclinical methods to assess the translation of a topical, single drop gel eyedrop formulation. An overview of the translation of the DDS is summarized in Figure 7. The dissertation studies contribute to the scientific and clinical understanding of improving treatment for rare diseases, an area with substantial potential for additional research in novel pharmacological, cell, or gene-based therapies.

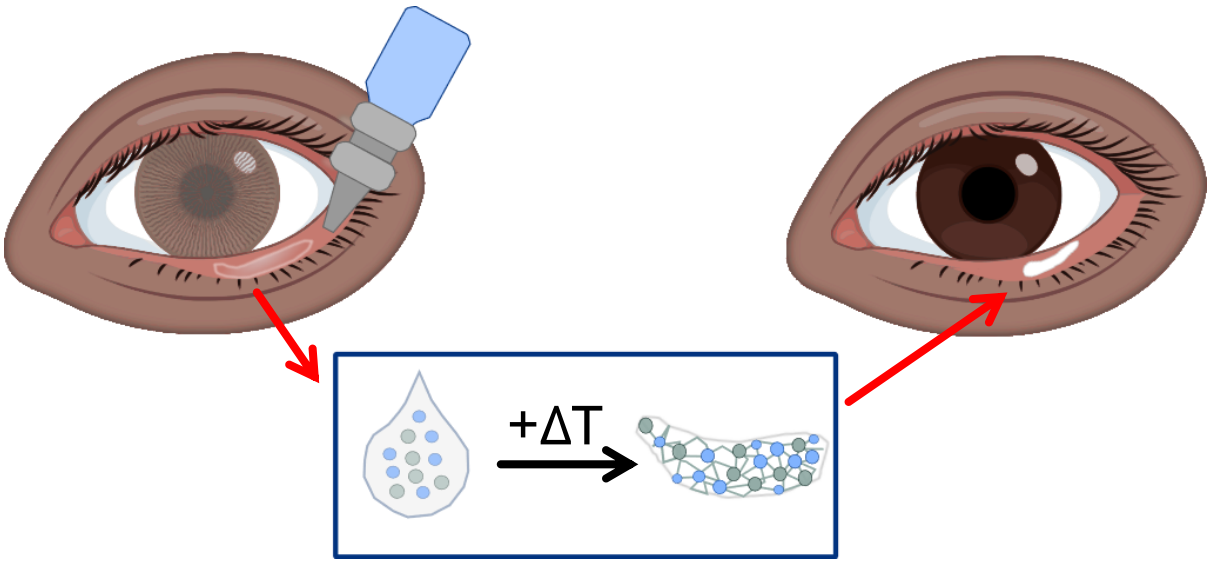

Figure 7 Overview of translational impact to cystinosis patients

2.0 Specific Aim 1

The focus of the aim was to develop and characterize materials in our DDS. In the timeline of this dissertation, the initial development (August 2016) took into consideration the clinical parameters set forth by Cystaran™ (0.44% cysteamine eyedrops), the only FDA-approved eyedrop at the time. Corneal cystine crystals are treated with Cystaran™ eyedrops when administrated 6 to 12 times day and used within 1 week after opening. The dosage and frequency of administration was clinically tested using titration studies [141, 142] to find the optimal dosing range. However, because these eyedrops are administered hourly and may require assistance from caregivers of pediatrics patients, the delivery of cysteamine can be inconsistent. This clinical practice may inhibit the ability to determine how much cysteamine (per mass) is delivered to the cornea. Furthermore, the FDA-approval did not require ocular pharmacokinetic data on cysteamine eyedrops which adds to the complexity of determining therapeutic concentrations in the eye. As such, the main strategy to determining a dosage to reformulate was focused on the concentration of cysteamine delivered from one 50µL drop at the minimum (6 drops) and maximum (12 drops). This aim highlights the scientific approach of encapsulating cysteamine microspheres (CMS). Several fabrication methods were conducted (Appendix A) and tested for compatibility with the pNIPAAm gel (Appendix A.2.3). The methods reflected in this chapter were iteratively used to design CMS formulations. Ultimately, the candidate formulation consisted of spray-dried cysteamine microspheres (SD-CMS) and was further investigated. The use of SD-CMS will henceforth describe a candidate microsphere formulation that was optimized after several formulations, which are compared and discussed in Appendix A.2.4 and Appendix A.2.5.

2.1 Introduction

Topical cysteamine has proven to be safe and effective in reducing and clearing corneal cystine crystals, resulting in clear corneal layers and reduction in light sensitivity [143-146]. However, cysteamine eyedrops require frequent administration—up to once per waking hour (6 to 12 times per day) and are highly susceptible to oxidative degradation, therefore requiring that the eyedrops are frozen until opening, stored in the refrigerator, and disposed of within 1 week [47, 143]. Furthermore, ocular irritation upon administration possibly associated with corneal epithelial erosions [147] leads to high levels of noncompliance with the prescribed drop regimen. This inconvenient therapy and its associated complications, particularly in the context of a disease as complex and multi-faceted as cystinosis, severely impact the quality of life of patients. To address the issues with ocular cysteamine delivery, including frequency of dosing and poor aqueous stability, cysteamine reformulation into various drug delivery systems has been investigated. Controlled release technologies including viscous gels [104, 108], hydrogels [103], contact lenses [106], and nanowafer discs [107] have recently been developed to increase the ocular retention and prolong the release of cysteamine. Of these studies, the nanowafer disc in particular has shown promise for extended release of cysteamine and moderately increased stability [107]. Despite these advances, development in this area, especially given the far-reaching implications for other rare diseases affecting vision [1] and the many new approaches for ocular drug delivery [18, 148], remains under investigated

The research presented in this chapter focuses on the development of a multicomponent extended-release drug delivery system for treatment of corneal cystinosis. This system incorporates spray-dried cysteamine-loaded poly(lactic-co-glycolic acid) microspheres (SD-CMS) within a thermoresponsive poly(N-isopropylacrylamide) (pNIPAAm) and poly(ethylene glycol)

(PEG) gel matrix (Gel) . The SD-CMS/Gel suspension is administered similarly to a traditional eyedrop but forms a pliable depot after exposure to ocular surface temperatures when placed in the lower eyelid. The Gel material is mixed with hydrolyzable PLGA microspheres, which are capable of delivering a range of ocular drugs for varying lengths of time, as with previous *in vivo* large animal studies demonstrating long-term efficacy, lower fornix retention and safety in glaucoma for 28 days [138], and bacterial endophthalmitis prophylaxis for 24 h [137].

This chapter describes the strategies for cysteamine encapsulation in PLGA microspheres and subsequent validation of microsphere morphology and in vitro drug release kinetics to achieve a minimum of 24 h of treatment, up to 12-fold reduction in dosing frequency. The resulting microsphere formulation demonstrated a dramatic increase in stability and ionic drug-surface tension interactions with the Gel carrier for sustained release of drug. Additional characterization including *ex vivo* corneal permeability studies, ocular irritation evaluation with organotypic models, and *in vivo* topical administration and retention further supported the use of this novel system for translation into preclinical models.

2.2 Materials and Methods

All materials and reagents were obtained from Sigma Aldrich (St. Louis, MO, USA) unless otherwise specified. The characterization methods (drug release and thermal properties) in this chapter also describe the methodologies performed in Appendix A.

2.2.1 Fabrication and Characterization of Cysteamine Microspheres

Spray dried cysteamine microspheres (SD-CMS) were fabricated using a Büchi B290 Mini Spray Dryer with a B29F Inert Loop (Büchi New Castle, Delaware, USA). Approximately 2 g of cysteamine hydrochloride and 8 g of 75:25 poly(DL-lactide-co-glycolide) (IV 0.14–0.22 dl/g, Mw: 4000–15,000) (Evonik Maryland, USA) in a cosolvent consisting of a methanol:dichloromethane (10:90,v/v) solution was used to generate a 5% cysteamine liquid feed. Büchi spray dry process parameters were set as follows: compressed nitrogen, flow meter (40 mm), aspirator (100%), inlet temperature (45 °C), atomizing gas flow (473 L/hr), feed rate (10% ml/min), and outlet temperature range (32–35 °C). Samples were collected using a Standard Cyclone and Product Collection Vessel. Cysteamine free microspheres (SD-BLANK-CMS) were produced using the same fabrication process without the addition of cysteamine hydrochloride. The shape and morphology of SD-CMS and SD-BLANK-CMS were examined using scanning electron microscopy (SEM). Samples were gold sputter-coated and imaged using a JEOL 6335F Field Emission SEM (JEOL, Peabody, MA, USA). The zeta potential of SD-CMS and SD-BLANK-CMS was determined using electrophoretic light scattering equipped in the Zetasizer Nano Series (Malvern, Westborough, MA, USA). SD-CMS and SD-BLANK-CMS were suspended in 10-mM potassium chloride (KCL) to achieve a 1% (w/v) ratio. A disposable folded capillary cell was filled with 0.75 mL of each suspension and measured at 37 °C..

2.2.2 Gel Fabrication and Thermal Characterization

Free radical polymerization of N-isopropylacrylamide (NIPAAm) was performed by adding 2 mL of an 0.5-mg/ mL solution of ammonium persulfate (APS) in MilliQ water to 100 mg of NIPAAm monomer. 5 μL of tetramethylethylenediamine (TEMED) initiator was added to the solution mixture and polymerization proceeded for 12 h at 4 °C. Residual TEMED and APS were removed from the synthesized poly(N-isopropylacrylamide) (pNIPAAm) via repeated phase transition cycling (T > 37 °C) in excess MilliQ water. The purified polymer was flash frozen in liquid nitrogen, lyophilized for 48 h, and stored at 4 °C prior to rehydration. A 9 wt% (m/v) gel was prepared via rehydration of ~ 470 mg of lyophilized pNIPAAm in 4.7 mL of MilliQ water with 470 μL of polyethylene glycol (PEG MW 200 kDa) as an additive. Hydration of the gels proceeded for 3 days with intermittent mixing and centrifugation at 4 °C, 1000 RPM (106 RCF). Samples were stored at 4 °C until use. After preparation, SD-CMS gel suspensions (SD-CMS/ Gel) and SD-Blank-CMS gel suspensions (SD-BLANK-CMS/Gel) were prepared by weighing out respective microspheres at a ratio of 1 mg: 100 μL gel. The lower critical solution temperature (LCST) of gel, SD-CMS/Gel, and SD-BLANK-CMS/Gel were determined via differential scanning calorimetry (DSC). DSC analysis was performed using a Perkin Elmer Pyris 6 calorimeter. Samples were heated in hermetically sealed aluminum pans from 2 to 50 °C at a rate of 2 °C/min under a nitrogen atmosphere with a flow rate of 20 mL/min. LCST values were calculated as the endothermic peak in the resulting DSC curves.

2.2.3 Evaluation of *In Vitro* Drug Release Kinetics

Quantifying cysteamine release from CMS formulations guides the optimization towards a candidate formulation of further characterization. In the initial development of a CMS formulation, emulsion-based techniques such as double emulsions and single emulsions produced CMS with unfavorable drug release kinetics as characterized below. It should be noted that the choice of SD-CMS as the candidate formulation is a result from the high drug encapsulation of a water-soluble drug from spray-dried techniques. Appendix A describes the optimization of CMS and SD-CMS process in more detail.

2.2.3.1 Detection of Cysteamine with Pre-Column Derivatization HPLC

Cysteamine was detected by derivatizing with 2-chloro1-methylquinolinium tetrafluoroborate (CMQT) and analyzed with a modified high-performance liquid chromatography (HPLC) method [149]. CMQT was synthesized in lab according to previously published methods [150]. Reduction of oxidized cysteamine (cystamine) with tris(2-carboxyethyl) phosphine hydrochloride (TCEP) was performed prior to CMQT derivatization. Standard cysteamine sample aliquots (100 µL) were added to 400 µL of a 0.1 M, pH 7.5 phosphate buffer solution. Approximately 20 µL of 0.1 M TCEP was added to the solution mixture, reacted for 15 min, followed by 20 µL of 0.1 M CMQT, which reacted for 5 min. The reaction mixture was then acidified with 50 µL of 3 M hydrochloric acid. Approximately 20 µL of reaction sample was injected into an autosampler on a 1220 Infinity Liquid Chromatography (Agilent Technologies, California, USA) attached with a 1220 DAD Liquid Chromatography UV detector (Agilent Technologies, California, USA). A reverse-phase Zorbax SD-C18 column (5 µm, 4.6 × 150 mm; Agilent Technologies, California, USA) was used to separate molecules undergoing a gradient

elution. The gradient elution consisted of mobile phases acetonitrile (A) and trichloroacetic acid pH 2.0 (B) at ratios: 0–3 min (12% A, 88% B), 3–9 min (30%A, 70%B), and 9–12 (12%A, 88%B) for 15 min at a flow rate of 1.2 mL/min. The column temperature was held at 25 °C. UV detector was set at 355 nm. Retention times of cysteamine-CMQT derivative and excess CMQT were 10.5 min and 11.3 min, respectively (Figure 8). The column was equilibrated for 5 min after each injection. Peak height from cysteamine-CMQT derivative was used from standard aliquots to create a 6-point standard curve over the range of 1 to 50 µg/mL (Figure 9).

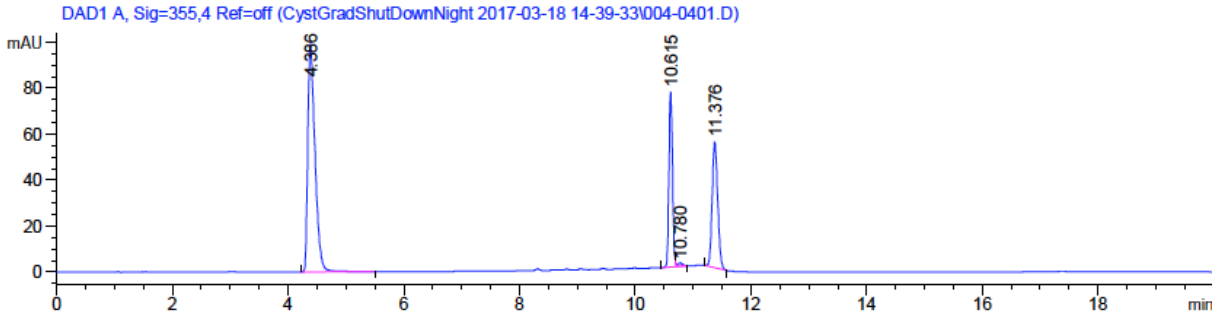

Figure 8 HPLC chromatogram of CMQT (10.5-10.6 min) and cysteamine-CMQT (11.3 min)

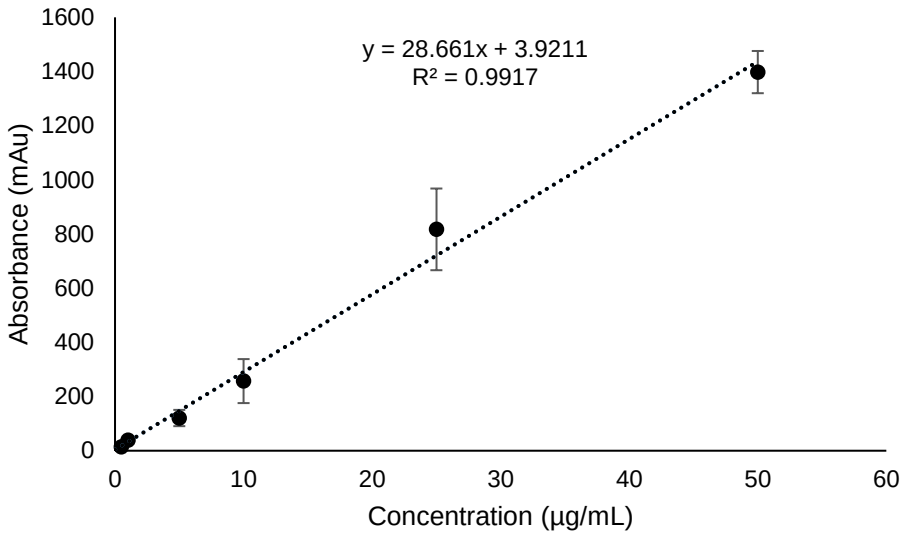

Figure 9. Standard curve of cysteamine-CMQT derivatves from HPLC

2.2.3.2 Release Studies on Cysteamine Microspheres and Gel Suspensions

Cysteamine loaded microspheres (SD-CMS) and cysteamine-free microspheres (SD-BLANK-CMS), along with their corresponding gel suspensions (SD-CMS/Gel, SD-BLANKCMS/Gel), were further characterized for *in vitro* drug release kinetics over 24 h. Known masses of SD-CMS were suspended in 0.1 M, pH 7.5 phosphate buffer solution (500 µL) in a 1.5 mL Eppendorf tube. Samples were placed in a rotator and incubator at 37 °C. For each predetermined time point, samples were spun down at 3500 RPM (106 RCF) or 5 min, and supernatant was removed for analysis. Fresh phosphate buffer solution was added to the remaining MS, vortexed, and placed back onto rotator to maintain sink-like conditions. Cysteamine concentrations in phosphate buffer solution were analyzed using the previously described HPLC method. Gel suspension release kinetics were determined similarly, by mixing MS at a ratio of 10 mg:100 µL (MS:Gel) in a 1.5 mL Eppendorf tube, sampling supernatant at 37 °C as not to

disturb microsphere/gel conformation, replacing supernatant with fresh 37 °C phosphate buffer solution, and evaluating release samples with HPLC.

2.2.4 NMR Quantification of Cysteamine in Microspheres

Cysteamine drug loading in PLGA microspheres was quantified using NMR spectroscopy. Reference spectra for PLGA quantification with NMR spectroscopy were implemented [151]. The 1 H-NMR spectra were obtained using a 500-MHz Bruker Avance III spectrometer at 293 K in deuterated dimethyl sulfoxide (DMSO-d6) with a sample concentration of 20 mg/mL. Spectra obtained from 32 scans were calibrated to the residual solvent peak at δ 2.50 ppm and processed with TOPSPIN™ software (Bruker, Billerica, Massachusetts, USA). Reference spectra of cysteamine, cystamine, and PLGA were utilized as standards, where non-overlapping methylene proton resonances at δ 2.70 ppm (cysteamine), δ 3.10 ppm (cystamine), and δ 4.88 ppm (PLGA) were utilized to determine mass of cysteamine in MS, drug-loading, and % cysteamine according to Eqs. 1, 2., and 3, respectively.

$$cys\ (mg) = \frac{MM_{CYS} \cdot \frac{I_{CYS}}{P_{CYS}}}{MM_{CYS} \cdot \frac{I_{CYS}}{P_{CYS}} + MM_{PLGA} \cdot \frac{I_{PLGA}}{P_{PLGA}}} \times mass\ MS\ (mg) \qquad \textbf{Equation 1}$$

In Equation 1, MM_{CYS} is the molar mass of cysteamine, 77.15 g/ mol; MM_{PLGA} is the molar mass of the PLGA repeat unit "LG," 126.0 g/mol; and I and P are the integral and number of protons, respectively.

$$drug\ loading\ \left(\frac{\mu g}{mg}\right) = \frac{mass\ of\ cys\ in\ MS\ (\mu g)}{mass\ of\ MS\ (mg)} \qquad \textbf{Equation 2}$$

In Equation 2, drug loading is the amount (mass) of cysteamine in a known mass of microspheres. A pre weighed sample of microspheres can be used to normalize between samples when determining the amount cysteamine.

$$\%\ Cysteamine = \left(\frac{\frac{I_{cysteamine}}{2}}{\frac{I_{cysteamine}}{2} + \frac{I_{cystamine}}{4}} \right) \times 100 \qquad \textbf{Equation 3}$$

In Equation 3, the percentage of cysteamine (%) is determined by finding the ratio of oxidized cystamine in the sample. The value $I_{cysteamine}$ is the integral value of NMR for cysteamine and is divided by the number of protons (2 protons) for cysteamine. The value $I_{\text{cystamine}}$ is the integral value of NMR for cystamine (the oxidized form of cysteamine) and is divided by the number of protons (4 protons) for cystamine.

2.2.5 NMR Study to Determine Cysteamine Stability in Microspheres and Eyedrops

Cysteamine drug stability in SD-CMS and eyedrop formulations was monitored using NMR spectroscopy. SD-CMS formulations and a control cysteamine eyedrop solution [139] consisting of cysteamine hydrochloride (66 mg) in 15 mL deuterate water (D2O) (Cabridge Isotope Laboratories Inc., MA, USA) with 0.01% benzalkonium chloride (1.5 mg) and 0.90% sodium chloride (135 mg) were evaluated at 4 °C and 25 °C, over a 7-week time period. The SD-CMS and eyedrop formulation samples were wrapped in aluminum foil and opened twice per day to simulate opening and closing of an eyedrop bottle. 1 H-NMR spectra were obtained bi-weekly using a 500-MHz Bruker Avance III spectrometer at 293 K. Approximately 1 mL aliquots of the D2O-based eyedrop formulation were utilized for analysis, whereas 20 mg samples of SD-CMS were weighed out, dissolved in DMSO-d6, and analyzed within 10 min to capture the

cysteamine:cystamine content within the SD-CMS. Spectra obtained from 32 scans were calibrated to the residual solvent peak at δ 2.50 ppm (DMSO-d6) and δ 4.80 ppm (D2O) and processed with TOPSPIN™ software (Bruker, Billerica, Massachusetts, USA). Cysteamine content within each sample was determined by monitoring the non-overlapping methylene resonance of cysteamine and cystamine at δ 2.70 ppm (DMSO-d6, Figure 10) or 2.85 ppm (D2O; Figure 11) and δ 3.10 ppm (DMSO-d6, Figure 10) or 3.05 ppm (D2O; Figure 11), respectively. Percent cysteamine (%) was determined according to Eq. 3.

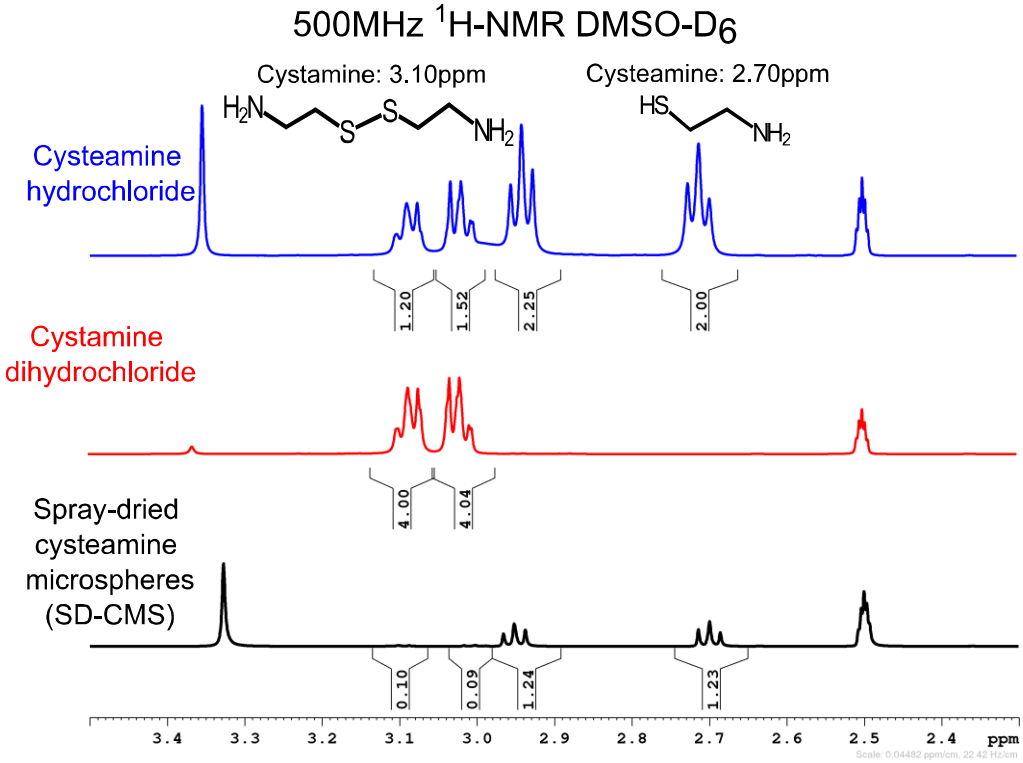

Figure 10 NMR profile of cysteamine and cystamine in SD-CMS

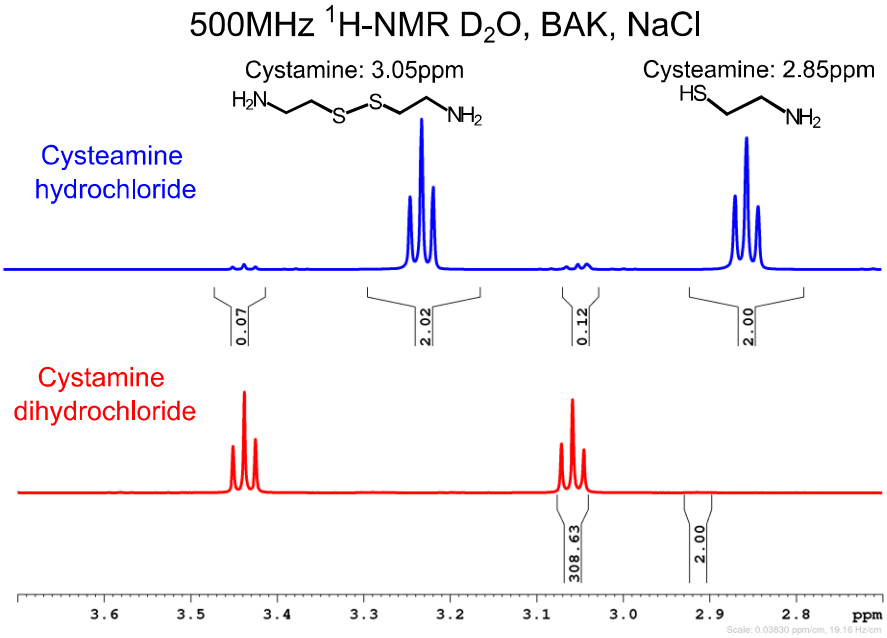

Figure 11 NMR profile of cysteamine and cystamine in eyedrops

2.2.6 Conjunctival Irritation on the HET-CAM Test

Fertilized white leghorn hen eggs (Moyer's Chicks, Quakertown, PA) were obtained and incubated for 9 days at 37 °C and 60% humidity. Eggs were placed pointy end facing down on egg holding racks and rotated twice a day manually. On the 6th day, eggs were candled using a candlar to observe embryo formation. Underdeveloped eggs were discarded. On the 9th day, eggs were removed from the incubator and were allowed to equilibrate to room temperature. A 1 cm radius circle was drawn on the top of the egg. A rotator tool (WEN Model #2305, Elgin, Illinois) with a cut-ofF wheel attachment was used to carefully cut through the eggshell, exposing a thin white membrane. For this study, a negative control of a 0.9% saline solution was fabricated by dissolving 9 g of sodium chloride in 1000 mL of milliQ water. A positive control consisting of a 0.1 M sodium hydroxide (NaOH) solution was obtained from Sigma Aldrich (St. Louis, MO, USA).

Approximately 500 µL of 0.9% saline was added to the white membrane for 5 min. Curved forceps were used to remove the white membrane and expose the chorioallantoic membrane (CAM). The CAM was noted of any defects, and egg shell debris was removed carefully without damaging the CAM. An initial image of the CAM was taken using an inverted slit lamp (Eyephotodoc Fullerton, CA). For liquid controls, 300 µL of test material was placed on the CAM. For microspheres controls, 10 mg of material to 300 µL of 0.9% saline was placed on the CAM. For gel controls, 100 µL of material was placed. Similarly, SD-CMS/Gel and SD-BLANK/Gel suspensions were applied at a ratio of 10 mg:100 µL SD-CMS:Gel. Images at 30 s, 2 min, and 5 min were taken for each test material. Any signs of vascular hemorrhage, coagulation, and/or lysis (Figure 12) were recorded based on previous studies [152]. Endpoint effects were scored based on in vitro toxicology studies [153] and summarized in Table 2.

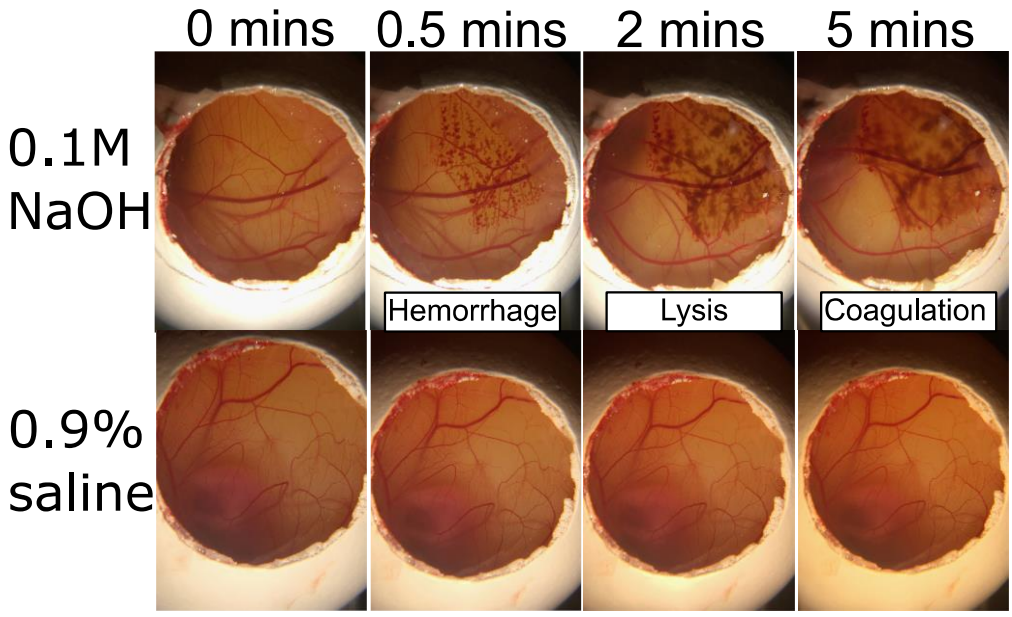

Figure 12 HET-CAM irritation from positive and negative controls

Table 2 HET-CAM score range

HET-CAM Score Range	Irritation Category
0.-0.9	Nonirritant or practically none
1-4.9	Weak or slight irritation
5-8.9 or 5-9.9	Moderate irritation
9-21 or 10-21	Strong or severe irritation

2.2.7 Corneal Irritation on the BCOP Test

Freshly enucleated bovine whole eyes were delivered on ice from Pel-freez Biologicals (Rogers, AR, USA) overnight, within 24 h of harvesting. Samples were inspected for corneal damage (scratches, cloudiness) or severe cataracts and were discarded from study. Viable bovine eyes were placed on aluminum dishes on top of 100 mL beakers filled with MilliQ water and placed in a 37 °C water bath. A silicon O-ring (RtDygert, Burnsville Minnesota) was placed on the center of the cornea. Prior to application of testing materials, a 150 µL drop of 0.9% saline was added to fill the O-ring. A khim wipe was used to blot of the saline and replaced with testing materials. Controls and test material masses and volumes were administered as a solution or suspension for dry powders, similar to the methods in the HET-CAM test. Corneas were exposed to materials for 30 s and subsequently rinsed of with 0.9% saline. Corneas post-exposure were incubated for 10 min and scored for corneal opacification and epithelial detachment. Epithelial integrity was determined by applying ophthalmic fluorescein strips (FluGlo, Akron Lakeforest,IL) and observed under blue cobalt light. Irritation scores were determined and categorized based on

overall cumulative scoring [153], summarized in Figure 13 and Table 3. These methods followed the OECD Test No. 437 guidelines for the testing of chemical eye irritants [154], which suggest a range of immediate exposure (30 s) to 4 h with longer exposure times suggested on case-by-case bases.

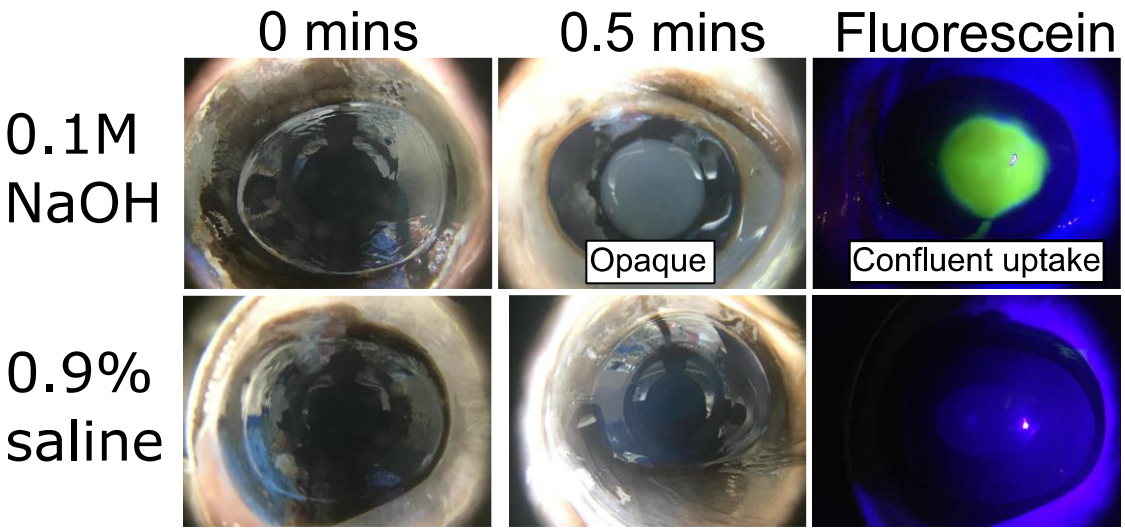

Figure 13 BCOP irritation from positive and negative controls

Table 3 BCOP scoring range

BCOP Score Range	Irritation Category
<= 0.5	Nonirritant or practically none
0.5-1.9	Weak or slight irritation
2.0-4.0	Moderate irritation
>4.0	Strong or severe irritation

2.2.8 *Ex Vivo* Corneal Permeation Studies

Trans-corneal permeation was studied using excised rabbit corneas (Pel-freez Biologics, Rogers, AR, USA) and Franz type diffusion cells as previously described [139]. Rabbit whole eyes were shipped in Dulbecco's modified Eagle's medium with antibiotic and antimycotic per Pel-freez Biologics formulation, shipped overnight on ice within 24 h of harvesting. Whole eyes were evaluated for corneal damage with slit lamp imaging and discarded if present with superficial damage. Selected corneas were excised with iris type dissecting scissors with 1–2 mm of surrounding sclera tissue and were placed epithelium side down in 0.1 M, pH 7.5 phosphate buffer solution. The corneal medium and storage conditions have been previously reported [155] to support epithelial cell survival and reduce the likelihood of ultrastructure changes required for corneal transplants in humans [156]. Corneas were fitted on Franz cells (9 mm OD spherical joint interfaced with sclera, 5 mL receptor volume) with a 0.64 cm^2 corneal permeation area (PermeGear, Hellertown, PA, USA). The donor chamber was filled with 0.3 mL of cysteamine eyedrops (0.44% cysteamine hydrochloride, 0.01% benzalkonium chloride (1.5 mg) and 0.90% sodium chloride (135 mg), adjusted to pH 4.1–4.5 with 0.01 M hydrochloric acid), and 0.3 mL of SD-CMS/Gel at a ratio of 10 mg:100 µL of SD-CMS:Gel. The receptor chamber was filled with 0.1 M, pH 7.5 phosphate buffer solution (approximately 5 mL volume). The receptor chamber was continuously stirred at 600 RPM on a magnetic stir plate and kept at 37 °C. Approximately 200 µL of receptor solution was sampled hourly for a 5 h period and analyzed using previously described HPLC (N = 3). Blank assays were conducted similarly to test assays to verify interferences due to biological tissues in HPLC. Data are presented as mass of cysteamine permeated across a 64 cm^2 permeation area (µg/cm^2) as a function of time.

2.2.9 *In Vivo* Topical Administration, Retention, and Preliminary Safety

Our study conformed to the Association for Research in Vision and Ophthalmology (ARVO) Statement for the Use of Animals in Ophthalmic and Vision Research and was approved by the University of Pittsburgh Institutional Animal Care and Use Committee. New Zealand white rabbits (0.95–1.4 kg) were purchased from Envigo (formerly Covance Research, Somerset, NJ, USA). The right eye of each subject (N = 3) was selected to undergo surgical resection of the nictitating membrane, a tissue that partially covers the surface of the rabbit eye, prior to treatment. This procedure has been previously described to be minimally invasive and safe with a healing time of 7 days [137, 138]. The nictitating membranes of the rabbit eyes were removed with a scalpel and cauterizing tool to excise the tissue and minimize bleeding. The rabbits were anesthetized intravenously via marginal ear vein by applying topical 5% lidocaine ointment (Amneal Pharmaceuticals LLC Bridgewater, NJ, USA) to the injection site 10 min prior to injection of 10 mg/kg of ketamine (Ketathesia; Henry Schein Animal Health, Dublin, OH, USA) and 1 mg/kg of xylazine (AnaSed Injection; Lloyd Laboratories, Shenandoah, IA, USA). To the eye, one topical drop of 0.5% proparacaine (Baush+Lomb, Bridgewater, NJ, USA) was administered before removal of the nictitating membrane. Following the procedure, one topical eyedrop of 0.3% tobramycin (Bausch+Lomb, Bridgewater, NJ, USA), and one topical eyedrop 1% prednisolone acetate (Pacifc Pharmaceticals INC, Rancho Cucamonga, CA, USA) was immediately administered and repeated once daily for the following 4 days to prevent infection and limit inflammation. The eyes of the rabbits were examined using slit-lamp photography (Eyephotodoc, Fullerton, CA, USA) throughout the study. After 7 days, one drop of 2% topical fluorescein ophthalmic suspension (Baush+Lomb, Bridgewater, NJ, USA) was administered and observed under cobalt light. After which, one 100 µL drop of SD-CMS/Gel (ratio 10 mg SD-

CMS/100 µL Gel) was topically administered using a 1 mL syringe capped with a 200 µL pipette tip (Figure 23A), and placed in the inferior conjunctival cul-de-sac (see Figure 23B) without local or systemic anesthesia. After 24 h, the rabbits were evaluated for eye health and gel retention via fluorescein drops and cobalt light imaging

2.2.10 Statistical Analysis

Zeta potential, drug release assays, stability, and ex vivo ocular irritation assays are represented as average ± standard deviation for N=3 samples. For corneal permeation studies, a Mann-Whitney U test was used to compare the amount of cysteamine permeated through rabbit corneas from cysteamine formulations (alpha = 0.05) reported from Minitab 19 software (State College, PA).

2.3 Results

2.3.1 Cysteamine Microspheres and Gel Characterization

Characterization of microspheres using scanning electron microscopy (SEM) was performed to evaluate their outer pore morphology and approximate size. The zeta potential (ZP) of microspheres were determined as indicative evidence towards the surface potential and nature of surface charge (positive/negative). Upon fabrication, SEM, and ZP characterization, microspheres were combined into Gel (pNIPAAm and PEG) and analyzed for thermal properties with differential scanning calorimetry (DSC) to ensure the lower critical solution temperature

(LCST) of the combined system was similar to ocular surface temperature ranges (32–34 °C) [140]. These measurements were taken prior to drug release assays to verify that the fabrication methods resulted in thermal properties compatible with the intended clinical use. Figure 14 shows representative SEM images of spray-dried cysteamine loaded microspheres (SD-CMS). SEM images represented spherical microspheres with a relative size of 2 µm, supporting microsphere fabrication with no appearance of free, unloaded cysteamine crystals. The ZP of SD-CMS and SD-BLANK-CMS was compared in Figure 15. Samples were measured at a range of pH (4–12) to compare surface potentials. SD-CMS ZPs were determined at pH 4–10 (between − 14.21 ± 7.235 mV and 0.29 ± 20.213 mV) and pH 11–12 (− 38.76 ± 1.939 mV and − 35.43 ± 7.569 mV). SD-BLANK-CMS ZPs were determined at pH 4–12 (between − 43.46 ± 4.556 mV and − 32.6 ± 3.469 mV). The differences in ZPs between SD-CMS and SD-BLANK-CMS support the inclusion of cysteamine ions within the fabrication process of SD-CMS. Having confirmed microsphere fabrication and characterization, the next step was to determine the LCST of our microsphere formulations and gel. Figure 16 presents differential scanning calorimetry thermograms of Gel (no microspheres), Gel with unloaded, cysteamine-free microspheres (SD-BLANK-CMS/Gel), and Gel with cysteamine loaded microspheres (SD-CMS/Gel). The thermograms confirm the LCST (°C) as endothermic transitions observed during the heating phase. The LCST for the gel formulation was determined to be 33.9 °C, whereas the LCST of the gels with cysteamine and cysteamine-free microspheres was 32.0 and 33.6 °C, respectively. These measures confirm the ability for our drug delivery system to be administered below their LCST as an aqueous gel, and when applied to the ocular surface and eyelid will transition to a pliable drug delivery system.

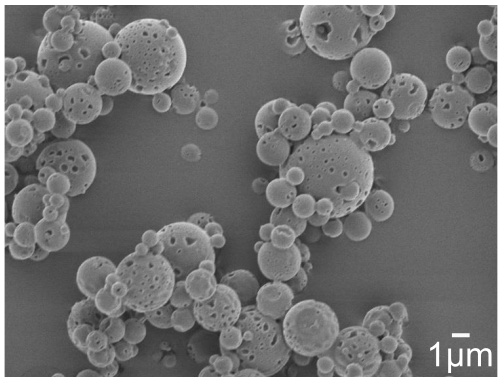

Figure 14. Scanning electronc microscopy (SEM) of SD-CMS

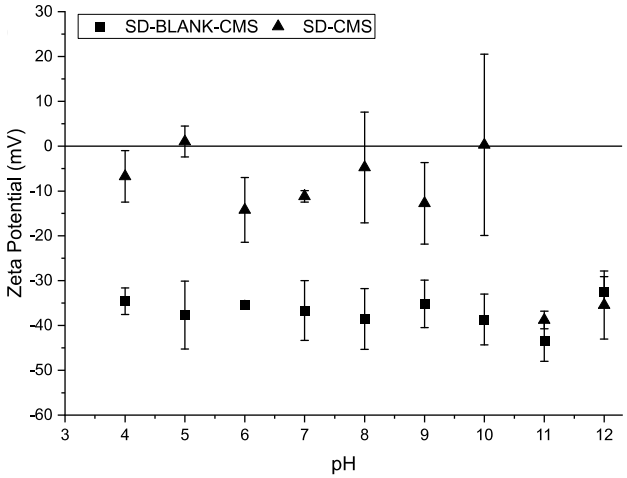

Figure 15. Zeta potential of SD-CMS and SD-BLANK-CMS. The data are represented by mean ± standard deviation (N=3)

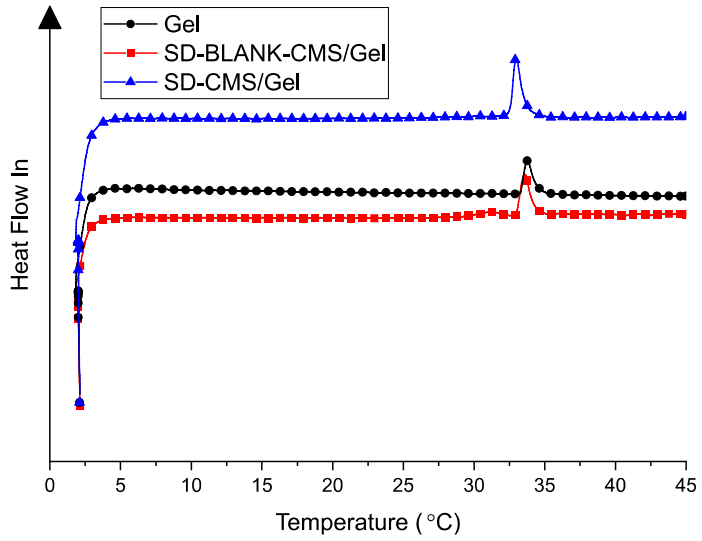

Figure 16. DSC thermal characaerization of gel and spray dried MS formulations

2.3.2 *In Vitro* Cysteamine Drug Release Studies

Having confirmed the fabrication of SD-CMS and thermal properties of our gel-microsphere delivery system, the next step was to determine the release profile of cysteamine from the SD-CMS and SD-CMS/Gel. *In vitro* cumulative release of cysteamine from a known mass of microspheres alone and microspheres within our gel for 24 h was compared in Figure 17. Analysis of percentage of total amount of cysteamine encapsulated was reported with the goal of verifying potential changes in release kinetics from our gel. Figure 18 present cysteamine release totals from our combined system relative to the amount of cysteamine delivered to the eye at the clinically recommended frequency, with a minimum 6 drops (1950 µg cysteamine) and maximum 12 drops (3900 µg cysteamine) daily (see Appendix A.1 for calculation) [47, 157]. As expected, cysteamine release from our system within 24 h was above the lower limit of cysteamine delivery with an average cumulative release of 2633.08 ± 61.797 µg/day released over 24 h.

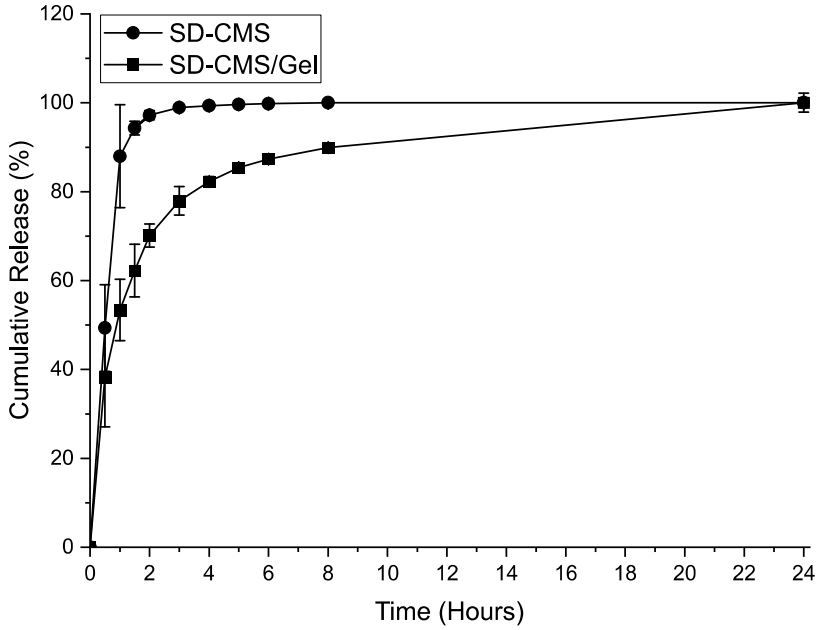

Figure 17 Cysteamine release from SD-CMS and SD-CMS/Gel. Data are represented as mean ± standard deviation (N=3)

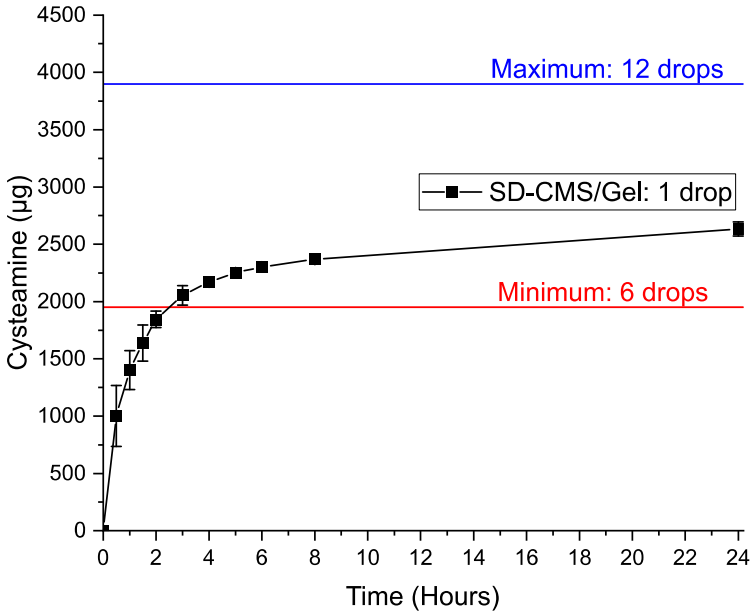

Figure 18 Cysteamine release from SD-CMS/Gel compared to eyedrop regiment (6-12 drops)

2.3.3 Stability Profile of Cysteamine Microspheres and Cysteamine Eyedrops

Cysteamine in eyedrop formulations has been well reported to be chemically unstable as it readily oxidizes to therapeutically inactive cystamine, the dimer of cysteamine [47, 99, 147]. Therefore, stability analysis of cysteamine in eyedrops and microspheres was evaluated at 25 ℃ and 4 ℃ with repeated opening and closing to introduce oxygen, much like the clinical use of the current cysteamine eyedrops. Figure 19 shows the stability of cysteamine (%) in an eyedrop formulation (n = 3) at 1 week at 4 ℃ with 92.5% ± 1.84% cysteamine, and 25 ℃ with 83.58% ± 3.25% cysteamine. Stability of cysteamine in microspheres (n = 1) at 7 weeks at 4 ℃ with 96.2% cysteamine and at 5 weeks at 25 ℃ with 93.1% cysteamine. Cysteamine encapsulated in PLGA microspheres remained in its therapeutic, effective form for 7 weeks, an improvement from cysteamine eyedrops, in which is stable for 1 week. Further, as seen in NMR spectra (Figure 10 and Figure 11), we can track the ratio of degradation by independently quantifying unique resonance for cysteamine (δ = 2.70 ppm) and cystamine (δ = 3.10 ppm) via 1 H-NMR.

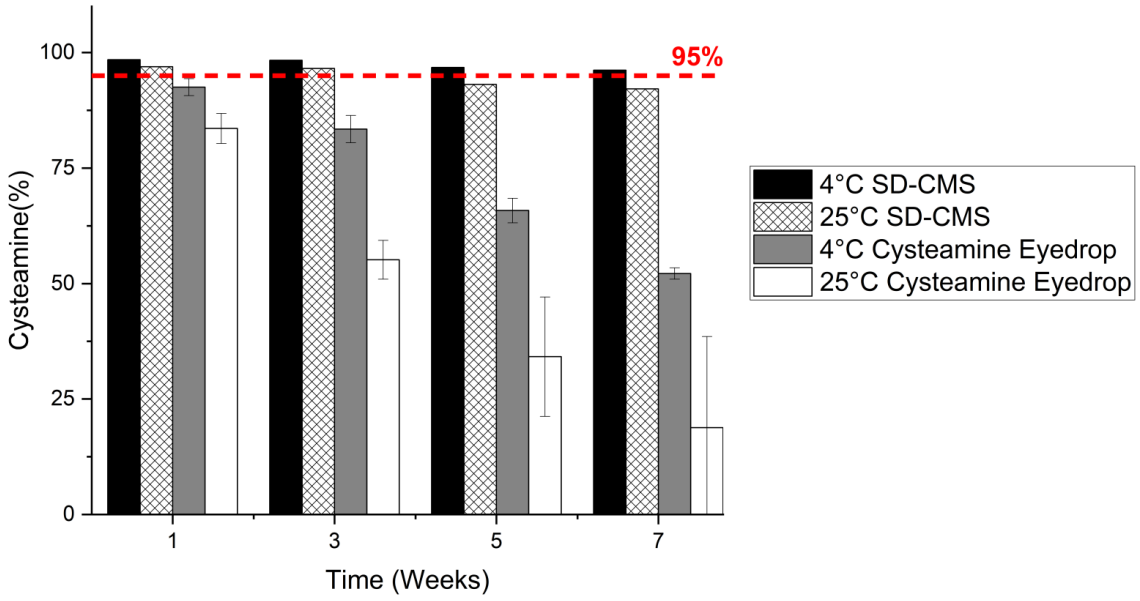

Figure 19. Stability plot of cysteamine in eyedrop formulations. Data is reprsented as mean ± standard deviation

2.3.4 *In Vitro/Ex Vivo* Ocular Irritation Studies

Previously developed organotypic ocular irritation models [158, 159] that are sensitive to irritating chemical materials were used to evaluate the potential irritation of our materials and cysteamine eyedrops. Figure 20 represents cumulative HET-CAM irritation scores indicating that cysteamine eyedrops (n = 3, 1.67 ± 2.86) and cysteamine loaded microspheres in gel (n = 3, 1.00 ± 1.73) had no irritation when compared with positive controls with severe irritation (0.1 M NaOH, n = 3, 20.33 ± 1.15) and negative controls with no irritation (0.9% saline, n = 3, 0 ± 0 None). The microsphere formulations with no cysteamine (SD-BLANK-CMS, n = 3, 1 ± 1.73) and cysteamine loaded (SD-CMS, n = 3, 2.33 ± 4.04) when applied as dry powders were categorized as no irritation and slight, respectively. Bovine Corneal Opacity (BCOP) results presented in Figure 21 show similar findings with all materials falling within the no irritation

category when compared with severely irritating positive controls of 0.1 M NaOH. These findings indicate that our materials have no irritation and the combined cysteamine loaded microspheres and gel is likely to be tolerated as an eyedrop when exposed to approximately 85% (8 h) of cumulative cysteamine release (Figure 17).

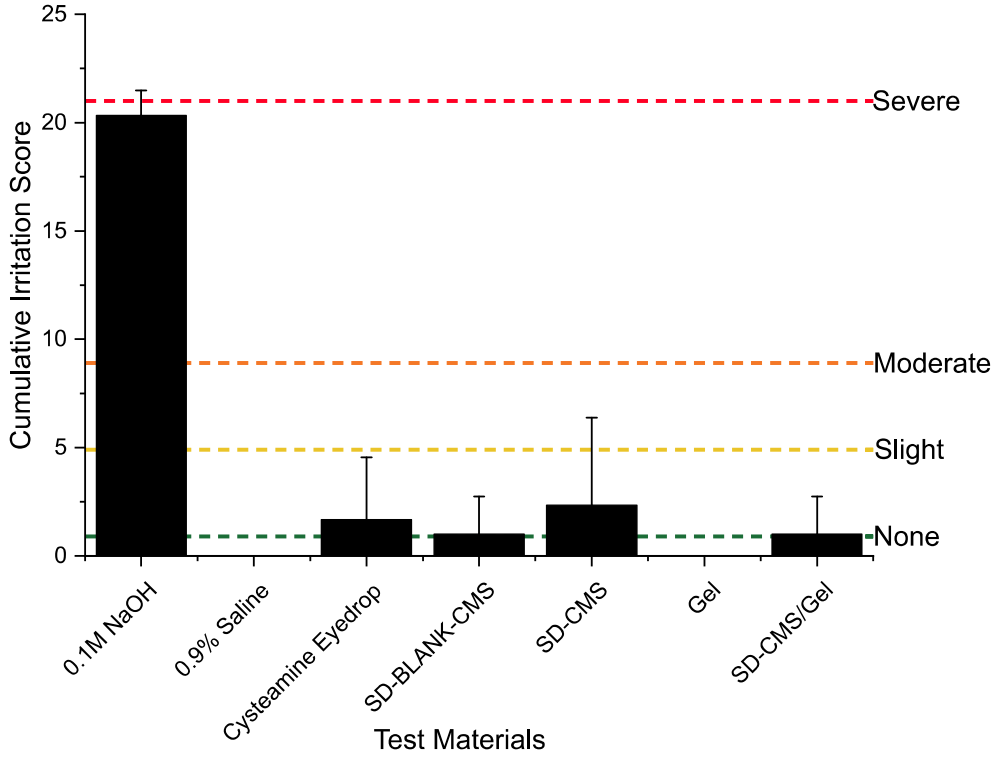

Figure 20 HET-CAM cumulative irritation scores

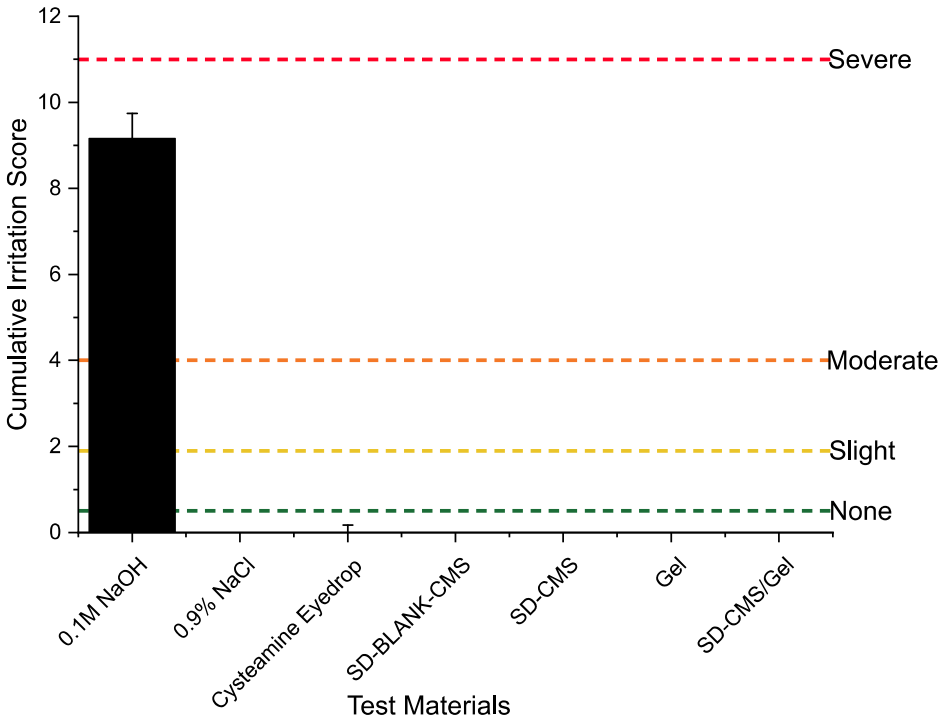

Figure 21 BCOP cumulative irritation scores

2.3.5 Corneal Permeation Studies

Cysteamine permeation through excised rabbit corneas in a Franz diffusion cell was investigated in our cysteamine microspheres/gel (SD-CMS/Gel) delivery system and compared with cysteamine eyedrops. We selected rabbit corneas for direct translation of our delivery system to our previous in vivo studies for glaucoma [138] and endophthalmitis [137], which suggest physiological and anatomical similarities to humans. Figure 22 presents cysteamine permeation data for each formulation for 5 h. We observed no significant difference in cysteamine permeation between cysteamine eyedrops (and SD-CMS/Gel). The resulting cysteamine permeation findings indicate cysteamine delivery from SD-CMS/Gel was readily absorbed through the cornea.

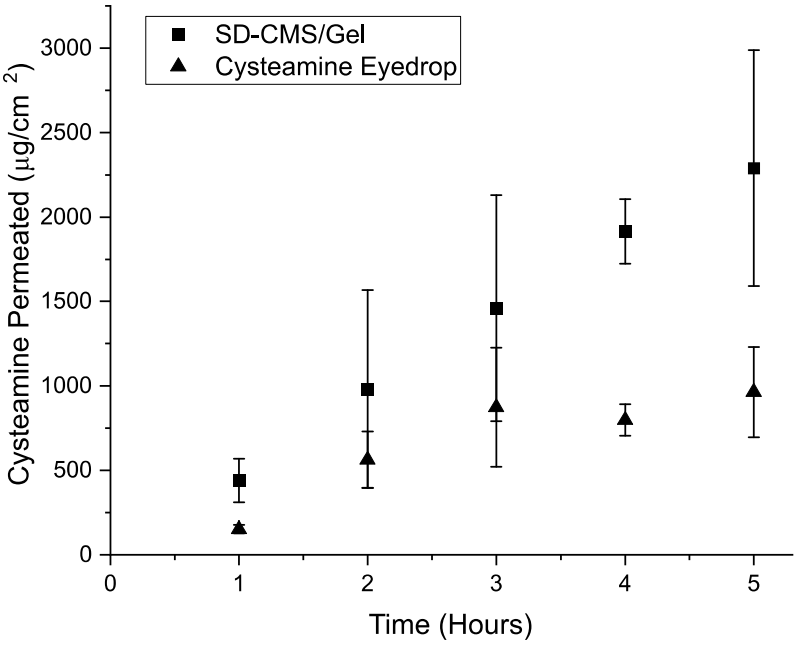

Figure 22 Corneal permeation from cysteamine formulations

2.3.6 *In Vivo* Retention Studies

The eyes of New Zealand white rabbits were surgically modified to anatomically resemble human eyes following safe surgical procedures and conventional after care. After monitoring eye health for 7 days, without anesthesia, our topical drug delivery system was administered to the lower eyelid at room temperature (Figure 23B) and transitioned upon administration at ocular surface temperatures (Figure 21C). For each subject (N = 3), one drop of 2% fluorescein was topically applied prior to SD-CMS/Gel administration (Figure 21, labeled D,F,H) and 24 h after (Figure 21, labeled E,G,I) to assess corneal health and retention. All subjects (N = 3) retained our drug delivery system at a volume of 100 µL (SD-CMS/Gel ratio 10 mg/100 µL) for 24 h. Cobalt light and fluorescein staining suggest no corneal or conjunctival damage.

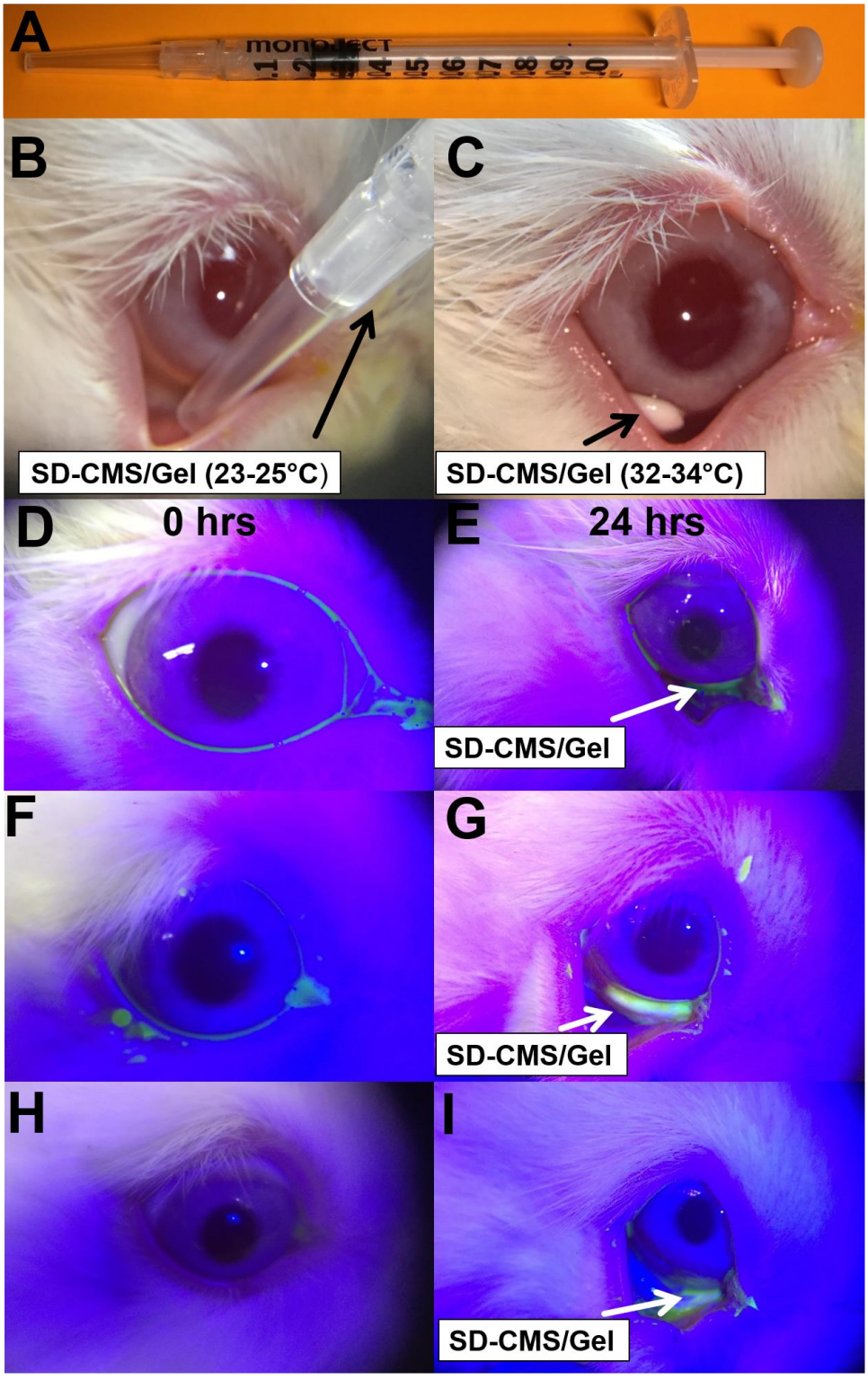

Figure 23 In vivo administration and retention of SD-CMS/Gel.

2.4 Discussion

The high instability of cysteamine in aqueous solutions is one of the greatest challenges in development of therapies for corneal crystals in cystinosis. Due to its unstable nature, clinical data regarding safety and efficacy required hourly cysteamine eyedrops to reduce corneal crystals—leading to the acceptance of a clinical standard of 6–12 drops daily [47, 99]. Often, administration of cysteamine eyedrops requires caregivers for pediatric patients further adding to the burden of therapy. While caregivers become experts in the clinical management of cystinosis, the irritation associated with disease and cysteamine eyedrop administration can lead to patients tolerating one drop per day, resulting in noncompliance. For these reasons, the area of controlled release with encapsulated materials may afford localized delivery of cysteamine that effectively treats cystine crystals in cystinosis patients' eyes, with a reduction in frequency of administration.

As seen in studies on the reformulation of cysteamine eyedrops in to controlled release systems, cysteamine release was extended to a few hours [104, 106-108] to a maximum of 24 h [103]. The small size and hydrophilicity of cysteamine may contribute to the difficulties in controlling the rate of diffusion and drug loading of cysteamine from these systems. Such was the case when designing a PLGA microsphere with a drug loading equivalent to the range of cysteamine delivered to achieve crystal reduction in patients. Achieving the proposed amount of cysteamine in traditional emulsion (single and double emulsions) based techniques as recommended by the literature [160] proved to be challenging with an ultra-small, hydrophilic, chemically unstable thiol.

Extensive efforts in microsphere formulation development and fabrication were conducted to achieve drug release magnitudes at the recommended amount of cysteamine equivalent in the range of 6–12 eyedrops/day [47]. Total amount of cysteamine delivered from standard cysteamine

eyedrops is the current clinical parameter for formulation development as the field lacks critical in vivo ocular pharmacokinetic data to determine efficacious cysteamine absorption amounts. Therefore, at a 0.05-mL dose volume of a 6.5- mg/mL cysteamine hydrochloride solution [157], a total of 0.325-mg (325 µg) cysteamine is delivered per drop. When scaled to the recommended frequency 6–12 drops/day, a minimum to maximum range is equivalent to 1950–3900 µg cysteamine (see Appendix A.1).

Several iterations of microsphere formulations were characterized and analyzed until ultimately, emulsion strategies were determined to be incompatible for encapsulation of cysteamine. As an alternative, removing potential interactions with larger volumes of aqueous solvents and thereby overcoming the hydrophilic nature of cysteamine, spray-dried fabrication of cysteamine achieved spherical microspheres (Figure 14). Inclusion of cysteamine ions from fabrication was indicated by differences in zeta potential magnitude and nature of surface charge (positive/negative) between SD-CMS and cysteamine free SD-BLANK-CMS (Figure 15). The presence of these ions slightly lowered the LCST after mixing in topical pNIPAAm and PEG gel (Figure 16). We observed 100% cysteamine depletion from PLGA microspheres within 2 h and extension of release from gel (SD-CMS/Gel) to 8–24 h (80%-100%). During sampling, the SD-CMS/Gel supernatant was sampled in a 37 °C water bath to prevent reversible transition and disruption of the microsphere-gel conformation. Cysteamine loading and delivery within daily minimum and maximum cysteamine mass delivery were achieved following our methods (Figure 17 and Figure 18).

The mechanism of release from our combined delivery system (SD-CMS/Gel) is based on diffusion from PLGA microspheres and extended in our pNIPAAm/PEG gel by potential molecular interactions of cysteamine ions between polymer-microsphere networks, attributed to a

change in LCST. The LCST property of pNIPAAm has been tailored to achieve different temperature ranges, with studies exploring the lowering effect on LCST by adding sodium salt ions following the Hofmeister series [161,162]. One study confirmed three mechanisms: surface tension effect, direct anion binding, and polarization of water molecules directly to hydrophobic portions of pNIPAAm (isopropyl groups and hydrocarbon backbone) [162]. In our zeta potential characterization of SD-CMS and SD-BLANK-CMS (Figure 15) we determined a difference in ZP magnitude at pH 4–10 between microspheres with cysteamine (SD-CMS) and cysteamine-free microspheres (SD-BLANK-CMS). When included into pNIPAAm/PEG gel, SD-CMS had a lowering effect on LCST (from base pNIPAAm gel 34 °C to 32 °C). The changes in ZP and lowered LCST may be attributed to the presence of cysteamine ions during the spray-dried fabrication process of cysteamine hydrochloride and PLGA. The inclusion of cysteamine ions and a potential increase in surface tension from SD-CMS into pNIPAAm is likely to delay the release of cysteamine as increased molecular interactions may occur through the microsphere polymer network. These experiments and our mechanistic insights represent the first cysteamine release kinetic profile from PLGA microspheres (Figure 17) and PLGA microspheres incorporated in thermoresponsive gels (Figure 18). Alone, SD-CMS release kinetics are similar to another spray-dried microsphere formulation [163]. While release occurs faster than what is typically noted in the literature for PLGA microspheres, [164] these results represent a 12-fold decrease in daily cysteamine eyedrop administration.

We further present the first long-term stability profile of encapsulated cysteamine in a direct comparison with traditional eyedrops using 1 H-NMR spectroscopy. This method is unique compared with other detection methods [107] because it can detect both cysteamine and cystamine. Further, our stability study took into account different storage conditions (4 °C and 25 °C), which

was not incorporated in other studies [107, 139]. We also performed repeated opening and closing as suggested by a study comparing cysteamine eyedrop stability under inert gas [165]. The stability profile for standard cysteamine eyedrops (Figure 19) demonstrates a temperature dependency of degradation behavior and a level below 95% after 1 week, as expected [47, 139]. A possible explanation for the poor aqueous stability of cysteamine is the pH influence of degradation into cystamine [139]. This study compared cysteamine stability in aqueous solutions at pH 7.4 and pH 4.0–4.2 and found that values of pH 7 oxidized more quickly due to the presence of ionized thiol groups. By encapsulating the drug, the influence of aqueous pH within the microspheres is minimized. We do, however, observe a temperature dependence of cysteamine degradation in microspheres, which is similar to previous studies [139]. Still, cysteamine entrapped within microspheres is stable for up to 5 and 7 weeks at 25 °C and 4 °C, respectively. This result represents a significant improvement over current storage methods, which greatly contribute to inconvenient shelf-life stability of current cysteamine eyedrops. These results further suggest that the cysteamine loaded in our microspheres is likely to release from the hydrogel delivery system to the cornea in its active form upon administration. Ongoing studies regarding the stability of cysteamine after gamma sterilization suggest a change in 3% cysteamine (N = 10) after storage, packaging under a nitrogen gas glove box, and shipping (Appendix A.2.5). Future studies will confirm the efficacy of stable cysteamine from ocular gel administration in a mouse model of cystinosis [166].

Confirmation of our target LCST via DSC (Figure 16) was performed and was comparable with previous LCST measurements of our gels administered in vivo [137, 138]. Our in vivo studies show the ease of administration, safety, and tolerability of our delivery system in a rabbit model (Figure 23) which is further supported in our previous studies [137, 138] for anti-glaucoma and

antimicrobial ocular drug delivery. As with previous testing of the gel eyedrop, irritation testing on models for conjunctiva (HET-CAM; Figure 20) and cornea (BCOP; Figure 21) showed negligible to mild irritation levels. This agrees well with previous reports for cysteamine [139, 159]. These data suggest that the irritation upon administration in patients may be partially due to the underlying disease which causes corneal sensitivity and corneal epithelial erosion. Hourly administration of traditional eyedrops containing the preservative benzalkonium chloride (BAK) is likely a major contributing factor to ocular irritation, which can be mitigated with our preservative-free delivery system using 1 drop versus 12 drops. These organotypic models, current in vivo studies, and previous long-term in vivo glaucoma study [138] support the potential use of our materials for cysteamine delivery as a non-irritating formulation. Repeated dosing and ocular pharmacokinetics will be investigated in future studies comparing our delivery system with cysteamine eyedrops in our large animal model. Data from previous human clinical trials [108, 109, 167] will guide our studies, which suggest no severe adverse effects (redness expanding 50% of the conjunctiva, pain affecting daily activities, and vision loss). We will focus on the local transient effects (stinging, burning, redness) observed in these studies that lasted less than 1 h from viscous gel formulations dependent on cysteamine concentration when administered 4 times daily in an open-label phase III 4-year study. Despite these local transient effects, patients expressed their preference for a 4 times daily formulation over an eyedrop after *a Comparisons of Ophthalmic Medications for Tolerability Questionnaire* [108, 109]. These studies will be of particular importance as there is currently limited knowledge regarding cysteamine absorption through the cornea.

The *in vitro* permeability studies presented herein demonstrated a trend of higher absorption after 5 h compared with standard drops. Pescina et al 2016 [139] demonstrated that

permeation enhancers were required to improve permeability compared with standard eyedrops, in contrast to our delivery system. The group further investigated pH dependence of cysteamine diffusion in aqueous formulations (without permeation enhancers) which resulted in a preference for higher permeation at pH 7.4 versus 4.2. This analysis offers an explanation for cysteamine permeation from our cysteamine delivery system, which has a pH 8.6 prior to thermal transition, compared with cysteamine eyedrops (pH 4.2). We aimed to limit variability in our samples by assessing the quality of corneas upon excision and using commercially manufactured Franz diffusion cells; however, validation studies on static Franz cells have indicated inadequate mixing in the side arm as influences to variability during sampling from receptor volumes [168], which may have contributed to our permeation variability. Overall, these data suggest that cysteamine is likely to be absorbed to the cornea upon administration and tolerated similar to alkaline hypromellose 0.3% lubricant eyedrops (pH 8.34) [169] for chronic dry eye, [170], which will be furthered explored in the aforementioned planned in vivo studies with improved tissue cysteamine detection via mass spec [171].

3.0 Specific Aim 2

3.1 Introduction

Investigation of drug delivery systems in animal models is a key component to developing therapeutics. These studies may be designed to inform the safety profile and efficacy of the delivery system, which informs the development of novel therapeutics towards clinical translation. In ocular drug delivery, topically applied drug delivery systems are commonly investigated when administered on the ocular surface or pre-corneal conjunctival cul-de-sac space [172] of animal models. The most common animal models for these type of studies are leporine (i.e., rabbits) [173] in addition to murine (i.e., rats and mice) [174], and non-human primates [175]. A goal of these studies is to observe the pharmacokinetic profile and biodistribution of the drug to ocular tissues and systemic organs. In general, studies are conducted on diseased models to also observe efficacy. However, if a disease model is not feasible – whether through genetic modification or experimental manipulation – healthy models can be justified. In the case of inherited rare diseases, genetic knockout models in smaller species are more common than in larger animals. This is highlighted in the field of cystinosis with only two established models including the C57BL/6 *CTNS* (-/-) mouse [166, 176] and *CTNS* (-/-) zebrafish [177]. A recent CTNS (-/-) rat model, still in peer-review, has been developed with CRSIP/Cas9-mediated gene editing a [178]. Due to the small mouse size and challenges with testing pharmacokinetics in aquatic environments, a health rabbit model would be the likely candidate for providing ocular pharmacokinetic insights towards clinical translation.

The New Zealand White and Dutch-Belted rabbit strains exhibit similarities in anatomy and physiology to humans. Shared similarities include corneal thickness, corneal surface area, and lacrimal volumes [172,173, 179]. One major difference between rabbits and humans is the presence of the nictitating membrane, a third-eyelid that is drawn laterally over the rabbit eye. The nictitating membrane is composed of conjunctival tissue that can act as a compartment for drug absorption, particularly for hydrophilic drugs [180]. Many studies overcome this difference by excising the nictitating membrane with minimally invasive surgery [181]. Removal of the membrane thus reduces the number of anatomical components where drug can reside and achieves a model closer to clinical translation for humans.

After surgical manipulation, eyes of a rabbit can be divided into two main components: ocular and systemic. The ocular components are separated by different ocular tissues and includes the pre-corneal area (i.e., tear-film), cornea, sclera, aqueous humor, trabecular meshwork, lens, vitreous humor, and retina [172]. The anterior portions are largely avascular with exception of the blood-aqueous barrier that has a supply of blood vessels in the iris of the eye; however, anterior chamber blood supply is considerably small compared to the posterior segment blood supply (e.g. blood-retinal barrier). Systemic components incorporate the conjunctival sac, or lower eyelid, and the nasal-lacrimal drainage ducts – which drain excess tears to the nasal and lymphatic system. Conjunctival blood vessels and the lymphatic system may lead to systemic drug uptake and potential side effects [182, 183]. Therefore, it is particularly important to sample blood plasma immediately prior to euthanatizing for drug quantification. By doing so, blood plasma is thus likely to serve as a proxy for overall systemic drug adsorption. In general, topical administration of aqueous solutions results in 50% drug loss in the precorneal area [172]. Typically 5% [184] of drug permeation to the cornea or sclera may occur based on the drug molecules properties

including size and hydrophilicity. The low bioavailability of topical eyedrops and multiple components in the eye make ocular pharmacokinetic studies challenging and are often performed within a time frame of less than 1 hour. It is particularly important that upon euthanizing that whole eyes are enucleated, frozen, and dissected to prevent drug transport in between components. Because there are many challenges to ocular pharmacokinetic studies, therapies for lesser-known diseases, like cystinosis, have little to no *in vivo* pharmacokinetic data.

Currently, both FDA-approved cysteamine eyedrops for cystinosis patients (e.g. Cystaran ™ and Cystadrops®) were approved following human clinical trials on the efficacy of reducing cystine crystals from the cornea. There were no previous *in vivo* ocular pharmacokinetic or biodistribution studies conducted for approval; likely due to efficacy studies on CTNS (-/-) knockout mice indicating drug adsorption to the cornea after confirmation of reduction of corneal cystine crystals. Furthermore, it is highly unfeasible to harvest ocular tissues in humans; sampling aqueous humor and vitreous humor requires costly and invasive procedures. Blood collection during clinical trials may have provided insight to the systemic absorption of cysteamine eyedrops, however many of these patients in the clinical trials were supplemented with a higher dose of orally administrated cysteamine [108, 109]. Thus, any blood-plasma concentrations determined would have likely been delivered from oral formulations and not eyedrops. While there is a large gap in ocular pharmacokinetic data for cysteamine eyedrops, the clinical trials reinforced their studies with patient experience and eyedrop tolerability surveys.

At instillation of Cystaran™, patients experienced transient adverse effects lasting up to an hour which included redness, stinging, and burning [47]. In addition to these transient adverse effects, when patients received Cystadrops ® some experienced sticky eyes and eyelashes as reported in open-label comparative phase III clinical trials [109]. Regardless of adverse effects,

patients were appreciative of a gel formulation that reduced the dosing frequency of traditional cysteamine eyedrops from 6-12 drops per day to 4 drops per day. As such, exploring the adverse effects of cysteamine eyedrop formulations upon instillation in an *in vivo* rabbit model would further contribute to the clinical translation to cystinosis patients. This can be accomplished by conducting *in vitro* and *ex vivo* ocular irritation studies to select a candidate formulation and then, evaluate candidate formulations in rabbits with the Draize eye test [185] and rabbit grimace pain scales [186].

3.2 Materials and Methods

3.2.1 Ophthalmic Animal Model and Timeline

Animal subjects were utilized for this research following the Association for Research in Vision and Ophthalmology (ARVO) Statement for the Use of Animals in Ophthalmic and Vision Research and was approved by the University of Pittsburgh Institutional Animal Care and Use Committee New Zealand white rabbits (0.95–1.4 kg) were purchased from Envigo (Somerset, NJ, USA). Prior to experiments, the nictitating membrane of the right eye (OD) of each subject was resected according to previous published methods [2, 137, 138]. Briefly, under systemic anesthesia (10 mg/kg of ketamine (Ketathesia; Henry Schein Animal Health, Dublin, OH, USA) and 1 mg/kg of xylazine (AnaSed Injection; Lloyd Laborato ries, Shenandoah, IA, USA)), one topical eyedrop of 0.5% proparacaine (Baush+Lomb, Bridgewater, NJ, USA) was administered to the ocular surface. Then, the nictitating membrane was surgically removed with a scalpel and cauterized. Following the procedure, one topical eyedrop of 0.3% tobramycin (Bausch+Lomb, Bridgewater,

NJ, USA), and one topical eyedrop 1% prednisolone acetate (Pacifc Pharmaceticals INC, Rancho Cucamonga, CA, USA) was immediately administered and repeated once daily for the following 4 days to prevent infection and limit inflammation. The eyes of rabbits were examined using slit-lamp photography (Eyephotodoc, Fullerton, CA, USA) throughout the study. After 7 days, baseline photography and baseline intraocular pressure (IOP) measured with tonometry (Tonovet Plus, Icare, Finland) were captured. An instillation safety study was carried out prior to PK and BD timepoints. For PK and BD, four timepoints (2 hr, 6 hr, 12 hr, 24 hr) consisting of two groups, one receiving 0.44% cysteamine eyedrops per hour (N = 3 per timepoint) and another group receiveing one dose of SD-CMS/Gel (N = 3 per timepoint) was conducted. A timeline of our study design and sample size is listed in Figure 24.

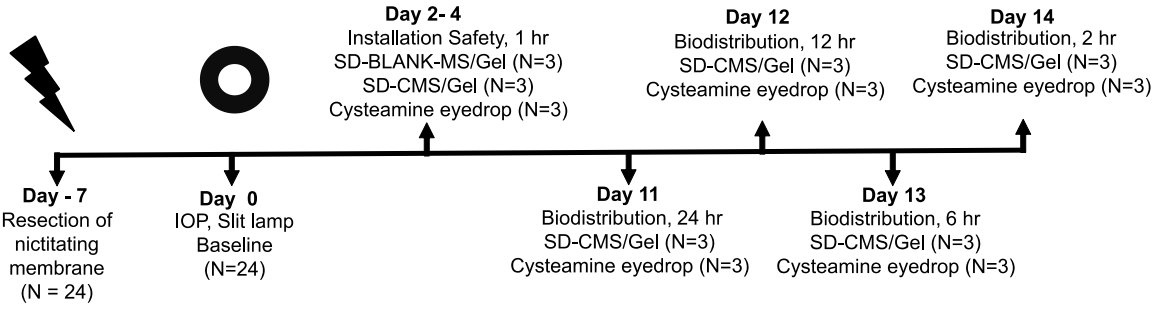

Figure 24 *In vivo* timeline for pharmacokinetic and biodistribution study

3.2.2 Cysteamine Formulations and Material Characterization

Cysteamine eyedrops were fabricated according to Cystaran™ product insert [157] by mixing cysteamine hydrochloride (66 mg) in 15 mL deionized water with 0.01% benzalkonium chloride (1.5 mg) and 0.90% sodium chloride (135 mg). A pH of 4.0 – 4.5 was achieved by titrating 0.1 N hydrochloric acid and 0.1 N sodium hydroxide, approximately 10 µL at a time. The

cysteamine solution was aliquoted into 1 mL volumes in 2.5 mL amber vials and bubbled with nitrogen gas in a glovebox (Fischer Scientific). Samples were stored frozen at -20°C and wrapped in parafilm until use – any unused cysteamine solution was immediately discarded within 24 hours of unsealing. For eyedrop instillation studies, a control of 0.9% saline solution was fabricated by dissolving 9 g of sodium chloride in 1000 mL of milliQ water.

The cysteamine microspheres in gel, SD-CMS/Gel, was fabricated according to our previous studies [2]. Briefly, 2 g of cysteamine hydrochloride and 8g of poly(DL-lactide-co-glycolide) (IV 0.14–0.22 dl/g, Mw: 4000–15,000) (Evonik Maryland, USA) in a cosolvent consisting of a methanol:dichloromethane (10:90,v/v) solution was mixed and fed to a mini spray dryer (Büchi, New Castle, Delaware, USA). Cysteamine free microspheres (SD-BLANK-CMS) were produced using the same fabrication process without the addition of cysteamine hydrochloride. The pNIPAAm based gel was fabricated using free radical polymerization with the addition of PEG 200 kDa. Suspensions of SD-CMS/Gel and SD-BLANK-MS/Gel were fabricated by mixing 10 mg of SD-CMS to 100 µL of Gel. All SD-CMS/Gel and SD-BLANK-MS/Gel suspensions were prepared by sterilizing respective microspheres with UV irradiation immediately before administration to subjects. For the present study, scanning electron microscopy (SEM) was utilized to obtain images of SD-CMS/Gel prior to administration (0 hours) and after administration (24 hours) of the delivery system. Samples were processed by freeze drying in a 1 mL syringe under liquid nitrogen. After drying, a razor blade was used to cut cross-sections. Cross sections were mounted on stubs with mounting tape and gold sputtered prior SEM imaging.

3.2.3 Eyedrop Installation Safety and Adverse Effects Testing

Semiquantitative Draize eye test scores [187] and rabbit grimace scores [186] were used to evaluate possible adverse effects at instillation. Subjects were randomly organized into three groups, where each group received one dose of a given formulation: 50 µL 0.9% saline solution (N=3), 50 µL of a cysteamine eyedrop (N =3), 10mg:100 µL of SD-BLANK-CMS/Gel (N=3) or 10mg:100 µL of SD-CMS/Gel (N=3). Rabbits were restrained (no anesthesia given) using the towel wrapped "bunny burrito" method [188] and given the specific eyedrop formulation. Slit lamp images were captured at the following timepoints 0 mins, 0.5 mins, 1 min, 5 min, 10 min, 15 min, 30 min, and 1 hour (Figure 25). Images were stored in a private server and identified by the research team. Then, images were de-identified and scored (single blind) by a clinical collaborator. Draize eye test scores included scoring for opacity in the cornea (0,1,2,3,4), iris hemorrhage (0,1,2) Conjunctiva redness (0, 1, 2, 3), and chemosis (i.e., swelling, 0, 1, 2, 3, 4) [187]. The rabbit grimace scores for orbital tightening as indicated by closure of the eyelid was scored at the following levels: not present (0), moderately present (1), and obviously present (2) [186].

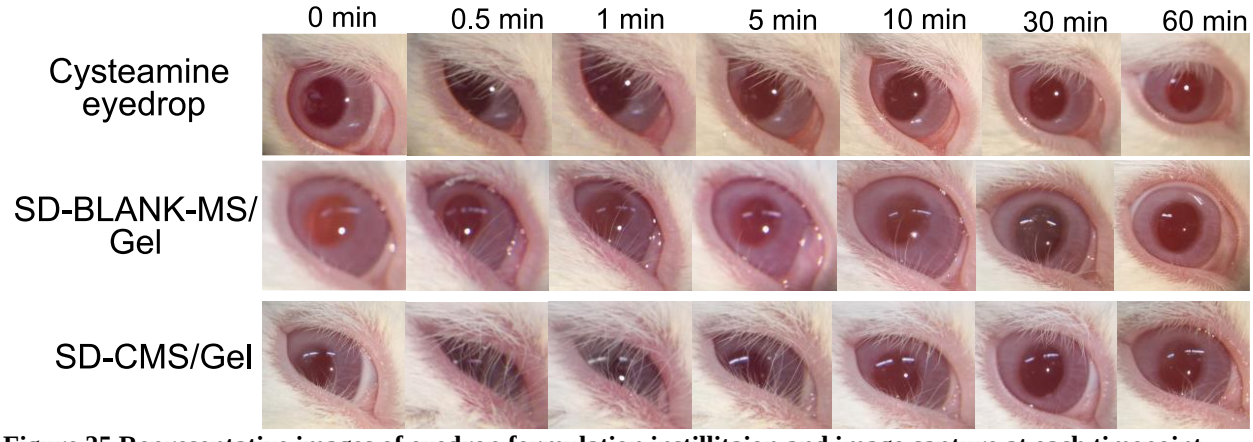

Figure 25 Representative images of eyedrop formulation instillitaion and image capture at each timepoint.

3.2.4 Treatment Timepoints, Ocular Tissue Collection, and Histology

Rabbits were randomly assigned into one of two groups based on treatment formulations. Each time point (2 hr, 6 hr, 12 hr, 24 hr) consisted of one group receiving 0.44% cysteamine eyedrops (N = 3, total 12 rabbits) and one group receiving SD-CMS/Gel (N = 3, total 12 rabbits). Each treatment group was run in parallel for each timepoint where the cysteamine eyedrops received one drop per hour (e.g. 2 hr received 2 eyedrops on the hour). For the cysteamine eyedrop group, the last dose was given at 12 hr for the 24 hr timepoint to simulate the recommended dosing frequency in patients. The SD-CMS/Gel group received a single dose for each timepoint. At each predetermined timepoint, the groups were staggered for sparse sampling of 1 mL of whole blood placed into heparinized glass tubes. Then, a lethal dose of ketamine/xylazine was administered via marginal ear vein. Immediately after, both whole eye globes were enucleated from subjects and immediately placed on dry ice. While frozen, the cornea was excised to access aqueous humor and vitreous humor. These fluids were distinguishable visually with reference to the lens and trabecular meshwork where the aqueous humor is anteriorly and vitreous humor resides posteriorly of these structures. Additionally, at sacrifice, eyelid tissue from both eyes were shaved and exenterated using iris scissors. Tissue samples were washed in PBS pH 7.4 for 1 hour. Then, eyelid tissues were placed in 10% formalin and fixed for 48 hours at 4°C then stored in a holding solution composed of 70% ethanol at 4°C for 1 week. Samples were embedded in paraffin. Cross sections of the eyelid (stood up on its side to observe layers of eyelid skin) were stained with hemoxylin and eosin (H&E) and Verhoeff Van Gieson (VVG). Paraffin histology was performed by the Histology Core Facility at the McGowan Institute for Regenerative Medicine. Stained sections were imaged with light microscopy (Echo A Bico Company, San Diego, CA). Images were

digitally archived and scored by a clinical ophthalmologist. Any morphological changes were observed and recorded.

3.2.5 Plasma, Aqueous Humor, and Vitreous Humor Cysteamine Measurement with Mass Spectrometry

To 80 µL of whole blood, 20 µL of 150 mM NEM in deionized water was immediately added and mixed. The reaction was performed at room temperature for 30 min. Then, samples were stored at -80 °C until cysteamine extraction for mass spectrometry. For aqueous humor and vitreous humor, 80 µL of each was treated similarly by adding NEM and reacting for 30 min and storing at -80 °C. Upon extraction for mass spec, samples were thawed and extracted with 800 µL of cold (-20 °C) extraction solution of 90% acetonitrile/1% formic acid containing an internal standard of a stable isotope consisting of 1µM NEM-d4-cysteamine, (d4-cysteamine HCL purchased from CDN Isotopes, Pointe-Claire, Quebec, CA). Samples were centrifuged at 4 °C at 16kg. The supernatant was collected and placed into a new microtube and stored at - 80 °C. Samples were shipped on dry ice and sent to Clarus Analytical LLC (San Diego, CA) for LC-MS/MS. Briefly, NEM labeled cysteamine in samples were quantified by LC-MS/MS. All endogenous levels were normalized to the stable isotope (NEM-d4-cysteamine). Area ratios were back calculated to an 8-point calibration curve for determining moles of cysteamine. Low and high quality control samples were run along sample batches to verify <15% error in accuracy and < 15% coefficient of variation. Values lower than 15 nM were considered below limit of quantification.

3.2.6 Corneal Tissue Cysteamine Measurement with Mass Spectrometry

Flash frozen corneal tissue was excised from the globe of harvested eyes. Corneal tissue was cryopulverized in liquid nitrogen with a stain-less steel pulverizer (BioSpec Products, Inc. Bartlesville, OK, USA). Corneal powder from cryopulverization was weighed into 10mg-25mg aliquots and placed into cold, pre-weighed microtubes. To tissue aliquot, 200 µL of 30 mM NEM in deionized water was added and mixed. The reaction was performed at room temperature for 30 min. Then, samples were stored at -80 °C until cysteamine extraction for mass spectrometry. For extraction, thawed samples received 1 mL of cold (-20 °C) extraction solution composed of 95% acetonitrile/1% formic acid containing an internal standard of 1µM NEM-d4-cysteamine, (d4-cysteamine HCL purchased from CDN Isotopes, Pointe-Claire, Quebec, CA). Samples were then placed into lysing matrices containing garnet beads and homogenized in a cold room (approximately 4 °C) using a FastPrep 24 homogenizer (MP Biomedicals, Solon, Ohio, USA). Homogenized samples were placed at -20 °C for 1 hr. Then, samples were centrifuged at 4 °C at 16kg. The supernatant was collected and placed into a new microtube and stored at -80 °C. Cysteamine levels were analyzed as indicated by the aforementioned mass spectrometry methods and normalized based on the corneal mass prior to cryopulverization.

3.2.7 Statistical Analysis

The means and standard deviations of N=3 samples for intraocular pressure (IOP), rabbit grimace scores, and Draize eye scores were reported. For the IOP of rabbits, a one-way, repeated measures ANOVA and a Tukey's Multiple Comparison test was performed to compare each timepoint between the treatment groups (four treatments). For rabbit grimace testing, a Man

Whitney U test was performed to compare clinical scores between four treatment groups. The concentration of cysteamine in tissues and fluids was analyzed with a Kruskal-Wallis one-way ANOVA and a Mann Whitney U post testt to compare each timepoint between treatment groups. All statistical analyses were performed using Minitab software (State College, PA).

3.3 Results

3.3.1 *In Vivo* Characterization of SD-CMS/Gel Formulation

SD-CMS/Gel samples were freeze-dried, sectioned, gold sputtered and imaged with SEM to verify the morphology and presence of microspheres within gel prior to topical administration (Figure 26A) and 24 hours after administration and retention *in vivo* (Figure 26B). The spray-dried microspheres aggregate prior to instillation *in vivo* which was anticipated from previous in vitro studies [2].

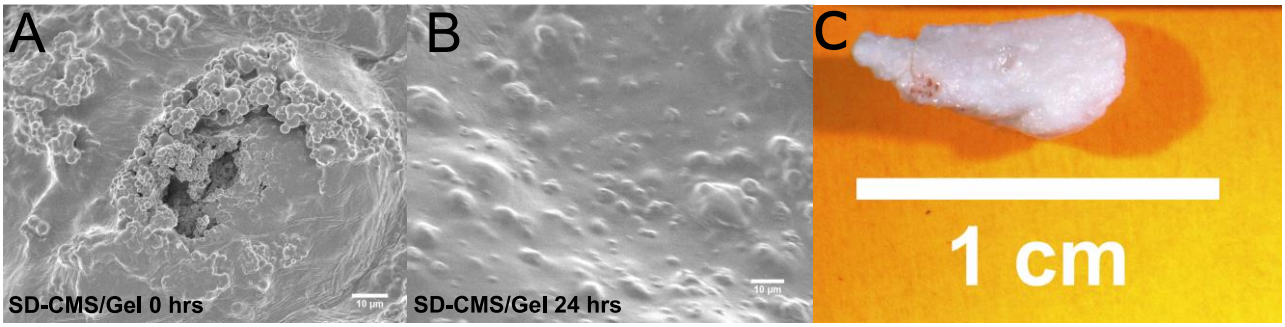

Figure 26 Representive scanning electron microscopy images of A.) SD-CMS/Gel prior to adminstration and B.) 24 hours after in vivo adminstration. The SD-CMS/Gel was recovered after 24 hours and freeze-dried (C)

3.3.2 Eyedrop Instillation Tolerability

Four treatment groups: 0.9% saline, 0.44% cysteamine eyedrops, SD-BLANK-MS/Gel, and SD-CMS/Gel were administered to the right eye of subjects and their images recorded at specific time points. Images for each timepoint were scored by an ophthalmologist for rabbit grimace scores (RGS) at the following levels: 0 - discomfort not present, 1 - moderately present, 2 - obviously present. There were no statistically significant differences between the treatment groups at any given timepoint. Baseline scores (time = 0 min) for each treatment was captured to obtain a reference point for potential discomfort of the subject during anesthesia-free restraint. In addition to baseline scores, a negative control of saline provided a reference of any discomfort of administration of a well-tolerated aqueous solution. The saline group maintained an average RGS below 1 between 0.5 mins to 5 mins (Figure27A RGS 0.333 ± 0.58). For the cysteamine eyedrop formulations, there was discomfort between 0.5 mins (Figure 27B – cysteamine eyedrops, Figure 27C – SD-CMS/Gel, Figure 27D – SD-BLANK-MS/Gel) with average RGS 1-1.33 ± 0.58. After 10 mins, average rabbit grimace scores returned to respective baselines (time = 0 min), which indicates a trend of discomfort during instillation and a transient effect of administration.

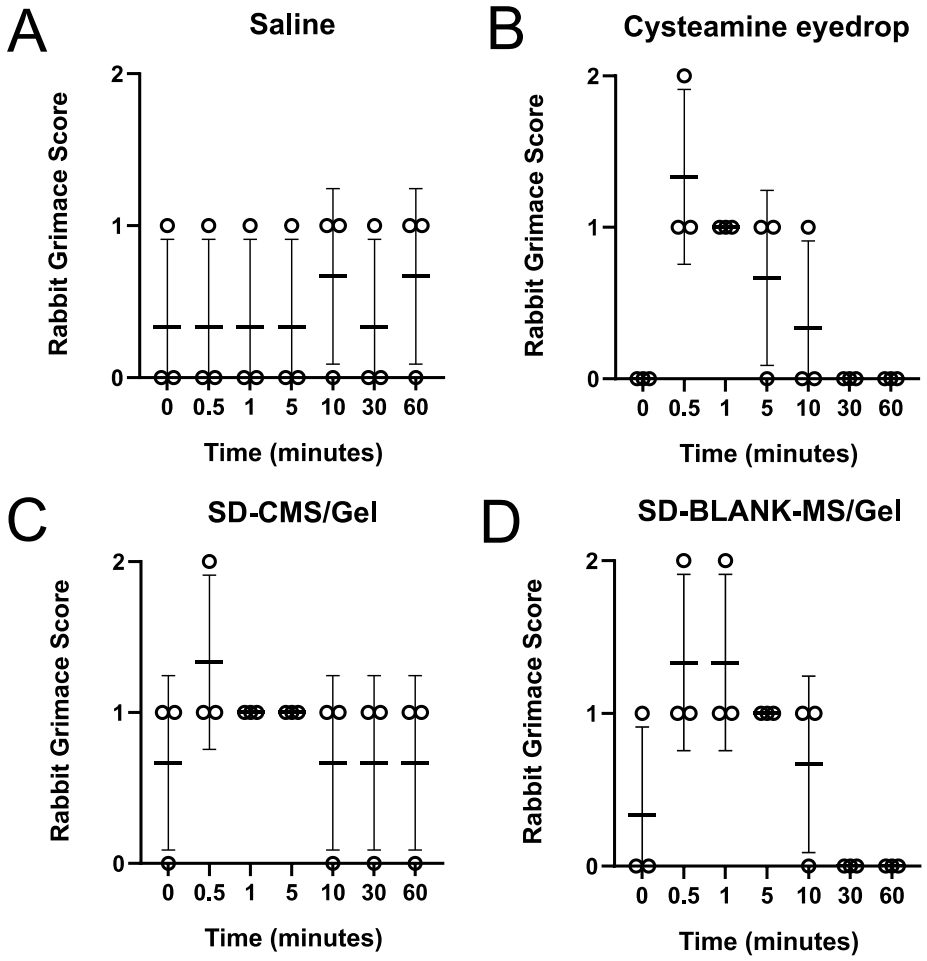

Figure 27 Rabbit grimace scores of A.) 0.9% saline, B.) 0.44% cysteamine eyedrop, C). SD-CMS/Gel and D). SD-BLANK-MS/Gel. The data are represented as mean ± standard deviation for N=3 subjects.

The images were also scored for the Draize eye test which summarized in Table 4. Scores for cornea and iris were statistically tested and resulted in no statistical differences between treatments at a given timepoint. Draize eye test for cornea indicated no ulceration or opacity (score of 0) and normal iris (score of 0) for all treatments and any given timepoint. Scores for conjunctiva and chemosis were not statistically tested as the ophthalmologist indicated difficulty in scoring a few images due to eyelid closure (indicated as not scorable). For the SD-CMS/Gel, SD-BLANK-MS/Gel and cysteamine eyedrop images that were scored, conjunctival scores were between 0

(normal) to 1 (some blood vessels hyperaemic) for conjunctiva and chemosis scores were between 0 (normal) to 1 (some swelling of the eyelids above normal). These scores were all below 1 at 60 mins after administration.

Table 4 Driaze Eye test scoring of treatments. The data are represented as mean ± standard deviation for N = 3 subjects

Treatment	SD-CMS/Gel				SD-Blank-CMS/Gel			
Time (min)	Cornea (Score)	Iris (Score)	Conjunctiva (Score)	Chemosis (Score)	Cornea (Score)	Iris (Score)	Conjunctiva (Score)	Chemosis (Score)
0	0 ± 0	0 ± 0	0 ± 0	0 ± 0	0 ± 0	0 ± 0	Not scorable	Not scorable
0.5	0 ± 0	0 ± 0	Not scorable	Not scorable	0 ± 0	0 ± 0	Not scorable	Not scorable
1	0 ± 0	0 ± 0	Not scorable	0 ± 0	0 ± 0	0 ± 0	Not scorable	Not scorable
5	0 ± 0	0 ± 0	Not scorable	0.5 ± 0.71	0 ± 0	0 ± 0	0.67 ± 0.58	Not scorable
10	0 ± 0	0 ± 0	Not scorable	0.33 ± 0.58	0 ± 0	0 ± 0	Not scorable	0.33 ± 0.58
30	0 ± 0	0 ± 0	0 ± 0	0 ± 0	0 ± 0	0 ± 0	0 ± 0	0.67 ± 0.58
60	0 ± 0	0 ± 0	0 ± 0	0 ± 0	0 ± 0	0 ± 0	0.33 ± 0.58	0.33 ± 0.58
Treatment	**Cysteamine eyedrop**				**Saline**			
Time (min)	**Cornea (Score)**	**Iris (Score)**	**Conjunctiva (Score)**	**Chemosis (Score)**	**Cornea (Score)**	**Iris (Score)**	**Conjunctiva (Score)**	**Chemosis (Score)**
0	0 ± 0	0 ± 0	0.33 ± 0.58	0.33 ± 0.58	0 ± 0	0 ± 0	0 ± 0	0 ± 0
0.5	0 ± 0	0 ± 0	Not scorable	Not scorable	0 ± 0	0 ± 0	0 ± 0	0 ± 0
1	0 ± 0	0 ± 0	Not scorable	0 ± 0	0 ± 0	0 ± 0	0 ± 0	0.33 ± 0.58
5	0 ± 0	0 ± 0	1 ± 0	0.67 ± 0.58	0 ± 0	0 ± 0	0 ± 0	0 ± 0
10	0 ± 0	0 ± 0	0 ± 0.58	0 ± 0	0 ± 0	0 ± 0	0.33 ± 0.58	0.33 ± 0.58
30	0 ± 0	0 ± 0	Not scorable	0.33 ± 0.58	0 ± 0	0 ± 0	0 ± 0	0 ± 0
60	0 ± 0	0 ± 0	0.33 ± 0.58	0.33 ± 0.58	0 ± 0	0 ± 0	Not scorable	0 ± 0

3.3.3 Intraocular Pressure Monitoring

The treated eyes (OD) and untreated contralateral eye (OS) of rabbits were measured for IOP over respective treatment time courses (Figure 28A – 2 hours, Figure 28B – 6 hours, Figure 28C – 12 hours, and Figure 28D -24 hours). For all eyes, a baseline IOP measurement indicated by time 0 hours was captured. Then, after treatment with each formulation and dosage in the right eye, IOP was measure for all eyes. Statistical analysis of each eye within timepoints resulted in no statistical significance – suggesting the mean IOP values of each eye were similar. At any given timepoint, all eyes, whether treated or untreated were within normal ranges (15-23 mmHg).

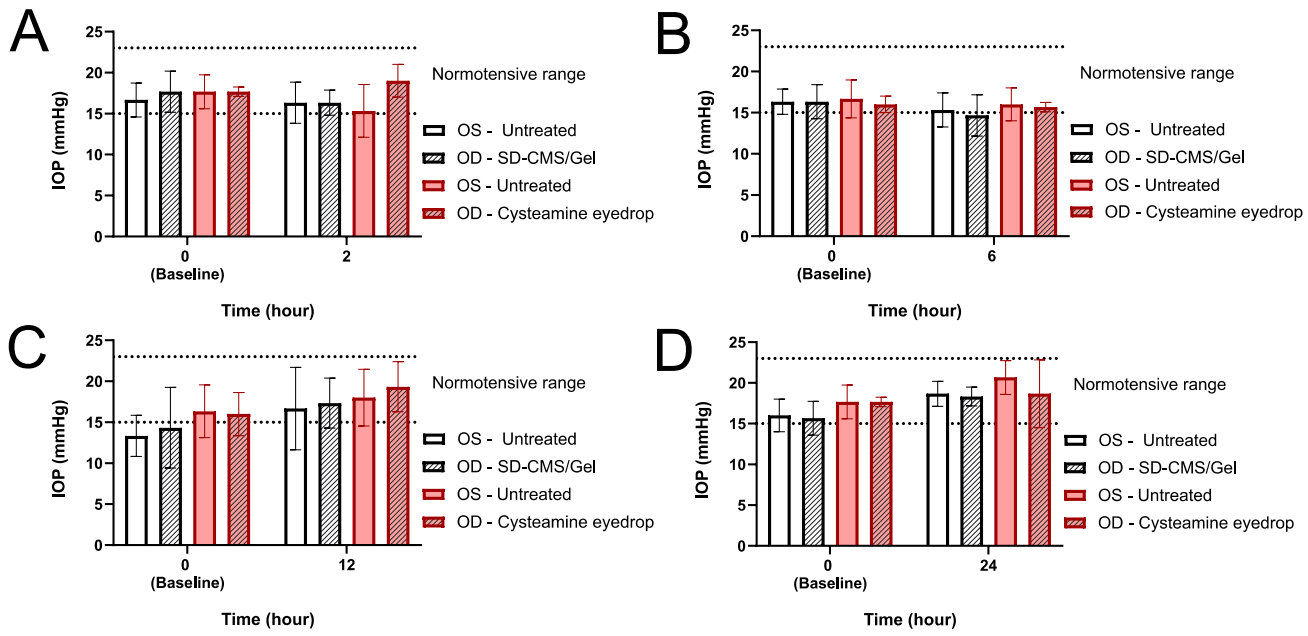

Figure 28. Intraocular pressure of treatment eyes (OD) and untreated contraleteral eye (OS) at A.) 2 hours, B.) 6 hours, C.)12 hours, and D.) 24 hours. The data are represented as mean ± standard deviation for N=3 subjects.

3.3.4 Histopathology of Eyelids

Tissue samples from all timepoints (2, 6, 12, 24 hours) were recovered and the 24 hour timepoint was selected to represent overall physiology and structural changes in Figure 27. Untreated eyelid (Figure 29A) H&E staining represent normal physiological and anatomical structures, such as an intact surface epithelium on the conjunctival side of the section – which is indicated by an asterisk (*). VVG staining of untreated eyes (Figure 29B) suggest no effect on collagen or elastin (stained red). Cysteamine eyedrops (Figure 29C-D) and SD-CMS/Gel (Figure 29E-F) are comparable to untreated eyes.

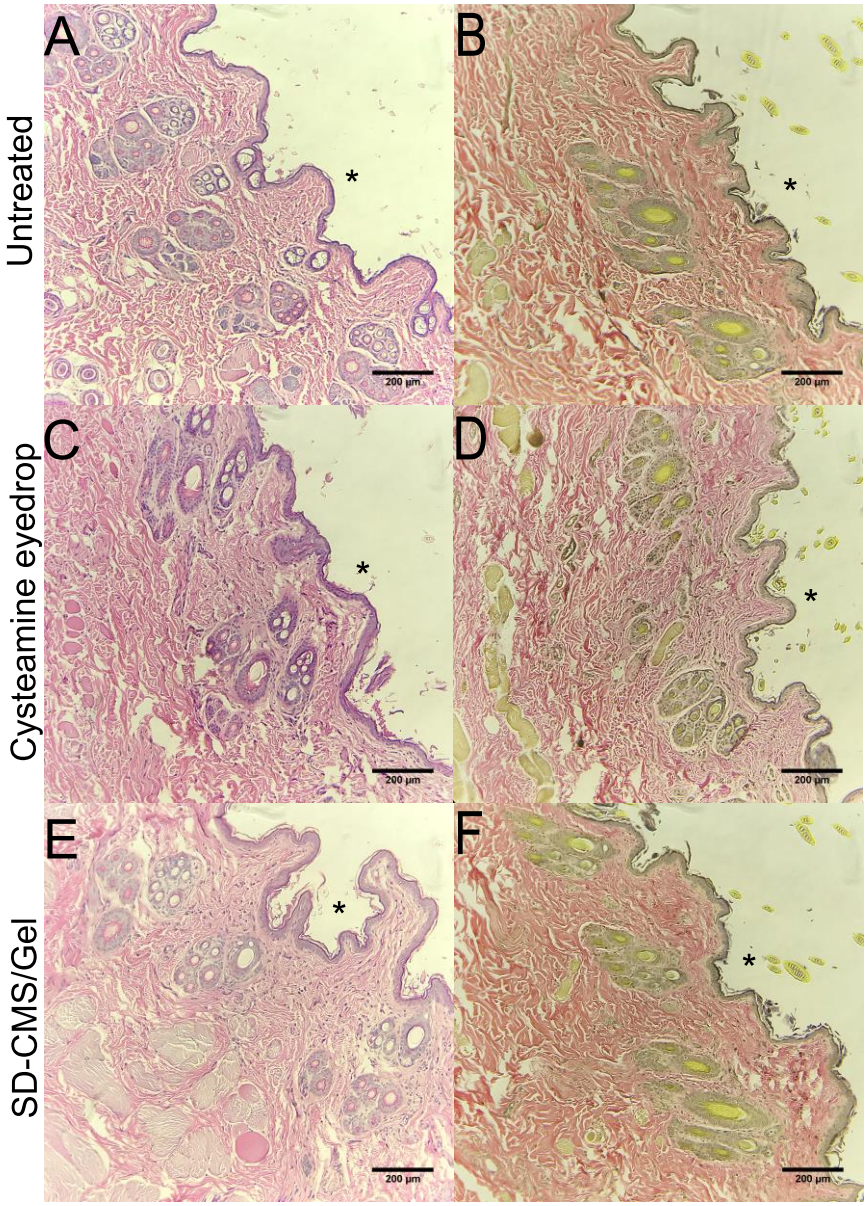

Figure 29 Hematoxylin and eosin (H&E) and Verheoff Van Gieson (VVG) staining of eyelids of untreated eyes (A. H&E, B. VVG), cysteamine eyedrops (C. H&E, D. VVG), and SD-CMS/Gel (E. H&E, F. VVG). Histologoly captures treatement after 24 hours. An asterisk (*) indicates the conjunctival side of the eyelid. Scale bar 200 µm.

3.3.5 Cysteamine Concentration in Ocular Tissues and Plasma

Cysteamine was topically delivered to the right eyes of rabbits at a frequency of administration of 12 hourly drops for cysteamine eyedrops and one drop of SD-CMS/Gel. For example, at 6 hours the cysteamine treated eye would receive 6 hourly drops and the SD- CMS/Gel would receive one drop at time 0 mins for the entire 6 hr time course. The contralateral eye was treated as independent for each timepoint. After serial sacrifice and tissue harvesting, cysteamine was extracted from corneas (Figure 30A) and normalized to the weight of corneal tissue (e.g milligram). Cysteamine in fluid samples were also quantified in aqueous humor (Figure 30B), vitreous humor (Figure 30C) and plasma (Figure 31). Several samples were below the limit of detection (< 15 nM) and were considered as a value of zero for plotting and statistical purposes. Statistical analysis indicated no statistical significance for ocular tissues and plasma mean values at any given timepoint. Based on descriptive statistics, cysteamine eyedrops presented a 3-fold magnitude higher cysteamine tissue concentration (pmol/mg) (e.g. 2 hr 66.93± 27.12, 6 hr 57.96 ± 25.45) than SD-CMS/Gel (2 hr 20.57 ± 11.15, 6 hrs 29.48 ± 10.72). After receiving 12 doses, cysteamine eyedrops at 12 hours was 5-fold higher than SD-CMS/Gel. Cysteamine was detected in the aqueous humor of treated eyes and follows a similar trend to corneal tissue – however, there was higher variability between samples in the cysteamine eyedrop treated eyes than SD-CMS/Gel treated eyes. Vitreous humor cysteamine concentrations were detected in all eyes, including the contralateral eye of subjects treated with cysteamine eyedrops and SD-CMS/Gel. Cysteamine was detected in plasma after 6 hours of treatment (cysteamine eyedrops- 23.55 ± 40.79 nM, SD-CMS/Gel 8.82 ± 15.28 nM) and had cysteamine concentrations below the limit of detection after 24 hours.

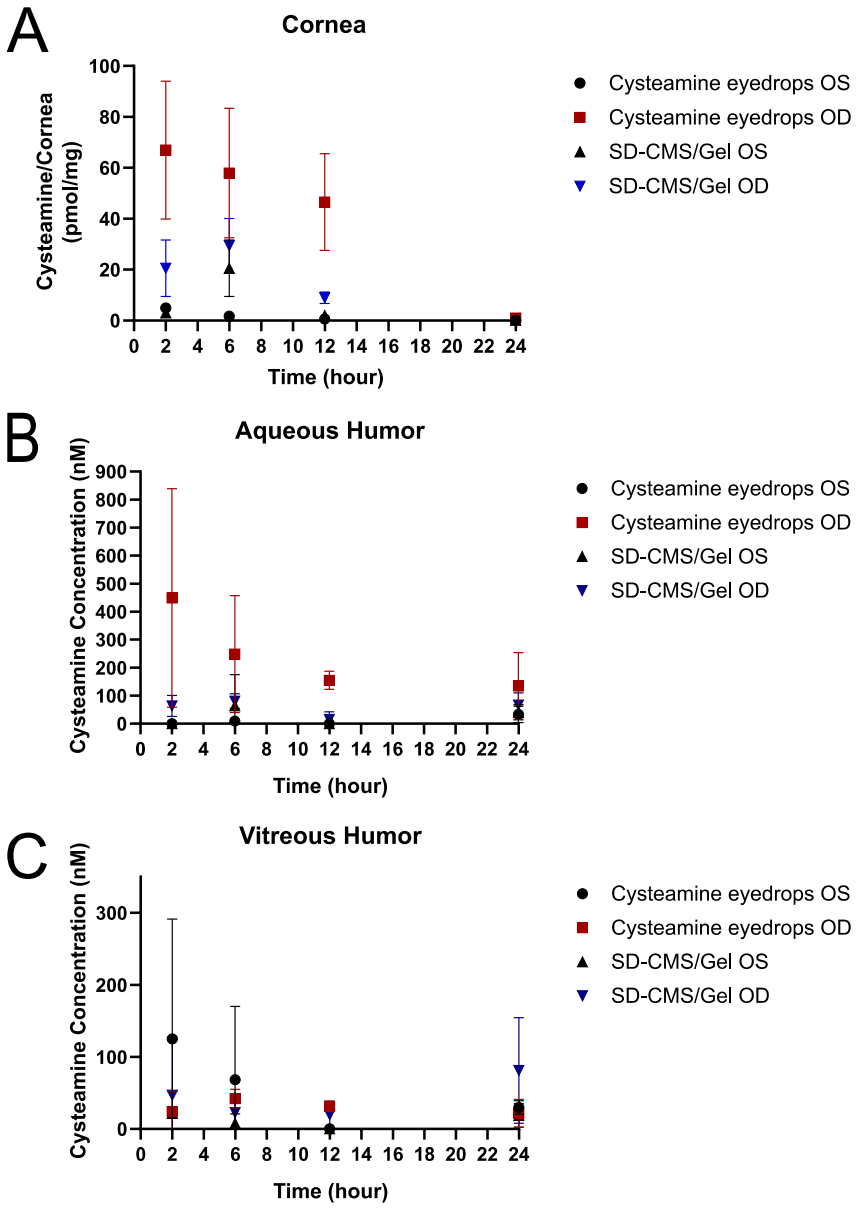

Figure 30 Cysteamine quantified in A.) corneal tissue and normalized based on tissue weight (pmol/mg) and B.) aqueous humor connentration (nM) and C.) vitreous humor concentration (nM). The data are represented as mean ± standard deviation for N = 3 per timepoint. The left eye (OS) are untreated contraletral eyes to the treated (OD) eyes and are categorized by respective eyedrop formulations.

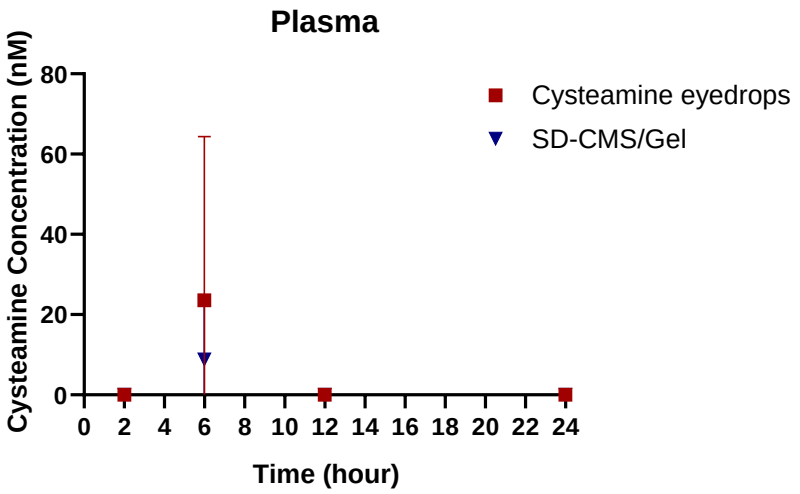

Figure 31 Systemic uptake of cysteamine in plasma after ocular administration of cysteamine eyedrops and SD-CMS/Gel

3.4 Discussion

The frequency of administration and concentration of cysteamine in ophthalmic solutions originates from clinical trials conducted in the EU with data that contributed to the FDA approval of Cystaran™ in the U.S. The exact therapeutic concentration of cysteamine in plasma and ocular tissues, specifically the cornea, has yet to be determined. Many of these formulations were not tested in large animal studies and their pharmacokinetic data after topical administration to the eyes was not studied. However, clinical trials on the efficacy of cysteamine hydrochloride (HCL) drops conducted titration studies with several cysteamine concentrations and evaluated cystine crystal clearance in humans. For example, a double-blind randomized placebo-controlled study

tested 0.1% and 0.5% cysteamine HCL at 1 drop per hour during waking hours [141]. Other clinical trials tested the addition of excipients, such as 0.02% disodium edetate in 0.2% cysteamine HCL at 6 times per day [142] and another tested 0.01% benzalkonium chloride (BAK) in 0.5% cysteamine once hourly during waking hours [189]. A combination of increased cysteamine HCL concentration at 0.55% with excipients consisting of 0.01% BAK was compared to 0.55% cysteamine HCL with 1.85% monosodium phosphate, 0.1% disodium Ethylenediaminetetraacetic acid , and 0.01 % BAK administered once hourly during waking hours [167]. The 0.55% cysteamine HCL (EU approved) since became the widely accepted concentration of drug to treat corneal cystine crystals. To add to the complexity of varying concentrations of cysteamine HCL and excipients, the FDA approval of 0.44% cysteamine HCL eyedrops (Cystaran™), which is equivalent to 0.55% cysteamine HCL, reports a different concentration due to labeling practices with the 0.55% cysteamine HCL accounting for the moisture content of the HCL [47]. Recently, the FDA-approval of a viscous formulation, Cystadrops®, contains 0.37% cysteamine HCl and prescribed at 4 times per day [190, 191]. This formulation suggests that a lower cysteamine concentration with reduced frequency of administration may be obtained if the formulation resides on the ocular surface longer than aqueous solutions. Despite these remarkable advances, the stability of cysteamine at 1-week in Cystaran ™ and Cystadrops® continues to be a detriment to treatment for patients with the burden of a rare disease and additional systemic therapies. To address these limitations, our group developed a controlled release eyedrop and encapsulated cysteamine into PLGA microspheres and embedded within a thermoresponive gel for sustained release behavior *in vitro* for 24 hours [2]. The studies within this chapter translates our technology to a preclinical model using New Zealand white rabbits and seeks to provide insight to the pharmacokinetic trends and biodistribution of cysteamine after ocular administration.

To our knowledge, we present the first large animal study quantifying cysteamine in ocular tissues and plasma after topical administration to the eye of rabbits. Current research on controlled release technologies have only performed *in vivo* retention and biopermenance studies on rats [103] and efficacy without pharmacokinetic data in genetic cystinosis mice models [107]. We improved the current status of *in vivo* studies exploring cysteamine eye formulations by working directly with a previously validated mass spectrometry protocol to determine drug concentrations in the eye. The mass spec protocol added further novelty to the filed by extending similar methodologies from cystine LC-MS quantification [192, 193]. Results from corneal tissue (Figure 30A) indicate cysteamine delivered from cysteamine eyedrops at hourly doses delivered approximately 60 pmol/mg cysteamine/corneal tissue at 2 hr receiving 2 drops and 6 hr receiving 6 drops. The SD-CMS/Gel achieved approximately 20 pmol/mg cysteamine/corneal tissue from one drop at the same time points. A full daily course of multiple doses (12 drops) of cysteamine eyedrops reached 5 times as much drug than SD-CMS/Gel at 12 hours. Although there are no comparable corneal tissue data, a pharmacokinetic study on rats after catheter intraduodenal delivery of 20mg/kg cysteamine achieved cysteamine liver concentrations of 0.2 nmol/mg protein at 6 hours and 0.11 nmol/mg protein at 24 hours [192]. These values are not directly comparable because the delivery methods are drastically different and the cysteamine tissue concentration in this study was normalized to protein content, however, it can be estimated that cysteamine presentation during topical application is on a scale of a magnitude a thousand times less than intraduodenal delivery, where topical delivery achieved nanomolar cysteamine concentrations and intraduodenal delivery achieved micromolar cysteamine concentrations. These methods are the first to extend current cysteamine mass spec protocols to the eyes of rabbits and offer processes that can be replicated in close collaboration with Clarus Analytical (San Diego, CA, USA).

Additional ocular samples consisting of aqueous humor and vitreous humor were quantified for cysteamine concentrations. Aqueous humor samples in the treated eyes achieved drug presentation at all timepoints with cysteamine eyedrops having wider variation in samples compared to SD-CMS/Gel. For example, at 6 hours cysteamine eyedrops delivered 248.7 ± 208.55 nM compared to SD-CMS/Gel 80.67 ± 26.47 nM. Interestingly, the untreated contralateral eyes at 2 hours had no detectable cysteamine concentrations (<15nM) in all samples while some samples had detectable drug amounts with wide variation at subsequent timepoints for both formulations (Figure 30B). Potential crosstalk between contralateral eyes may explain this phenomenon and is further speculated in our analysis of vitreous humor samples. Several samples from untreated eyes presented cysteamine at detectable concentrations. These concentrations were less than aqueous humor levels at the same magnitude, which may indicate less posterior segment drug adsorption as reported in other pharmacokinetic rabbit studies of small molecules delivered topically [194].

Our study also revealed a trend of cysteamine plasma concentrations below detectible limit of quantification at timepoints 2 hr, 12, hr 24 hr. There was detectable cysteamine concentrations in a few samples at 6 hrs, however, the deviations between samples implies there was likely little to no systemic adsorption of cysteamine from all formulations when topically delivered. These observations are particularly important due to the inability to obtain peak plasma concentration of cysteamine following ocular administration of cysteamine during clinical trials in humans. It is likely that patients enrolled in these trials were pretreated with prescribed oral cysteamine which is far greater than one daily ophthalmic dose of cysteamine [191] and would be the main contributor of plasma cysteamine concentrations and not eyedrops. We furthered evaluated the

translation of cysteamine formulations in instillation tolerability studies with semiquantitative clinical scoring.

We evaluated rabbit grimace pain scales and Draize eye test for irritation during eyedrop instillation between cysteamine eyedrops, our delivery system materials without cysteamine (SD-BLANK-MS) and cysteamine-loaded materials (SD-CMS/Gel). These studies were guided by adverse effects observed in clinical trials as noted by redness expanding over 50% of the conjunctiva [167] and transient effects lasting less than 1 hour which included stinging and burning [108, 109]. Based on our model and clinical scoring by an ophthalmologist, the formulations were well tolerated and any pain upon instillation was relieved between 10 to 60 mins (Figure 27A-D). This was expected as the clinical trial observers saw relief after 1 hour. They also suspected that any increase in resident time of a formulation as well as a higher concentration of cysteamine HCL may cause discomfort from viscous cysteamine studies [109, 195]. Draize eye test scores also supported transient effects of irritation lasting up to 10-30 mins as noted in Table 4. Overall, the sustained release materials were tolerated during instillation in the pre-corneal area. In addition to instillation tolerability, we also monitored the safety profile of subjects prior to tissue collection for intraocular pressure and structural changes to eyelids after treatment with histopathology.

The intraocular pressure of rabbits in untreated and treated eyes was quantified. Overall, all measurements were within normotensive range 15-23 mmHg [196, 197] for all subjects at each timepoint. There was no increase in IOP from any of the formulations, which was expected and supported by previous rabbit studies conducted by our group [138]. Histopathological analysis of eyelid tissue was used as a proxy for irritation at the ocular surface. H&E staining revealed no structural differences in untreated and treated eyes with an intact conjunctival epithelium in all samples at 24 hours (Figure 29). VVG staining also presented no changes in elastin or collagen as

indicated by uniform red structures observed in all samples. Thus, the visible similarities between sections suggest no effect of cysteamine and materials in SD-CMS/Gel effect the structure of eyelids. We previously performed irritation assays on hen's eggs and bovine eyes which observed little to no irritation within 8 hours [2] and our eyelid histology agrees with these findings. It is important to note that we were unable to obtain corneal histology due to the tissue processing for cysteamine extraction with subsequent mass spectrometry analysis.

In addition to our limitation in obtaining corneal histology, the challenges to maintaining cysteamine stability during in vivo topical administration and tissue post processing may contribute to variability observed in our mass spectrometry data. At administration, cysteamine may be exposed to oxidative degradation while simultaneously metabolized endogenously into thiol derivatives (e.g S-methylcysteamine and hypotaurine) [198]. The tissue sample processing with NEM for mass spectrometry targets the free sulfhydryl group in cysteamine; if the sulfhydryl group is blocked, as in the disulfide bond formation in cystamine, then cysteamine cannot be quantified with NEM derivatization. Therefore, the data presented is a best-case scenario for quantifying active cysteamine after quickly and humanely excising tissue post-mortem. To overcome this, adding a reducing agent like TCEP prior to NEM derivatization would reduce cysteamine thiol derivatives to determine total cysteamine prior to oxidation. Subsequent mass spectrometry analysis would thus require validation to ensure extraction ratios are not inhibited by the reducing agent. Furthermore, the variability in our preliminary pharmacokinetic may be lessened by increasing the current sample size (N=3) for each time point to a sample size large enough for statistical power with careful consideration of retaining the ability to quickly sparse sample subjects. The literature supports the use of satellite groups [199], which are subjects undergoing pharmacokinetic studies only, for sparse sampling performed in the current studies

across four timepoints. However, to reduce the variability in determining pharmacokinetic disposition of cysteamine, performing sparse sampling at earlier timepoints would potentially offer less variable data. A future *in vivo* study consisting of earlier timepoints (1 min, 5 min, 10 min, 30 min, 60 min) with a single dose of cysteamine eyedrops may provide a true pharmacokinetic profile of cysteamine when topically delivered. We did not investigate the pharmacokinetic profile of a single drop of cysteamine eyedrops. Rather, our study replicated the prescribed dosing regimen of Cystaran™ eyedrops and readministered every hour up to the 12th hour. In doing so, we developed a model that is in direct translation to patients and provides a basis for comparing future ophthalmic formulations.

4.0 Specific Aim 3

4.1 Introduction

Upon design, optimization, and translation to large animal *in vivo* ophthalmic models, our sustained release drug delivery system containing cysteamine was tested for efficacy in the cystinosis knockout mouse (CTNS (-/-)). Corneal cystine crystals in the eyes of the CTNS(-/-) knockout mouse were first evaluated during the generation of the transgenic mouse and preliminary therapeutic oral cysteamine trials [166]. The CTNS (-/-) mouse was further characterized in subsequent efficacy studies with *in vivo* confocal microscopy (IVCM) [200, 201]-B]. The same research group performed the first efficacy study on a murine model of cystinosis by treating eyes with 0.55% cysteamine eyedrops and confirming cystine crystal reduction with longitudinal IVCM. Presently, two additional studies on the efficacy of experimental therapies for cystinosis have utilized the CTNS (-/-) knockout mouse and IVCM – which include systemic hematopoietic stem cell transplantation [202] and reformulation of cysteamine into a polymeric nanowafer [107]. While IVCM is the most established imaging modality for murine models of cystinosis, patients with cystinosis are regularly examined with a combination of IVCM and optical coherence tomography (OCT), with OCT becoming the preferred clinical imaging modality for its low-light emission and fast scanning rates [203]. In the clinic, longitudinal OCT on the cystinotic cornea is utilized to obtain cystine crystal depth and corneal thickness over a patient's lifetime [204]. Recently, spectral-domain OCT was used to observe retinochoroidal cystine crystals in cystinosis patients [205] and suggests a trend in harnessing imaging modalities with low light emission to reduce photophobia that cystinosis patients experience during eye

examinations [206]. Thus, the studies herein utilize OCT to determine intensity backscatter from corneal cystine crystal in the CTNS (-/-) mouse and examine mouse corneas during cysteamine treatment from our formulation.

Investigating our experimental delivery system and OCT techniques required careful consideration of previous established methods. Quantification of hyperreflective cystine crystals by IVCM required corneal volumes to be processed with thresholding techniques to isolate bright pixels (i.e. white) from darker, non-reflective corneal structures (i.e grey and black). IVCM methodologies utilized a grey scale threshold between 100-255 pixels (i.e., 1 pixel value equal to black, 255 pixel value equal to white) [107] to determine a crystal volume index (CVI %). The CVI% for eyes in the CTNS (-/-) mouse during efficacy studies were quantified by normalizing crystal volumes to stromal volumes [200]. Initial CVI% for each eye was compared to each timepoint after treatment to evaluate the absence or progression of crystal growth for all controls during topical cysteamine administration. The amount of cysteamine delivered in these studies are inconsistent, however, they emphasized the importance of the duration of treatment and age-dependence of corneal cystine crystal deposition in the CTNS (-/-) mouse.

At 5-months cystine crystals are detectable with IVCM and are likely to increase with density up until 7-months [166, 200, 2021]. Within this time frame, seminal studies focused on delaying the onset of crystal progression by treating with 0.55% cysteamine eyedrops (no known volume) administered 4 times a day for 4 weeks (28 days) [201]. Initial IVCM prior to treatment at 5 months was compared after treatment when the mice were 6-months old. The eyes in the treatment group resulted in a 15% increase of crystal volume from baseline, whereas the untreated group (N = 5) resulted in 178% increase. Comparison of crystal volumes significantly supported 0.55% cysteamine eyedrops as a therapy to delay cystine crystal progression [201]. In the

polymeric nanowafer study, the researchers administered treatment of mice at 7-months. One group of 7-month-old mice received a 0.44% cysteamine eyedrop administered 2 times a day at a volume of 5 µL (44µg cysteamine) and compared to a once-daily cysteamine nanowafer formulation containing 10 µg cysteamine for 30 days. IVCM was used to calculate crystal volume at 7-months before treatment in one eye of each subject, and then compared after treatment to the same eye when the mice were aged to 8-months. Interestingly, the cysteamine nanowafer reduced cystine crystal volume by 90% and the 0.44% cysteamine eyedrop reduced crystal volume by 55%. The statistical findings supported a once daily cysteamine formulation in a rodent model of cystinosis. The systemic hematopoietic stem cell transplantation studies did not use cysteamine as a treatment modality, however, their studies compared the eyes of CTNS (-/-) mouse receiving low HPCS doses or high HPCS doses over 12 months [202]. In total, these studies support multiple approaches to treating corneal cystine crystal in the CTNS (-/-) and provide data to encourage cysteamine reformulation into controlled drug delivery systems.

Despite the limitations of efficacy studies in the CTNS (-/-) mouse and lack of published ocular pharmacokinetic studies in available models, there is scientific premise towards investigating topical cysteamine further in cystinosis animal models. When conducting efficacy studies on the CTNS (-/-) mouse it is particularly important to utilize established positive controls receiving 0.55% cysteamine eyedrops (0.44% cysteamine hydrochloride FDA equivalent) that are administered at volume of 5 µL (22µg cysteamine) for a minimum 2 [202] to 4 times per day [107]. In total, this equates to 22-88 µg cysteamine delivered in one day. Reformulated cysteamine therapies would thus be adjusted similarly to deliver 88 µg cysteamine per day with a careful balance of eyedrop tolerability. Lastly, mice would be aged between 7-12 months to take advantage of dense crystal deposition with limited effect of untreatable corneal disease (e.g scarring).

4.2 Materials and Methods

4.2.1 Establishing a Colony of CTNS (-/-) Knockout Mice, Husbandry, and Genotyping

Eight breeding pairs of C57BL/6J CTNS (-/-) knockout mice were obtained through the Cherqui Lab at the University of California San Diego. Beginning on 2019 and through 2021, breeding pairs were pair mated and housed in cages with automatic water with a 12-hour night-day cycle. Dames were fed a prenatal diet (DietGel® Prenatal, Clear H_20, Westbrook, ME) until their first litters were born to support maternal health and prevent cannibalism. Upon litter generation, C57BL/6J CTNS (-/-) pups were weaned after 21 days. Mice born (within ages of less than 7 days) with abnormalities such as missing one or both eyes (anophthalmia), visibly small eyes (microphthalmia), or hydrocephalus were euthanized humanely via cervical dislocation. Pups born to homozygous CTNS (-/-) breeding pairs are 100% homozygous knockouts of the CTNS (-/-) gene. Therefore, genotyping was not consistently performed on candidate pups. However, a genotyping protocol was developed for the potential need to rederive the CTNS (-/-) knockout mouse colony after cryopreservation (i.e. colony reduction during global pandemic in 2020). Briefly, 3 primers GT10F1(5′-GATCTTCGGAGACCCAACC-3′), GTgalF(5′-TCCAGCGGGGGATCTCATGT-3′), and GT10R(5′-CAGGGCAGCTTACTGATTGA-3′) (Thermo Fisher Scientific, Pittsburgh, PA) were selected for PCR in collaboration with University of Pittsburgh's Health Science Core Research Facilities. Mice toe clippings approximately 2 mm^3 were safely cut with fine precision scissors from pups (< 7 days old) and placed in PCR tubes. Then, 88 µL of PCR-grade water (Thermo Fisher Scientific, Pittsburgh, PA) , 10 µL of KAPA Express Extract Buffer (Roche, Basel, Switzerland) , and 2 µL of KAPA Express Extract Enzyme (Roche, Basel, Switzerland) was added. The tissue was then lysed for 10 mins at 75 °C using a

thermocycler (C1000 Touch™, Bio-Rad Laboratories, Hercules, CA). Enzyme activation then occurred for 5 mins at 95 °C. Cellular debris was then pelleted by centrifugation at 2000 RPM at 25 °C. The top layer containing DNA was extracted and placed into fresh PCR-Tubes. Samples were stored at -20°C for 6 months unit PCR genotyping occurred. Candidate CTNS (-/-) knockout were raised to maturity and evaluated for corneal cystine crystal presentation, abnormal corneal defects due to aging (e.g., clouding, opacity), or systemic complications of their disease. A dissecting microscope (Leica Si9, Leica Camera Inc., Allendale, New Jersey) was used to obtain gross morphological images of the CTNS (-/-) knockout eye and was compared to C57BL/6 WT eye at 7-months of mice age.

4.2.2 Gel Administration, Retention, and Safety Studies

Topical administration of SD-CMS/Gel onto a murine model was performed on C57BL/6 wild type (WT) mice (The Jackson Laboratory, Bar Harbor, ME) . First, preliminary studies were conducted by mixing SD-CMS into Gel using a 1mL syringe and 25G needle at a ratio of 10mg SD-CMS:100µL of Gel. Drops of SD-CMS/Gel were placed on glass slides and observed using a microscope. After confirming delivery of SD-CMS/Gel after 25G needle administration, feasibility trials on Gel placement and retention were performed on mice. In short, when the Gel was applied without any protection from mice grooming the Gel was not retained for more than a few minutes. To overcome this challenge, a mouse postoperative eye patch consisting of a transparent thin polyurethane film coated with acrylic adhesive (Tegaderm™, 3M Company, Saint Paul, MN) and Elizabethan collars (E-collars) (Kent Scientific Corporation, Torrington, CT) were tested for retention and safety. Briefly, C57BL/6 mice (N = 3) were anesthetized using inhaled isoflurane delivered by an oxygen transported nebulizer and rodent facemask (World Precision

Instruments, Sarasota, FL). Fine tweezers were then used to pluck the fur in a 4mm radius circle around the eye. One 5 µL drop of lubricating eyedrops (Refresh Tears, Allergan, Irivine, CA) was placed to wash any fur off the ocular surface and then wiped off gently with a microfiber swab. Then, a drop of Gel ranging from 1-5 µL was then placed on top of the ocular surface and eyelid space of the right eye of each subject. After placement, the Gel underwent a phase change with an external overhead irradiated heat lamp (Braintree Scientific Inc., Braintree, MA) which was required due to the body heat loss rodents naturally experience during anesthesia. An 8 mm biopsy punch (AcuDerm Inc., Fort Lauderdale, FL) was used to punch out circular eye patches from Tegarderm™ films and was placed with forceps on top of the transitioned gel and firmly pressed onto the skin around the eyelid. E-collars were then placed around the neck of the mice such that the collars could rotate 360°. Mice were then placed single housed and observed for 26 days. Their body weight was measured using a digital scale to confirm adjustment to eating and drinking.

4.2.3 Non-Contact Optical Coherence Tomography Acquisition, Image Processing and Analysis for Central Corneal Thickness and Corneal Intensity

Images of the cornea and anterior segment were obtained with optical coherence tomography (OCT) (Bioptigen Envisu R2210 Leica, Durham, NC). Two groups, C57BL/6 CTNS (-/-) mice (N = 3 mice, N=6 eyes) and C57BL/6 WT mice (N=5 mice, N=10 eyes) were aged to 7-months and imaged under isoflurane inhalation anesthesia with a facemask mounted on a mouse bite bar. Central corneal radial scans (scan range: 2.0 mm, scan resolution - A scan: 1000, B scan: 100) on both eyes were obtained. First, a drop of artificial tears was placed on each eye during induction of isoflurane anesthesia. Then, a microfiber swab was used to remove excess tears near

the eyelids. Volumetric images (.OCT) of each was then stored in a password protected hard drive and analyzed for corneal intensity and thickness.

OCT volumes obtained from randomized eyes C57BL/6 CTNS (-/-) mice (N=5) and C57BL/6 WT mice (N=5) were first processed using ImageJ FIJI (National Institutes of Health, Bethesda, MD) [207]. Raw OCT files were processed to register and average the frame to the center of the cornea from the middle of the stack (e.g. 100 stacks would be centered at stack 50). Then, a rectangle (400 x 100, WxL pixels) was centered above the ocular surface to capture the cornea and specular reflection. Specular and Purkinjean artifacts were removed manually using the 3D viewer. Each file was then saved as in TIFF format and stacks were saved as individual image sequences of .TIFF files (e.g 100 .TIFF images for each eye scan). For all image sequence files the corneal intensity was measured by selecting the entire cornea with the wand tool and setting a pixel threshold between 100-255 [107]. All intensity values from individual images were added to calculate pixel intensity/volume (grey scale value/voxel) per eye. The central corneal thickness (CCT) of C57BL/6 WT eyes (N=10) and C57BL/6 CTNS (-/-) (N=6) were measured by first calibrating .BMP files to calipers in the Bioptigen software to obtain a pixel/distance ratio (e.g 319.33 pixels/mm). After calibration, the line tool was used to measure the pixel distance from the ocular surface to the endothelium at a 90° angle for all eyes. Then, the pixel value from the line tool was divided by 319.33 pixels/mm to obtain CCT in millimeters and converted to micrometers.

4.2.4 Cysteamine Drug Escalation and Longitudinal Anterior Segment OCT Towards Efficacy

Materials for this study followed similar procedures outlined within in vivo rabbit studies (Section 3.2.2). Briefly, 0.44% Cysteamine eyedrops were fabricated by mixing cysteamine hydrochloride (66 mg) in 15 mL deionized water with 0.01% benzalkonium chloride (1.5 mg) and 0.90% sodium chloride (135 mg). A pH of 4.0 – 4.5 was achieved by titrating 0.1 N hydrochloric acid and 0.1 N sodium hydroxide, approximately 10 µL at a time. The cysteamine solution was aliquoted into 1 mL volumes in 2.5 mL amber vials and bubbled with nitrogen gas in a glovebox (Fischer Scientific). Samples were stored frozen at -20°C and wrapped in parafilm until use – any unused cysteamine solution was immediately discarded within 24 hours of unsealing. SD-CMS/Gel, was fabricated according to our previous studies [2]. Cysteamine free microspheres (SD-BLANK-CMS) were produced using the same fabrication process without the addition of cysteamine hydrochloride. Suspensions of SD-CMS/Gel and SD-BLANK-MS/Gel were fabricated by mixing 6.5 mg of SD-CMS to 100 µL of Gel. All SD-CMS/Gel and SD-BLANK-MS/Gel suspensions were prepared by sterilizing respective microspheres with UV irradiation 30 mins immediately before administration to subjects.

CTNS (-/-) knockout mice were aged and used to test the tolerability and efficacy of cysteamine from SD-CMS/Gel over 30 days. Baseline OCT (e.g 2 days prior to treatment) images were acquired for fifteen mice, with mixed sexes and between the ages of 7 and 10 months. Initial OCT scans revealed enlarged corneal stroma and opaque layers in three mice (i.e., one or both eyes succumbed to corneal disease), which were excluded from the study. Thus, twelve mice were randomly organized into three treatment groups for their right eyes: 1). Once daily SD-CMS/Gel 6.5mg/100µL with eyepatch and E-collar, 2) Once daily cysteamine-free microspheres (SD-

BLANK-MS)/Gel 6.5mg/100µL with eyepatch and E-collar, and 3). Four times per day 0.44% cysteamine eyedrops at 5 µL drops. The left, contralateral eye, was untreated for all subjects and served as controls. For 4 weeks (28 days) the mice were treated with their respective dose each day. The E-collars were removed for 1 hour of self-grooming each day prior to topical administration of treatment for the respective eyepatch and E-collared groups. Mice weight for the E-collared group were recorded every other day. All mice were imaged with OCT at days 7, 14, 21, and 28. OCT volumes for both right (OD) and left eyes (OD) were processed and analyzed for corneal intensity and CCT. After the study, the subjects were humanely euthanized and the eyes were harvested and processed for histology. A summary of the timeline for the experiments is depicted in Figure 32.

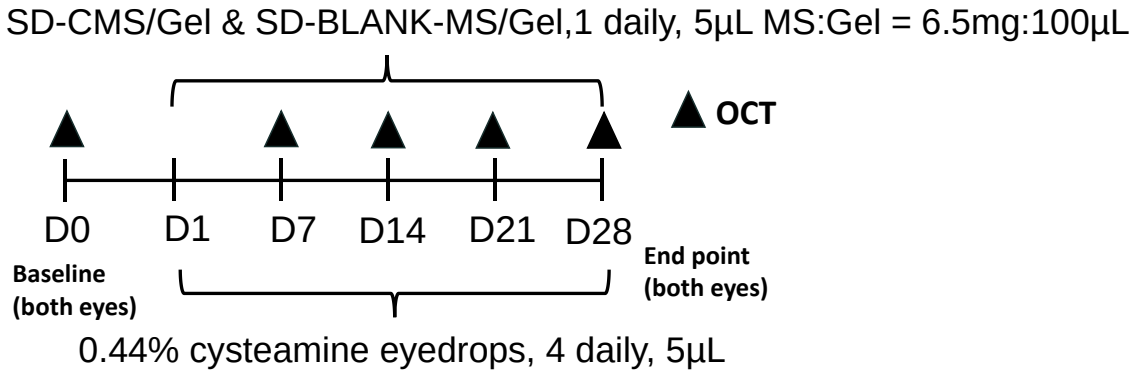

Figure 32 Timeline of longitudinal OCT study on CTNS (-/-) mice

4.2.5 Statistical Analysis

Descriptive statistics (mean ± standard deviation) were obtained for mass % change, central corneal thickness, and pixel intensity/volume. A nonparametric analysis consisting of the Mann Whitney U was performed to compare C57BL/6 WT mice and C57BL/6 CTNS (-/-) pixel intensity/volume for statistical significance (p-value = 0.05). For longitudinal OCT analysis in

C57BL/6 CTNS (-/-) a repeated-measures one-way ANOVA was performed (p-value). All statistical analyses were performed using Minitab 19 software (State College, PA).

4.3 Results

4.3.1 Corneal Imaging of CTNS (-/-) Knockout Mice

From 2019-2021, CTNS (-/-) knockout mice were aged and imaged with light microscopy to observe corneal health. A wild type of the same background strain (C57BL/6 WT) was aged to 7-months and their corneas imaged. Representative corneal images (Figure 33) of light microscopy indicated the presence of cystine crystals in the cornea of 7-month-old CTNS (-/-) knockout mice (Figure 33A, white arrows) and their absence in the wild type cornea (Figure 33B).

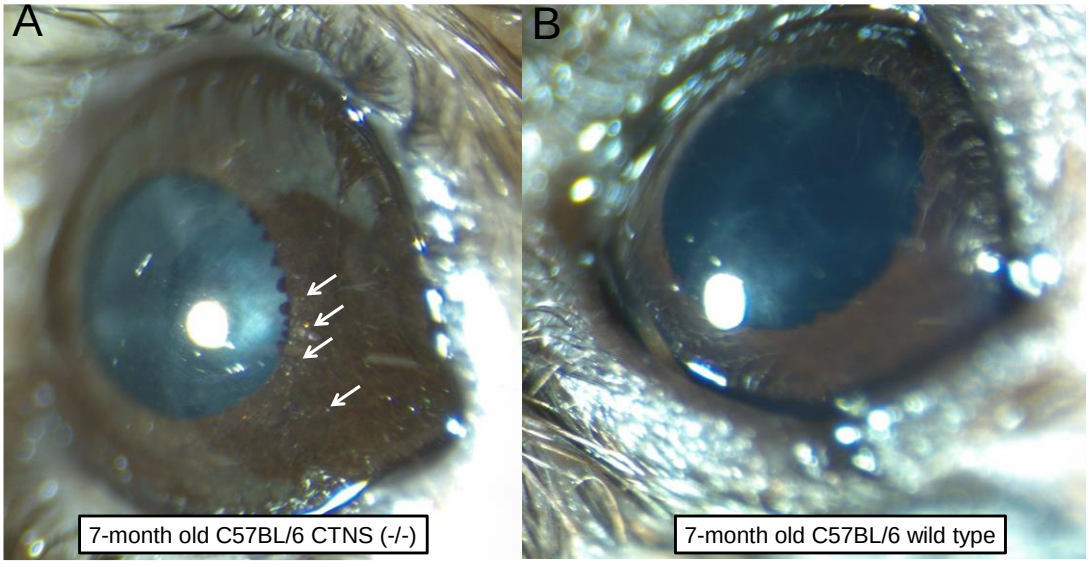

Figure 33 Light micrscopoy of C57BL/6 wild-type and C57BL/6 CTNS (-/-) mouse. White arrows indicate hyperreflective cystine crystals.

4.3.2 Topical Application and Retention with Modified Eyepatch and Elizabethan Collars

Several trials of topical application and retention of our delivery system were conducted in rodent models. Due to mice grooming behavior, retention of Gel for 24 hours was not obtained without eye protection. Representative images of transitioned gel with eyepatch and E-collars (Figure 34A and Figure 34B) were obtained. The health of mice (N=3) were observed by weighing their masses with eye protection over 26 days. Mass percent was calculated based on initial mass and plotted as an average ± standard deviation. Overall, weight loss was observed through the first week above 20% and weight maintenance after 11 days (Figure 34C).

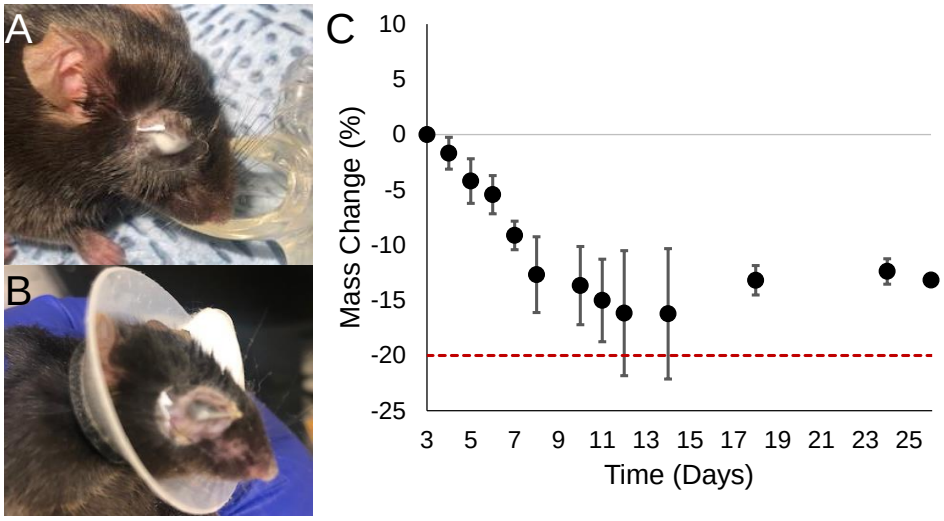

Figure 34 Gel application with eyepatch (A) and retention with elizabethan collar support (B). The mass change in mice (C) is reported as mean ± standard deviation (N=3).

4.3.3 Central Corneal Thickness and Corneal Intensity in Untreated Mice

OCT volumes of eyes from C57BL/6 CTNS (-/-) mice and C57BL/6 WTe mice were processed for central corneal thickness (CCT) (Figure 35) and corneal intensity (Figure 36). CCT of both mice were within 50-100µm. The pixel intensity of randomized eyes from the C57BL/6

CTNS (-/-) mice had statistically different means than C57BL/6 WT mice means. Statistically significant differences (p-value = 0.05) indicate the pixel intensity of C57BL/6 CTNS (-/-) were higher than C57BL/6 WT at an age when cystine crystals are present.

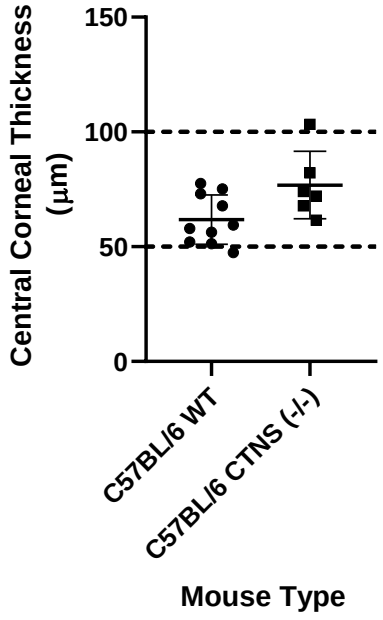

Figure 35 Central corneal thickness (CCT) of C57BL/6 wild type mice eyes (N=10) and C57BL/6 CTNS (-/-) mice (N=6). Values are reported as mean ± standard deivation. Dotted lines indicate the range of CCT for murine models as reported in the literature.

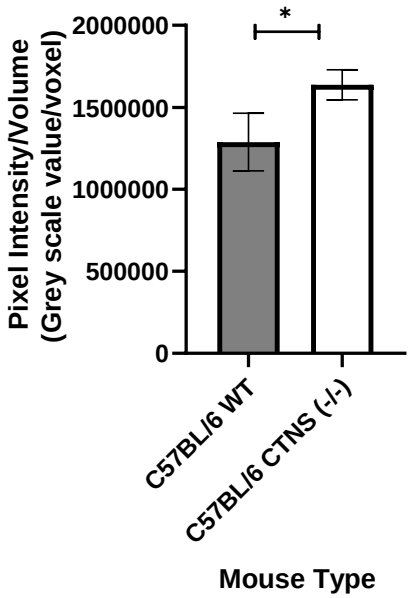

Figure 36 Pixel intensity normalized to volumes of C57BL/6 mice eyes (N =5) and C57BL/6 CTNS (-/-) mice eyes (N=5). Grey scale intesnity is reported by mean ± standard deviation. Statiscal signifcance is indicataed with an asterisk (*) (p-value = 0.05).

4.3.4 Longitudinal OCT on CTNS (-/-) Mice for Central Corneal Thickness and Corneal Intensity

The right eyes of CTNS (-/-) knockout mice were treated with their respective eye formulations for 28 days. OCT images were acquired at baseline and once weekly (e.g D0, D7, D14, D21, D28). Some of the subjects in the SD-BLANK-MS/Gel group (Figure 38 E-H) and SD-CMS/Gel group (Figure 38 I-L) experienced corneal opacity. There was low observed opacity in cysteamine eyedrop eyes (Figure 38 A-D).

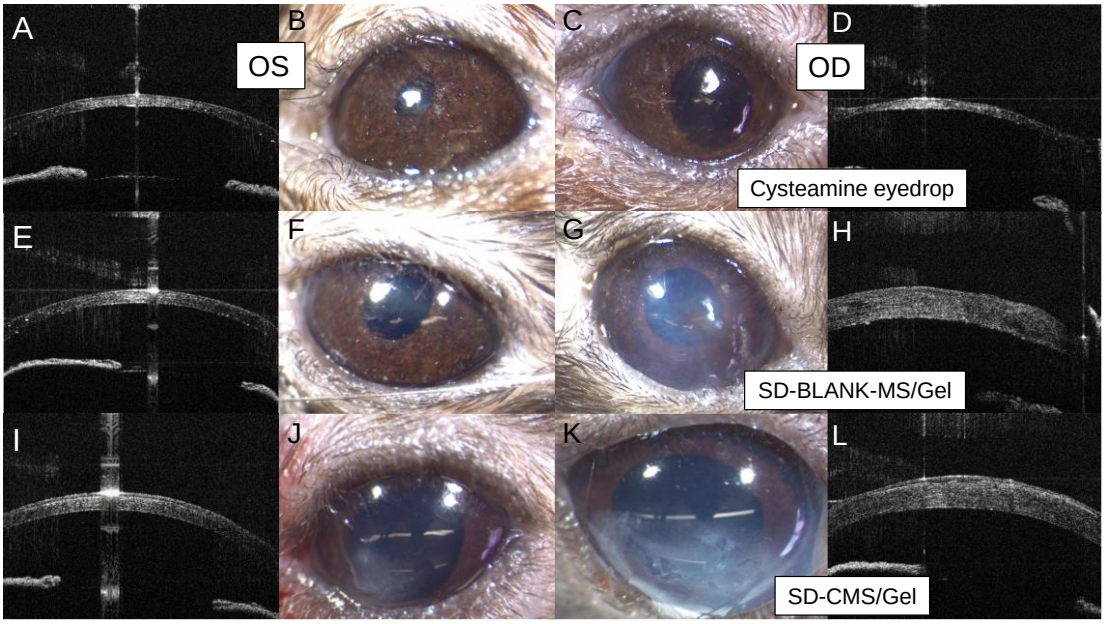

Figure 37 CTNS (-/-) mice corneal images treated with cysteamine eyedrops (A-D), cysteamine-free microspheres (SD-BLANK-MS/Gel) (E-H), and cysteamine micropsheres (SD-CMS/Gel) (I-L) on day 28.

OCT analysis of CCT of each eye was determined at each timepoint and compared in Figure 39. Both eyes of CTNS (-/-) knockout mice treated with cysteamine eyedrops remained within 50-100 µm. The mean values of SD-CMS/Gel and SD-BLANK-MS/Gel treated eyes (OD) were above 100 µm after D14 (Figure 39, week 2). The contralateral eyes of SD-CMS/Gel, which did not receive any treatment, were above 100 µm at D28 (Figure 39, week 4).

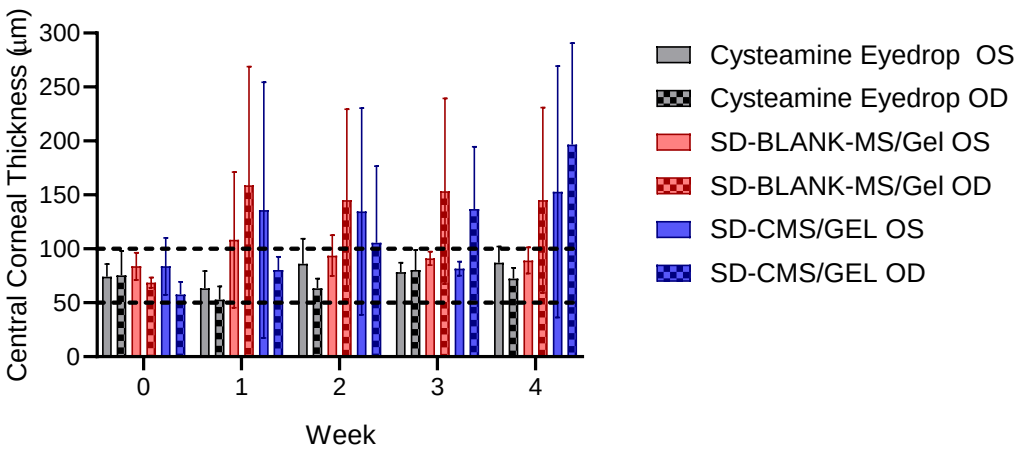

Figure 38 Central corneal thickness of CTNS (-/-) knockout mice (N=3 per eye). Right eyes (OD) received treatmeht. Left eyes (OS) were not treated and categorized based on the contralteral eye treatment. Data is presented as mean ± standard deviation.

OCT volumes were processed for corneal intensity for all eyes in the study and presented in Figure 40. Statistical analysis of corneal intensity values reported no significant differences. Descriptive statistics (mean values) for right eyes treated with SD-BLANK-MS/Gel and SD-CMS/Gel were higher in grey scale values/voxels than their respective untreated, contralateral eyes. For cysteamine eyedrop treatments, there were no statistically significant differences in intensity values between right and left eyes (Figure 41A). However, when the right eye (OD) values were normalized to left eyes (OS), there was a trend towards a decrease in intensity values after 4 weeks (Figure 41B).

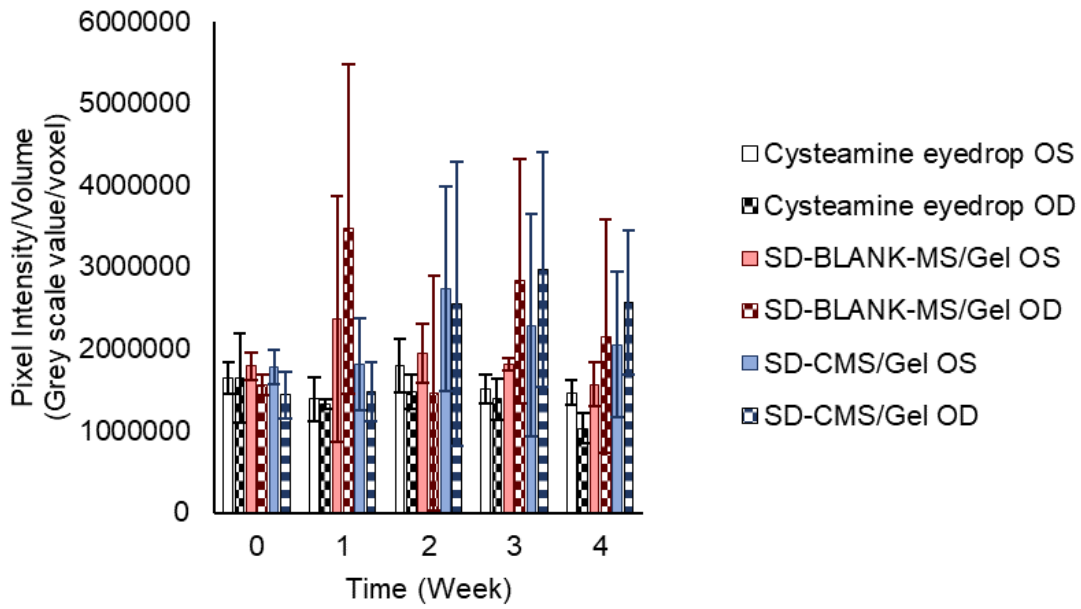

Figure 39 Pixel intensity per volume of treated (OD) and untreated, contralteral eyes (OS) of CTNS (-/-) mice. Data are presented as mean ± standard deviation for N=3 eyes.

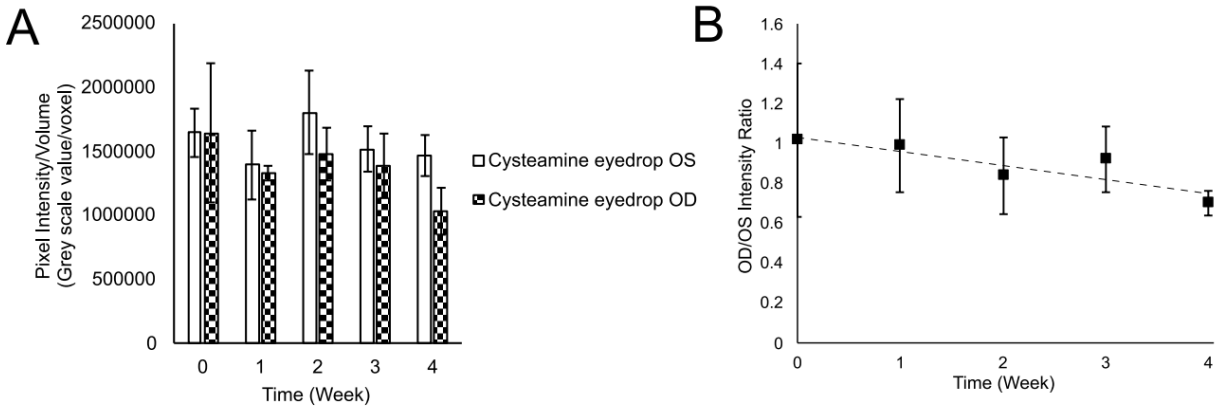

Figure 40 Pixel intensity of cysteamine eyedrops (A) and right eye (OD, treated) intensity normalized to left eye (OS,untreated) intensity (B). Data is presented as mean ±standard deviation for N=3 eyes.

4.4 Discussion

The goal of the studies within this chapter was to test the efficacy of cysteamine delivered from spray-dried cysteamine microspheres in thermoresponsive gel (SD-CMS/Gel) in a murine model of cystinosis. The murine model of cystinosis is the most widely characterized and established genetic model of cystinosis – with major *in vivo* studies investigating efficacy of topical cysteamine formulations [107,201] and hematopoietic stem cell transplantation [202] for treatment of corneal cystine crystals. In these studies, light microscopy and IVCM were utilized to quantify hyperreflective cystine crystals in the cornea during treatment. To improve upon current imaging modalities for cystine crystals, while also considering imaging modalities appropriate for pediatric patients, optical coherence tomography was used to evaluate corneal health and to quantify corneal intensity of corneal cystine crystals. Upon optimization of OCT acquisition and processing, longitudinal studies were conducted on CTNS (-/-) mice treated with cysteamine released from our novel drug delivery system.

The goal of the studies within this chapter was to test the efficacy of cysteamine delivered from spray-dried cysteamine microspheres in thermoresponsive gel (SD-CMS/Gel) in a murine model of cystinosis. The murine model of cystinosis is the most widely characterized and established genetic model of cystinosis – with major *in vivo* studies investigating efficacy of topical cysteamine formulations [107, 201] and hematopoietic stem cell transplantation [202] for treatment of corneal cystine crystals. In these studies, light microscopy and in vivo confocal microscopy were utilized to quantify hyperreflective cystine crystals in the cornea during treatment. To improve upon current imaging modalities for cystine crystals, while also considering imaging modalities appropriate for pediatric patients, optical coherence tomography was used to evaluate corneal health and to quantify corneal intensity of corneal cystine crystals. Upon

optimization of OCT acquisition and processing, longitudinal studies were conducted on CTNS (-/-) mice treated with cysteamine released from our novel drug delivery system.

The feasibility of topical application and retention of microspheres embedded in our thermoresponive gel was optimized for smaller animal species in these studies. Our previous studies in large animals with anatomically similar eyes to humans have evaluated retention for 24 hours to 30 days [2, 137, 138]. In larger animal studies, anesthesia-free handling and restraint was performed and compatible with our materials. However, direct translation of anesthesia-free methodologies to a murine model of cystinosis was unfeasible. Despite manual restraint (e.g, neck scuffing) of mice [208] topical administration was prevented by mice clawing and biting at the microsphere/gel applicator. After establishing isoflurane inhalation anesthesia and heat lamp protocols for thermoresponive gel application and phase transition, the retention of the delivery system was prevented by the natural self-grooming behavior of mice on their oculofacial regions [209]. As such, microsphere/gel retention methodologies were engineered iteratively until an eyepatch and Elizabethan collar successfully retained our delivery systems for 24 hours (Figure 34A&B). These methods were influenced by post-operative eye procedures to protect eyes in pediatric patients [210] and restraint collars for mice surgeries [211], which were deemed safe with careful aftercare. In parallel to troubleshooting microsphere/gel application and retention strategies, OCT acquisition set-up and parameters were also optimized.

OCT acquisition and processing was optimized against a background strain (e.g, C57BL/6 WT) of the CTNS (-/-) knockout mouse. The background strain shares similar anatomical structures of the cornea and anterior chamber, thus comparative imaging strategies to untreated CTNS (-/-) mice (i.e., no systemic or topical cysteamine) would support quantification of intensity produced by corneal cystine crystals. Central corneal thickness (CCT) (Figure 35) between

C57BL/6 wild type background strains (CCT 61.82 ± 10.79 µm) and C57BL/6 CTNS (-/-) (CCT 76.85 ± 14.66 µm) were similar and within range of studies measuring CCT in the same background strain and knockout mouse [202]. Comparison of corneal intensity suggested differences in grey scale values per voxels of OCT volumes, with the CTNS (-/-) mouse having higher values than background strain corneas (Figure 36). These data suggest the light scatter from corneal cystine crystals in the knockout mouse is captured by OCT. To our knowledge, these data support the first studies utilizing OCT to determine corneal cystine crystal light scatter intensity in a murine model. Clinically, OCT is used to image the cornea of cystinosis patients in combination with slit-lamp photograph to observe corneal health throughout their lifetime [204], and to determine optimal treatment of cysteamine eyedrops. Similarly, we extended these methodologies to evaluate cysteamine efficacy from our delivery system.

Longitudinal OCT captured CCT and corneal intensity of CTNS (-/-) mice receiving cysteamine eyedrops and microsphere/gel formulations our studies. For cysteamine eyedrops the right eye (OD) received 4 drops of a 5 µL aqueous cysteamine suspension, which resulted in normal CCT mice corneal thickness in the OD and contralateral left eye (OD) (Figure 39). While there were no statistically significant differences in corneal intensity between OD eyes receiving cysteamine eyedrops and their contralateral OS eyes (Figure 41A), there was a trend towards a decrease in intensity ratios when OD eyes were normalized to OS eyes (Figure 41B). Normalizing to contralateral eyes as controls for OCT studies has been previously performed for corneal intensity determined by light scattering [212]. In contrast, the mice receiving a dose of SD-CMS/Gel (6.5 mg MS/100µL Gel) and SD-BLANK-MS/Gel (6.5 mg MS/100µl Gel) in their OD eyes resulted in corneal opacity, increased corneal thickness, and increase in corneal intensity (Figure 38-40). The contralateral OS eyes of some subjects treated with microsphere/gel and

restrained with Elizabethan collars shared similar pathologies. For example, one OS eye (Figure 38 I&J) had opacity when visualized via light microscopy and OCT at 28 days and increased CCT. These data are confounding to the previously established safety profile our materials on ex vivo irritation assays (HET-CAM and BCOP in Chapter 2) and histological analysis of eyelid tissue in rabbits (Chapter 3) at a ratio of 10mg/100uL of microsphere/gel. These studies supported a non-irritating formulation for both cysteamine loaded and cysteamine free materials. It is speculated that our material and cysteamine are not contributing to the opacity observed in these studies, particularly because the ratio was reduced from 10 mg/ 100uL to 6.5 mg/100 L to match the drug per mass delivered from 4 drops of cysteamine eyedrops. Furthermore, the use of PLGA particles containing ocular therapeutics were deemed safe and nonirritating to the ocular surface after topical application in mice [213] and rabbit models [214, 215]. We speculate the methodologies used to apply our delivery system and restrain mice were the source of abnormal ocular effects.

A major challenge in these studies was to maintain the body temperature of mice during isoflurane inhalation to promote temperature phase transition at the ocular surface. Studies have shown that mice body temperatures are strongly correlated to heart beat count and respiratory breathing; at normal physiology the starting temperature of mice is at 36°C and drops in heart rate and breathing during isoflurane inhalation causing a reduction of temperature to 28°C [216, 217]. Several methods to maintain physiological body temperatures in mice include the use of heated blankets [218], thermogenic gel packs [217], metallic heating plates [219], and overhead infrared heat lamps [220]. Of these methods, the infrared heat lamp methodology was used to prewarm the ambient temperature (23-25°C) surrounding the subject during anesthesia. After prewarming, the microsphere/gel was then applied to the ocular surface and the heat lamp was focused on the subject's oculofacial region to support phase transition above the LCST (T > 32°C). While

necessary for optimal formulation application, the repeated exposure (7 times per week) to various temperatures above 32°C with infrared light may have resulted in dryness at the occur surface of both eyes leading to subsequent exposure keratitis. Exposure keratitis has been experimentally induced on murine models of dry by exposing mice to dry environments with speculums to prevent eyelid closure [221] and ultraviolet light to induce photokeratitis [222]. A combination of dry environments and heat lamp exposure may have led to the opacity observed in our studies (Figure 38). Furthermore, the inability for mice to self-groom may have led to further ocular surface complications. Mice spend 40% of their waking time self-grooming their oculofacial regions for hygienic purposes which includes removing discharge from eyes [209, 223]. In our study, we inhibited mice from self-grooming with E-collars for more than 12 waking hours to prevent removal of microspheres/gel. The combination of potential exposure keratitis from heat lamps during application and prevention of self-grooming may have contributed to the opacity, corneal thickness and increase in corneal intensity observed in our studies.

Despite the major drawback in exposing mice to various environmental conditions (i.e., temperature, humidity), housing conditions with restraints that prevent self-grooming, and potential increase in stress from E-collars [224] during studies, our work contributes to the translation of novel ocular drug delivery systems to rare corneal disease. Specifically, the methodologies herein suggest the ability to measure corneal intensity as a marker for treatment of highly reflective structures, a common effect observed in similar lysosomal storage disorders [225-227]. To determine a positive effect of cysteamine treatment from our delivery system, future studies will engage in modulating ambient temperatures to prewarm mice within a controlled humidity environment as performed in murine models of dry eye [228] or using a warming blanket used for infants experiencing hypothermia [229]. Furthermore, an alternative to using an eyepatch

to retain our formulation includes a partial tarsorrhaphy where sutures are tied together to laterally close the eyelids [230]. Tarsorrhaphy is advantage over an eyepatch as it is accessible for the topical administration of eyedrops with retention of partial eye sight [231]. We can perform a drawstring tarsorrhaphy in mice using nylon sutures to repeatedly open and close the eye for microsphere/gel instillation. In order to keep the sutures intact, the mouse e-collar would likely be required prevent mice from scratching and ripping sutures out. This method may offer further insight to whether any debris or interaction from eye patches contributing to the opacity observed in treatment groups.

5.0 Summary and Future Directions

5.1 Overall Summary

In this dissertation, studies investigated an eyedrop technology to address the unmet need for an improved drug delivery system to the diseased cornea while retaining the ease of administration of traditional eyedrops. Our technology utilizes biodegradable polymeric microspheres that degrade through hydrolysis and release encapsulated ocular therapeutics upon degradation or diffusion. After engineering microspheres based on in vitro release studies, candidate microsphere formulations are combined into an in situ thermoresponive gel that is administered to the precorneal area, undergoes a temperature-dependent phase change from solution to a semi-permanent depot, and is retained in vivo. Within the context of cystinosis, a rare corneal disease, the potential for the platform technology was rigorously tested to encapsulate cysteamine while improving drug stability and translate to preclinical in vivo models.

Cysteamine, the active drug used to treat corneal cystine crystals in the cystinotic eye, was encapsulated into PLGA microspheres and combined into our thermoresponsive gel. Spray-dried encapsulation of cysteamine into microspheres dramatically improved the stability of cysteamine to 7-weeks. Cysteamine drug loading and release from gel was equivalent to a daily course of drug administration from traditional eyedrops, representing a 12-fold decrease in dosing frequency. The formulation was shown to be non-irritating in vitro and ex vivo through organotypic models. A daily course of our therapy was administered topically without anesthesia and retained in vivo. The retention studies and observed tolerability *in vivo* informed potential to engage in preliminary

pharmacokinetic and biodistribution studies in large animals and efficacy studies in the only cystinosis animal model, a knockout of the CTNS gene in mice.

An *in vivo* ophthalmic model consisting of the New Zealand white rabbit was utilized to provide ocular tissue and systemic drug concentrations after topical administration of our delivery system and traditional eyedrops. Multiple doses of aqueous cysteamine eyedrops, when administered hourly, maintained drug concentrations within the cornea at a magnitude 5 times higher than a single dose of our technology over 12 hours. Despite the difference in drug uptake, our technology-maintained drug release across 12 hours from a single drop, potentially reducing the need to readminister by 8-11 drops. Systemic uptake of cysteamine from our formulation was below our limit of detection after plasma cysteamine concentrations were quantified during sparse-blood sampling. During these studies, clinical scores from an ophthalmologist indicated our sustained release formulation and controlled release materials without drug were tolerable and any observed transient effects were diminished within 10-30 mins. Histological evaluation of eyelid tissue served as a proxy for irritation at the ocular surface during in vivo studies and observed no structural changes. These findings were comparable to the effect from traditional cysteamine eyedrops. In total, these studies inform the first large animal ocular biodistribution of multiple doses of cysteamine eyedrops – when previous studies failed to provide imperative ocular tissue drug levels. We further investigated the efficacious potential of our encapsulated cysteamine microspheres/gel after topical application and retention in the CTNS (-/-) mouse.

Our objective of establishing a local colony of CTNS (-/-) mice was successfully accomplished. Upon aging select mice to adulthood, corneal cystine crystals were evaluated with light microscopy and OCT. Corneal cystine crystals were evident in CTNS (-/-) mice at age 7 months and compared to background strain wild types, which had no presence of corneal cystine

crystals. OCT imaging processing utilized light scattering to quantify the intensity reflected from corneal cystine crystals. Longitudinal OCT on mice treated with cysteamine eyedrops provided evidence towards a positive effect trend on cystine crystal reduction over 28 days. On the other hand, the challenges in maintaining body heat during topical administration of our formulation and preventing mice from self-grooming with E-collars resulted in no conclusive efficacy data from our microsphere/gel formulation.

5.2 Summary of Challenges and Limitations

The candidate formulation developed for cysteamine release from our topical drug delivery system has potential for further investigation despite the numerous challenges and limitations. Stability studies were limited to quantifying cysteamine within PLGA microspheres only. Our NMR methodology, while selective for active cysteamine and inactive cystamine, was not capable of selectively quantifying PLGA from pNIPAAm. Therefore, the stability of cysteamine in MS is deemed as a shelf-life profile prior to mixing microspheres into pNIPAAm gel. However, this limitation may be strategized when translating to manufacturing and processing procedures by including the MS separate from the gel and requiring users to premix before topical administration. Furthermore, the challenges associated with controlling diffusion of cysteamine from our delivery system limited our fabrication to emulsion-free encapsulation strategies. Thus, the release profile from spray-dried materials afforded drug release less than the initially proposed 1 week release profile.

For translation to *in vivo* models, the established rabbit model was ideal in anatomical size and ability to administer without anesthesia. However, the stability of cysteamine in vivo continues

to be a hindrance for quantification. The mass spectrometry methodology utilizes NEM derivatization on the active thiol of cysteamine. Unfortunately, any degraded cysteamine, whether through oxidation or enzymatic processes, was not detected. Reduction of cystamine or any enzymatic by products with TCEP was performed, however did not result in reproducible data at 24 hour timepoints (data not shown). For examination of tissue structural changes, our study was limited to daily course of our formulation and did not provide long-term toxicity in vivo. While we were successful in administrating our formulation in rabbits, there remains the substantial challenge of topically administering to translating this technology to pediatric patients.

As indicated in the CTNS (-/-) knockout studies, the major challenge of this work was controlling the heat loss during isoflurane anesthesia and protecting the materials from self-grooming behavior. The longitudinal study did not include a group of mice that were untreated and fixed with Tegaderm™ eyepatches and E-collar. This control would potentially support identifying the root-cause of corneal opacity in several of the mice treated with eyepatches and collars. Furthermore, the dry atmosphere under irradiated heat lamps may have limited our findings by introducing a negative effect on corneal health. The number of mice in our study could also be improved to achieve statistical significance. At baseline, several mice were excluded from the study due to scratches and abnormalities at the corneal surface. Furthermore, during the first week of studies, a mouse became dehydrated and required subcutaneous injections of fluids and were removed from the study after euthanizing. Some mice experienced swollen faces and accumulated nesting debris with their E-collars; we suspect that mice were dragging the collars around their cages due to stress. Additionally, the constraints on the number of animals used during the study arose from housing limitations on breeding during the global pandemic. Despite these challenges, we were able to bring novelty to the field of cystinosis by providing OCT parameters on the

cystinotic mouse cornea. An improvement to OCT processes would be to stratify post-image processing into automatic algorithms (e.g Matlab, Python) that precisely remove artifacts automatically as seen in automatic segmentation processes of retinal OCT.

5.3 Future Directions

Future studies will focus on large scale manufacturing of spray dried materials and improvement of preclinical models. The fabrication of spray-dried PLGA MS may be improved to increase the aqueous dispersibility with gel. This may be accomplished by adding non-ionic surfactants to reduce aggregation of particles (e.g., leucine [232], triton-100 [233]). Comparing the rheology of microspheres/gel when embedded with future particles to the current SD-CMS formulation would provide additional insight to material properties. For the rabbit model, an early-timeframe ocular pharmacokinetic study with increased sample size would compare a single dose of cysteamine eyedrops to a single dose of microspheres/gel at a shorter time scale (e.g., 0.5 mins, 10 mins, 30 mins, 60 mins). In doing so, we would obtain cysteamine half-life, max concentration, and clearance mechanism [234] and potentially reduce variability in pharmacokinetic drug dispositions [199]. Lastly, to improve longitudinal OCT efficacy studies on the CTNS (-/-) mouse, a controlled humidity chamber would be added to maintain an ideal environment to prevent drying of the cornea [228]. An alternative to using a Tegarderm™ patches would involve surgically sewing the eyelids partially with sutures and adding a drawstring to open and close the eyelids for daily gel administration [230]. OCT post-image processing may also be improved by developing automatic segmentation based on deep-learning algorithms [235]. One such network utilizes human OCT images and neural networks to distinguish corneal layers [236]. This may be extended

similarly by feeding the neural network with inputs from OCT volumes from our wild type mice and CTNS (-/-) knockout mouse. After which, including a pixel threshold to the images similar to our studies may support distinguishable pixels between intense, reflective cystine crystals and darker corneal structures. As an extension of the preclinical animal studies, performing iterative usability studies with an applicator designed for our materials can potentially bring light to patient's experiences with our technology.

Usability and feasibility studies are an important research goal for translational technology and is required by the FDA further down the translational pipeline during clinical trials [237]. One area for usability consideration our research is the design of an applicator for the microsphere/gel technology. A usability study exploring an applicator prototype and its feasibility on a silicone mannequin head with replaceable eyes and eyelids [238] can be used to evaluate patient experience with our technology during topical administration. Participants can be recruited through the annual conference held by the Cystinosis Research Foundation to identify key clinical stakeholders (e.g., clinicians, nurses, ophthalmologists,) and community stakeholders (e.g., patients and family members). Mixed methods studies would seek to quantify squeezing force and dispensing time [239] while also evaluating participant's experience with qualitative eyedrop satisfaction questionnaires [240], [241]. This exploratory study would offer user informed technical specifications for the applicator, highlight any barriers to translation to pediatric patients, and incorporate user feedback for future applicator devices.

Beyond using cysteamine to treat cystinosis, cysteamine has been researched to examine the drug's antimicrobial properties for cystic fibrosis [242], prevention of oxidative stress that contribute to neurodegenerative and neuropsychiatric disease [243] and inhibition of SARS-COV-2 variants of concern [244, 245]. An oral formulation of cysteamine and an inhaled nebulized form

(Lynovex®) has been marketed as a combination mucolytic-antibiofilm-antimicrobial agent. This formulation has been investigated *in vivo* when directly administered to the lungs of mice [242] and has on going exploratory clinical trials in adults with cystic fibrosis [246]. The antiviral activity of cysteamine against multiple variants of SARS-CoV-2 was confirmed *in vitro* and the compound is likely reducing disulfide bonds in the spike proteins of variants, inhibiting binding of the receptor binding domain [245]. In addition to antimicrobial and antiviral properties, cysteamine mitigates oxidative stress and its oxidized form cystamine mitigates inflammation [243]. Oxidative stress and inflammation contribute to upregulation of neuroprotective pathways involving brain-derived neurotrophic factor and nuclear factor erythroid 2-related factor 2 signaling [243]. These pathways have been associated with the progression of Huntington's diseases and led to a randomized clinical trial of oral delayed release cysteamine bitartrate in humans for 18 months [247]. Clinical trials of cysteamine for Huntington's disease have been largely unsuccessful – with researchers suspecting that patients who were enrolled were in late stages of disease progression and oxidative stress was beyond prevention [243, 247]. However, promising data in reformulation of cysteamine into dendrimers ameliorate autophagy deficits in cystic fibrosis animal models, which is suspected to also impact autophagy in brain tissue [248]. These studies support evidence on cysteamine formulation into different drug vehicles that may offer improvement to current cysteamine formulation. Overall, our spray dried methodologies for cysteamine encapsulation may be extended to develop aerosolized particles that increase the bioavailability of cysteamine in lung tissue for patients with cystic fibrosis and novel coronavirus. Lastly, to improve targeted delivery for oxidative stress in Hunting disease, modification of PLGA with polyethylene glycol to obtain a copolymer particle can increase blood-brain-barrier diffusion [249] when administered through delivery routes to the brain, such as intranasal routes. Current research from our group utilizes our

microsphere and thermoresponsive materials to achieve otic drug delivery for antibiotic therapies [250] and paranasal administration of corticosteroids [251]. These recent studies lay the foundation for material compatibility and safety for exploring cysteamine delivery with our technology for the clinical applications in lung illnesses and neurodegenerative disease.

Appendix A Cysteamine Microsphere Formulation Trials and Candidate Formulation

Appendix A.1 Introduction

The target parameters for cysteamine microspheres for drug release, drug loading and release kinetics were based on clinical data and prescribed dosing of cysteamine eyedrops (Cystaran™). The current clinical dose of cysteamine hydrochloride (HCL) is 6.5mg/mL (equal to 4.4 mg/mL, 0.44% cysteamine). The recommended dosage is 1-12 eye drops a day, once per waking hour. The total amount of cysteamine in an eyedrop containing a volume of 50µL is is 0.325mg/drop (i.e. 6.5mg/mL x 1mL/1000µL x 50uL). At 1% absorption of eyedrops, 3.25µg is absorbed, with 10% absorption equating to 32.5µg. Based on these calculations, the total range of cysteamine is 325-3900 µg/day. An ideal controlled release formulation would release 3.25-39µg/day (1% absorption) or 32.5-390g/day (10% absorption). The time frame for delivery was suggested to be 1 week, to retain familiarity of cysteamine shelf life, or up to 1 month. As such the anticipated goal, assuming 1 % absorption, was a release profile of 7 days at 20µg/day. The following sections present the iterations of PLGA microspheres and our rationale for the candidate formulation presented in Chapter 2. Several of the methodologies discussed in Chapter 2 are reference throughout this section and were omitted for conciseness. For clarity on methodologies used for characterization of cysteamine microspheres (i.e., morphology with SEM, drug release, HPLC detection, DSC, and NMR), refer to Chapter 2.

Appendix A.2 Materials and Methods

All materials were sourced from Sigma Alrich (St. Louis, MO) unless otherwise specified.

Appendix A.2.1 Water in Oil in Water Double Emulsion

A water-in-oil-in-water (W/O/W) double emulsion was first performed according to previously established protocols [137]. Double emulsion cysteamine microspheres (DE-CMS) were fabricated by adding 200mg of poly(d-lactic-co-glycolic) acid (PLGA) (502H MW 7,000-17,000) to 4mL of dichloromethane. To this mixture, 200μL of 1g/mL cysteamine HCL in deionized water was added. The dissolved drug and polymer solution was sonicated for 10s at 30% amplitude (EpiShear Probe Sonicator, Active Motif, Carlsbad, CA) followed by homogenization in 60mL of 2% poly(vinyl alcohol) (PVA) (W2) with 13.2% sodium chloride (7.9g NaCl in 2% PVA) e ((w/v) (Polysciences, Warrington, PA) for 1 minute at 2300 rpm (Silverson L5M-A, East Longmeadow, MA). The double emulsion was added to 80mL of 1% PVA and stirred at 600rpm for 3 hours. Resulting microspheres were washed 4 times by centrifugation, then resuspended in deionized water with, flash frozen in liquid nitrogen, and lyophilized for 48 hours (Speedvac Freezone, Labconco, Kansas City, MO). Blank, cysteamine free microspheres were fabricated by substituting cysteamine with DI water. The release of cysteamine from microspheres were determined by measuring releastes with HPLC.

Appendix A.2.2 Solid in Oil Single Emulsion

Aa an alternative to the high aqueous environment of double emulsions, a solid in oil in oil (S/O) emulsion was conducted to eliminate cysteamine diffusion during fabrication. Solid in oil cysteamine microspheres (SE-CMS) were first explored by attempting to micronize cysteamine [160]. Sonication at a high amplitude (>60%) was performed and resulted in degraded cysteamine HCL, that was a pungent smelling. Therefore, 50 mg of cysteamine HCL was partially solubilized in 1 mL of a co-solvent composed of 90:10 (v/v) acetonitrile: deionized water. An oil phase consisting of 200mg of PLGA (RG 502H) in 4mL of acetonitrile was mixed. 250 µL of the partially solubilized cysteamine (~50mg/mL) was added to the oil phase (PLGA/acetonitrile). A secondary oil phase consisted of 40 mL of mineral oil and 200µL of Span-80 was mixed and stirred on a magnetic rotator at 600 RPM. Then, the S/O emulsion was slowly added wise into the secondary oil phase while under stirring. The emulsion was stirred for 3 hours, centrifuged at 1000 RPM, flash frozen and lyophilized. Materials were then characterized with SEM.

Appendix A.2.3 Double Emulsion, Salt Balance, and Salt Washing

Cysteamine microspheres were fabricated following the double emulsion procedure. For these microspheres, a initial drug content from cysteamine was lowered from 1g/mL to 200mg/mL to reduce the osmolality of the initial water phase. A 200mg/mL Cysteamine HCL solution was measured with an osmometer and resulted in 2850mOsm/kg. The external water phases consisting of PVA, were then salat balanced. A 2% PVA 60 mL solution was mixed with 8.3%, 4.99g NaCL (w/v). A 1% PVA 80 mL solution was mixed with 8.3%, 6.66g NaCl. The polymer phase was mixed by adding 200mg of poly(d-lactic-co-glycolic) acid (PLGA) (502H MW 7,000-17,000

Sigma Aldrich, St Louis, MO) in 4mL of dichloromethane for the oil phase. To this mixture, 200μL of 200mg/mL cysteamine hydrochloride in deionized water was added. The dissolved drug and polymer mixture was sonicated for 10s at 30% amplitude followed by homogenization in 60mL of 2% poly(vinyl alcohol) (PVA) (W2) with 8.3%, 4.99g NaCL (w/v) for 1 minute at 2300 rpm (Silverson L5M-A, East Longmeadow, MA). The double emulsion was added to 80mL of 1% PVA with 8.3%, 6.66g NaCl (w/v) stirred at 600rpm for 3 hours. Resulting microspheres were washed with deionized water 4 times by centrifugation, then resuspension in deionized water, frozen, and lyophilized for 24-48 hours. A second batch of DE-CMS were fabricate following the same protocol but instead washed with 20% NaCL (w/v) during the washing and centrifugation steps. Microspheres were characterized with SEM, HPLC, and DSC when mixed with pNIPAAm gel.

Appendix A.2.4 Spray Dried Manufacturing and Candidate Formulation Characterization

Several spray-drying trails were conducted in partnership with Dr. Gary Hollenbeck at the University of Maryland Pharmacy Lab. The spray drying manufacturing process utilizes a standard cyclone (upper and lower) and collection vessel (Figure 32). The spray-dried materials in each chamber were collected and analyzed for morphology and drug loading using SEM and NMR.

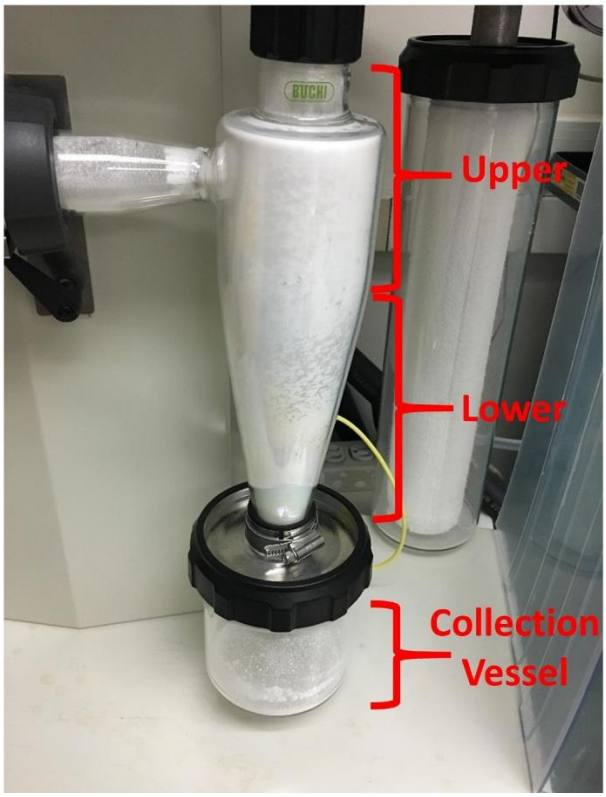

Figure 41. Spray-dried standard cyclone and collection vessel containig cysteamine microspheres

Appendix A.2.5 Sterilization of Candidate Spray Dried Formulation

Spray-dried cysteamine microspheres were weighed and placed in sterilized amber vials in a protective glove box (Fisher Scientific, Hampton, NH) under inert nitrogen gas. Amber vials with samples were capped and sealed with parafilm. Samples were shipped and stored at 4°C for 16 days prior to sterilization with -25kGy ± 10% for 48 hours using a gamma irradiator (Sterigenics U.S, LLC, USA). The drug loading with NMR was compared between an internal control (N=1) that was not shipped and sterilized, to sterilized samples (N=10)

Appendix A.3 Results

Appendix A.3.1 Double Emulsion Microspheres with Low Drug Loading and 7-Day Release Kinetics

Double emulsion cysteamine microspheres (DE-CMS) were spherical and in between 5-10 µm in size (Figure 33A). HPLC analysis of release medium indicated a total of 0.5 µg/mg cysteamine /DE-CMS over a 7 day period (Figure 33B). The release profile was pseudo-linear with a burst release within the first day of release, approximately 3 µg cysteamine in 10 mg of DE-CMS. Efforts to reformulate for higher drug loading were attempted by following encapsulation strategies for small hydrophilic drugs [Ramazani et al 2016].

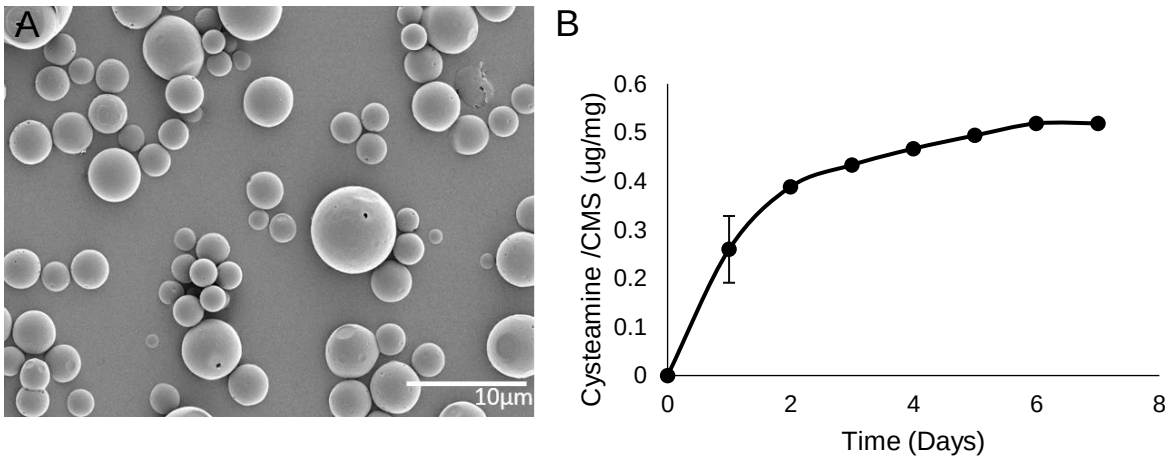

Figure 42 Scanning electron microscopy image of double emulsion cysteamine microspherfs (A) and release profile with HPLC analaysis (B). Data for release is mean ± standard derviation.

Appendix A.3.2 Solid in Oil in Oil PLGA structures

Solid oil and oil cysteamine microspheres produced large structures of PLGA and cysteamine after lyophilization. Scanning electron microscopy revealed interconnected PLGA microspheres. Cysteamine content was not verified and solid oil and oil trials were discontinued.

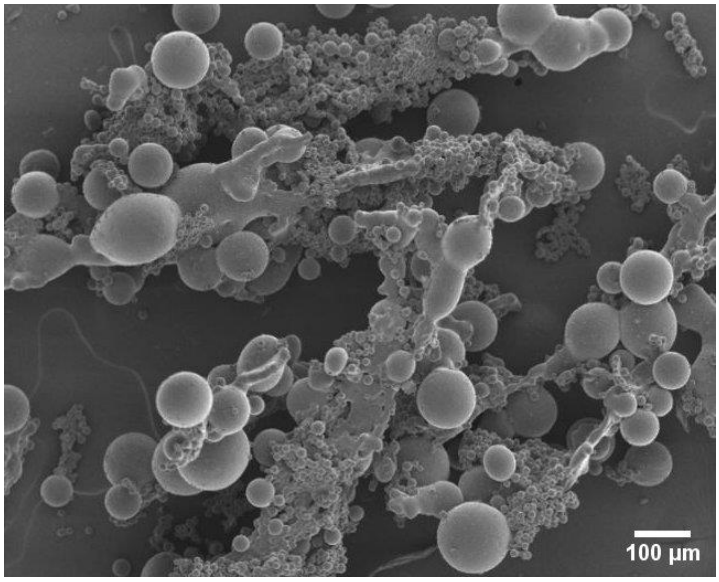

Figure 43 Scanning elecron micrscopy of solid-oil-in-oil of cysteamine-PLGA strucutures larger than 100µm

Appendix A.3.3 Double Emulsions CMS with Salt Washing Release and LCST

Double emulsion cysteamine microspheres with a salt balance were fabricated. Their morphology and size (10-20µm) were characterized with scanning electron microscopy (Figure 25A). Cyseamine release from cysteamine microsphers achieved 20µg/day of drug release at day 1 (Figure 35A). There was low magnitude of cysteamine release on subsequent days up to day 9. However, the target of drug per day was achieved for 1 day.

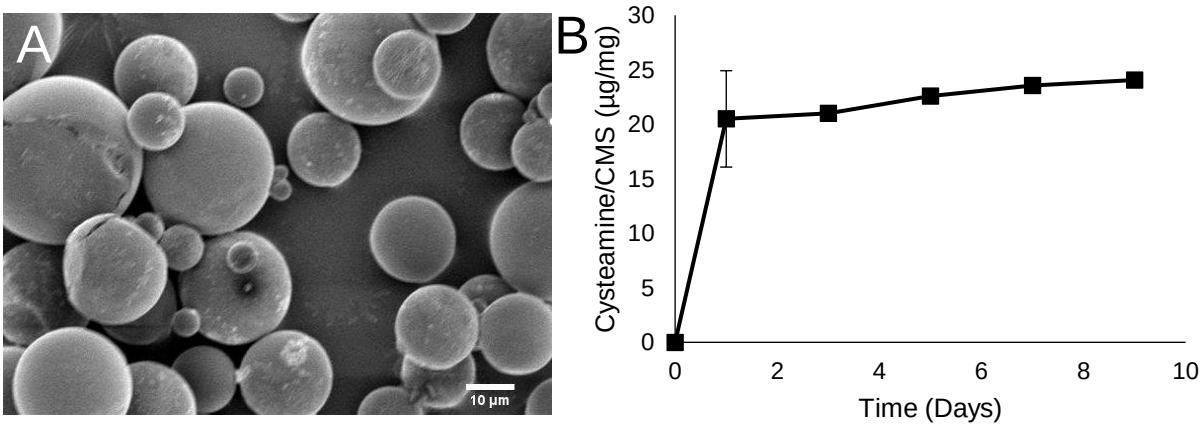

Figure 44 Salt balance double emulsion microspheres (A) and release profile analyzed with HPLC (B). Data is represented as mean ± standard deviation

Drug loss in the washing steps was confirmed at all four washing steps (Figure 36). A salt balance was added to the washing step and drug loss was reduced at steps two through four. These experiments indicated that cysteamine diffusion occurred when cysteamine microspheres immediately made contact with water during fabrication.

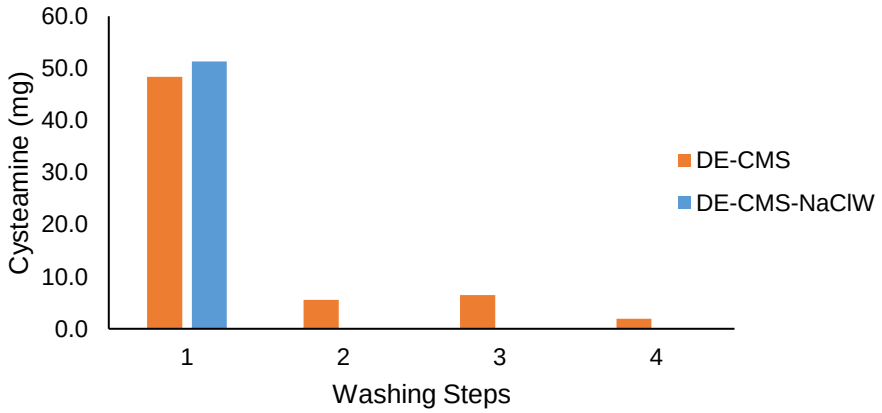

Figure 45 Cysteamine drug loss during washing steps and compared to the washing steps with sodium chloride (DE-CMS-NaClW)

The double emulsion cysteamine microspheres with the sodium chloride washing steps (DE-CMS-NaCLW) were characterized with scanning electron microscopy. DE-CMS-NaClW had uniform size (10µm, Figure 37A). Cysteamine drug loading of double emulsion cysteamine microsphers without sodium chloride washing (DE-CMS) and DE-CMS-NaClW were compared (Figure 37B). The addition of the washing steps reduced the variation of between samples (N=3) and had drug loading at the target of 20 µg/day.

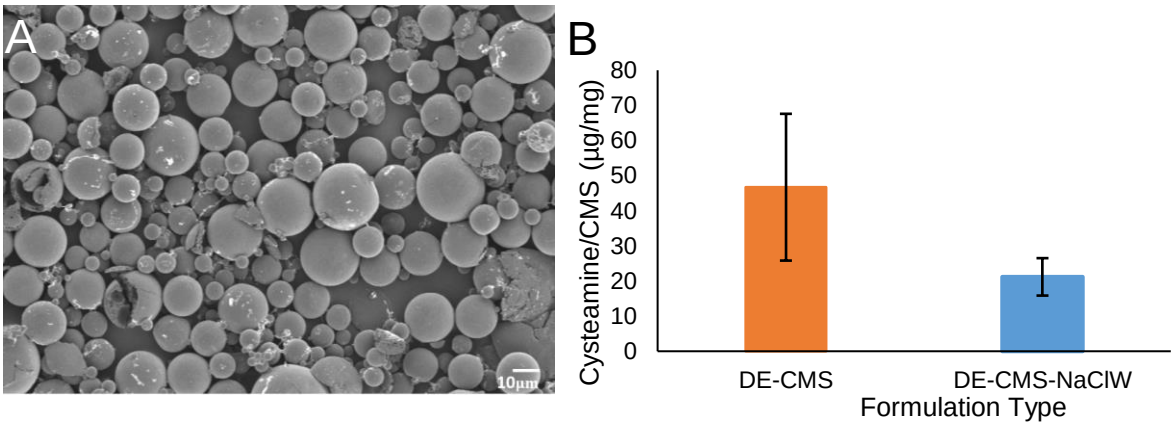

Figure 46 Scanning electron microscopy (SEM) of Double Emulsion fabrication of cysteamine microspheres with sodium chloride washing (DE-CMS-NaCLW) (A) and cysteamine loading (µg/mg) comparison to Double emulsion fabrication of cysteamine microspheres (without sodium chloride washing) (DE-CMS) (B). Data is represented as mean ± standard deviation.

The candidate double emulsion formulation with washing (DE-CMS) was incorporated into pNIPAAm gel at a ratio of 10mg to 100µL. Cysteamine-free microspheres (DE-BLANK-MS/Gel) were also mixed into gel at the same ration. Differential scanning calorimetry (DSC) was performed to determine the lower critical solution temperature (LCST) of each mixture. The LCST gel without microspheres (pNIPAAm) was compared to each material. The LCST was lowered

for the formulations (27°C for DE-BLANK-MS+Gel, and 20°C for DE-CMS+Gel). These LCST were lower than 34°C pNIPAAm alone. The LCST of the formulations were below ocular surface temperatures and incompatible for topical administration to the eye. In the literature, [Zhang et al 2007] explored the relationship of different salts on LCST of pNIPPAm, including sodium chloride which lowered the LCST.

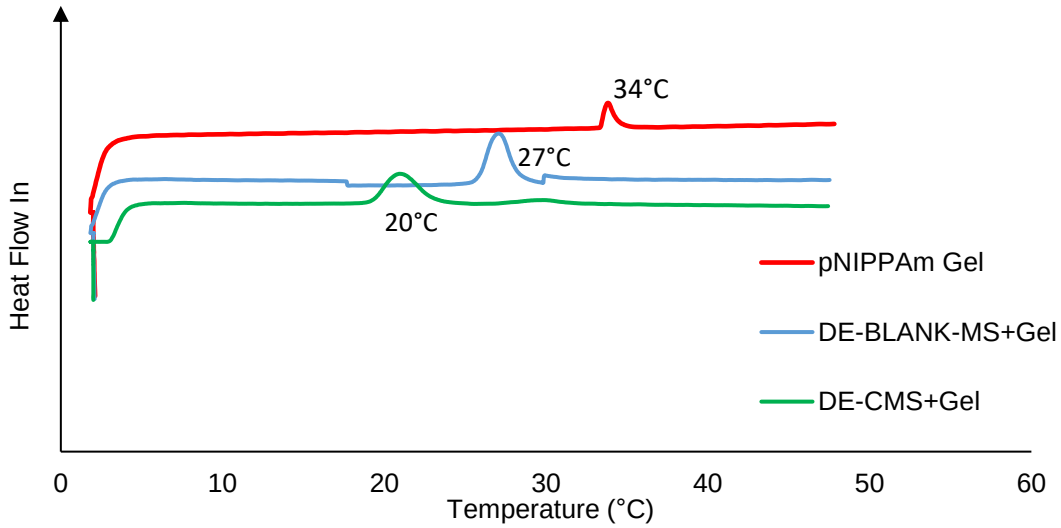

Figure 47 DSC of DE-CMS after washing and the addition of sodium chloride reduced the LCST below ocular surface temperatures

Appendix A.3.4 Spray Dried Microspheres Characterization and Candidate Selection Vessel

Scanning electron microscopy of material from upper cyclone (Figure 39A), lower cyclone (Figure 39B), and collection vessel (Figure 39C) indicated microspheres at 1-5µm in size with irregular morphology.

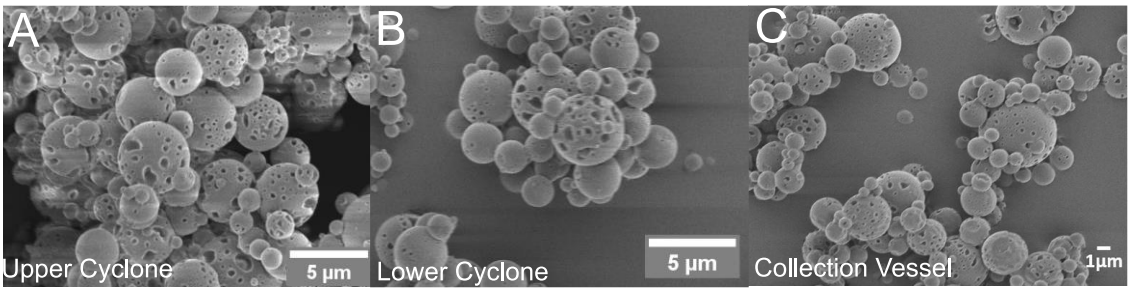

Figure 48 Scanning electron micrscopy of spary-dried microspheres manufactured with a cyclone and collection vesse

SD-CMS at each chamber was evaluated for drug loading and resulted in equivalent drug loading (270 µg/mg, Figure 40) from all materials, regardless of location after manufacturing.

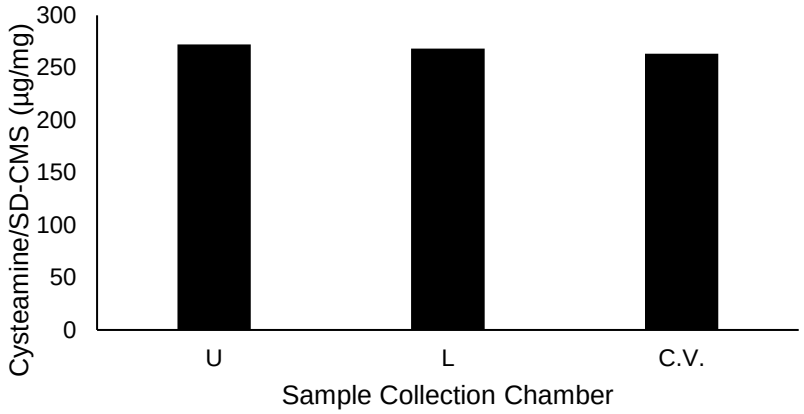

Figure 49 Cysteamine loading in upper cyclone (U), lower cyclone (L) and collection vessel (CV). The data represent mean ± standard deviation (N=3).

The candidate SD-CMS from the collection vessel was compared to previous double emulsion formulations and achieved a 10-fold increase in drug loading per mass of microsphere (Figure 41). The SD-CMS was further characterized and discussed in Chapter 2.

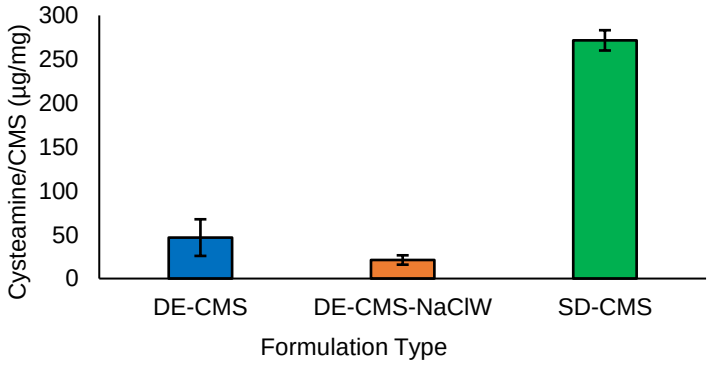

Figure 50 Comparison of cysteamine loadin in optimized cysteamine micropheres. The data represents the mean ± standard deviation of N=3.

Appendix A.3.5 Sterilization of Spray Dried Microspheres

Sterilized samples of SD-CMS had a reduction in 3% drug loading compared to the internal control (Figure 42). The time from fabrication, storage, and shipping resulted in 16 days of varying temperatures. As such, while gamma irradiation may have reduced the drug content by 3% when comparing to the internal control, which was stored at 4°C for 16 days, the loss of drug may have also resulted from cysteamine instability during shipping (temperature greater than 25°C).

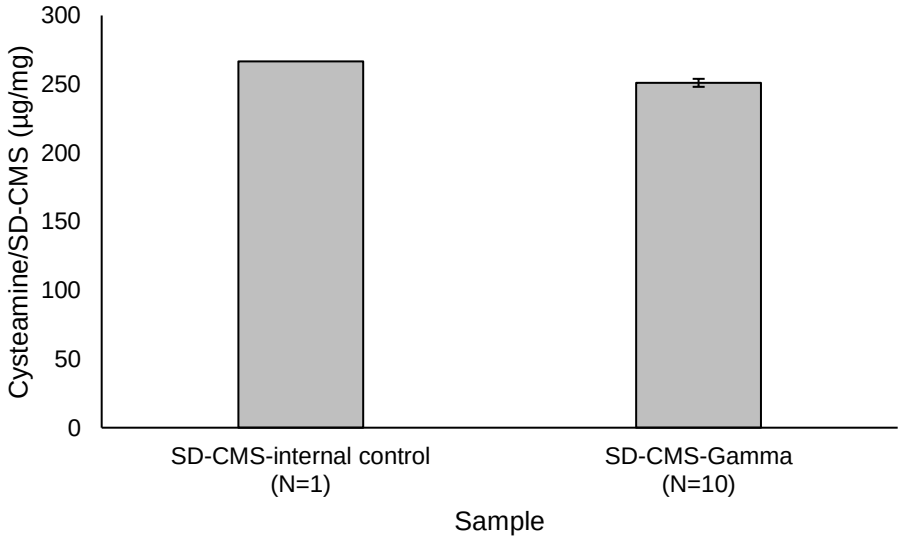

Figure 51 Cysteamine loading in spray dried micosphers (SD-CMS) after gamma sterilzation. The data for SD-CMS-Gamma represent the mean ± standard deviation for N=10 samples.

Appendix B A Controlled Release Formulation of a Small Molecule for Inherited Retinal Degeneration

Appendix B.1 Introduction

The research motivation and techniques utilized to develop ocular drug delivery systems for cystinosis, an inherited rare disease, can be extended for rare diseases that impact the retina. A collaboration with Dr. Yuanyuan Chen was formed to develop a controlled release system of a small molecule chaperone of rod opsin (YC-001) for inherited retinal degeneration. YC-001 was discovered by Dr. Chen to target P23H rod opsin, a protein that is commonly mutated among autosomal dominate retinitis pigmentosa patients (adRP) [252, 253]. YC-001 is effective in rescuing P23H-opsin transport in retina degenerated mice, but suffers from a short half-life at 34.5 min [252]. Thus, developing a controlled release system that release YC-001 over an extended time may afford longer drug presentation after intravitreal injection. While YC-001 remains in the investigative therapy pipeline, there is a substantial clinical need to develop effective treatments for adRP and similar inherited retinal disorders with rod opsin mutations like Stargardt disease [254] and Leber congenital amaurosis [255].

Appendix B.2 Materials and Methods

YC-001 was received from Dr. Yuanyuan Chen.. Dimethyl sulfoxide (DMSO), dichloromethane (DCM), and PLGA were obtained from Sigma Aldrich (St. Louis, MO, USA). Poly-vinyl alcohol (PVA) was obtained from Polysciences

Appendix B.2.1 YC-001 Single Emulsion Encapsulation and Characterization

YC-001 is highly water insoluble and was compatible with DMSO and DCM for a co-solvent solution capable of solubilizing both YC-001 and PLGA. Therapeutic amounts of YC-001 were experimentally determined in a P23H mouse model to be 700 picomoles of YC-001 per day, which equates to 0.197 µg of YC-001 (MW 282.7 g/mol) . This value guided initial formulation parameters along with the ability to inject microspheres in a homogenous aqueous solution with a 33-gauge needle used specifically for intravitreal injections in murine models (Hamilton Company, Reno, Nevada, USA). Hamilton needs are capable of injecting up to 1µL of solution. In our previous experience, a homogenous mixture of microspheres in phosphate buffer saline solution is composed of 10 mg of microspheres per 100 µL of saline solution. Therefore, 1 µL would contain 0.1mg of microspheres. Ideally, 1.97 µg YC-001 per mg of microspheres would afford therapeutic drug levels to the mouse retina.

To fabricate microspheres, 200mg of PLGA (MW 24,000-38,000 kDa (503) and 38,000-54,000 kDA (504)) were dissolved in 4 mL of DCM. To this solution, 200 µL of a 20 mg/mL YC-001/DMSO was added. The solution was then placed into a 2% PVA solution (60 mL) and homogenized for 1 min at 2300 RPM. The emulsion was then mixed into a 1% PVA solution

(80mL) for 3 h to allow residual DCM to evaporate. The microspheres were then washed via centrifugation with deionized water prior to lyophilization for 48 hours (Virtis Benchtop K Freeze Dryer, Gardiner, NY). Dry microspheres were stored at -20°C until use. Blank microspheres (Y-BLANK-MS) were fabricated following the same method with the exclusion of YC-001 and only 200µL of DMSO in the initial solution.

YC-001 loaded microspheres (YMS) were characterized for average size and surface morphology using volume impedance measurements (Multisizer 3 Coulter Counter, Beckman Coulter, Indianapolis, IN) and scanning electron microscopy (SEM, JEOL 6335 F Field Emission SEM, Peabody, MA), respectively. The volume average microsphere diameter was determined for a minimum of 10,000 microspheres.

Appendix B.2.2 YMS Drug Release and HPLC Detection

YC-001 release studies were performed to determine the release behavior of YC-001 from microspheres. Lyophilized YMS (10 mg) were suspended in phosphate buffered saline (PBS) and incubated at 37 °C on a rotator. These samples were centrifuged for 5 min at 1000 rpm and the supernatant removed for analysis of YC-001. The supernatant was then replaced with fresh PBS and samples were vortexed briefly prior to additional incubation. The same procedure was repeated for Y-BLANK-MS. YC-001 concentration in supernatant samples was determined via high performance liquid chromatography (HPLC). Briefly, the samples were diluted with methanol and then injected onto Eclipse XDB-C18 column (4.6 x 150 mm, 5 µm) (Agilent Technologies) equilibrated with solvent composed of 30% acetonitrile in water (v/v), 0.1% formic acid. YC-001 was eluted in a gradient of acetonitrile in water (30 – 100%) developed within 15 min at the flow rate of 1 mL/min, detected at 334 nm, and quantified by correlating peak areas with known

quantities of an original YC-001 synthetic standard. Background signal from Y-BLANK-MS (no drug) was subtracted prior to reporting the results of the average of n = 3 YMS samples ± standard deviation.

Appendix B.3 Results

YMS and Y-BLANK-MS were fabricated and resulted in spherical morphology after lyophilization as confirmed with scanning electron microscopy (Figure 52). The size of YMS formulations (Figure 53B) were within similar ranges between 503 (20.03 ± 5.8 µm) and 504 (17.63 ± 7.7 µm) formulations at a homogenization speed of 2300 RPM. YMS formulations released YC-001 at similar drug levels (0.12 µg/mg) when normalized to the mass of YMS during release studies (Figure 53A).

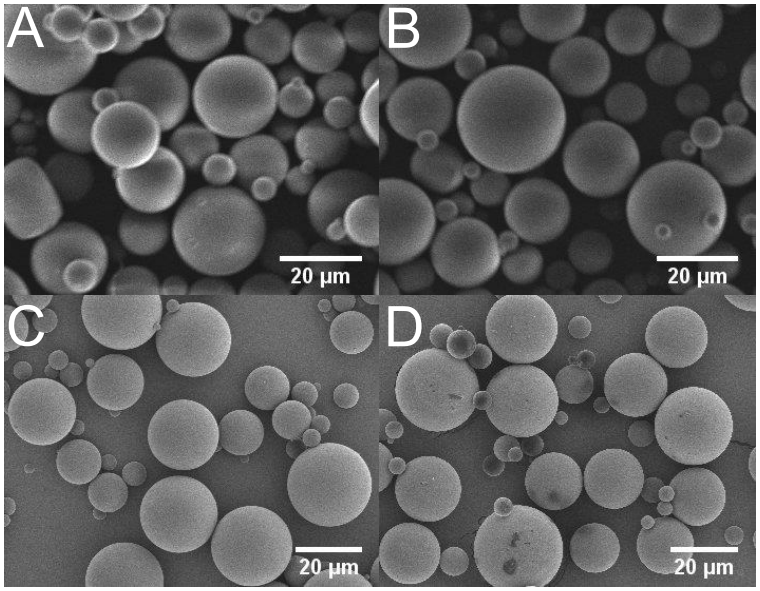

Figure 52. Microsphere formulations fabricated for YC-001. A) Y-BLANK-MS 503, containing no YC-001, B). YMS 503, C) Y-BLANK-MS 50, cotaining no YC-001 and 4 D) YMS 504. Scale bar 20 µm.

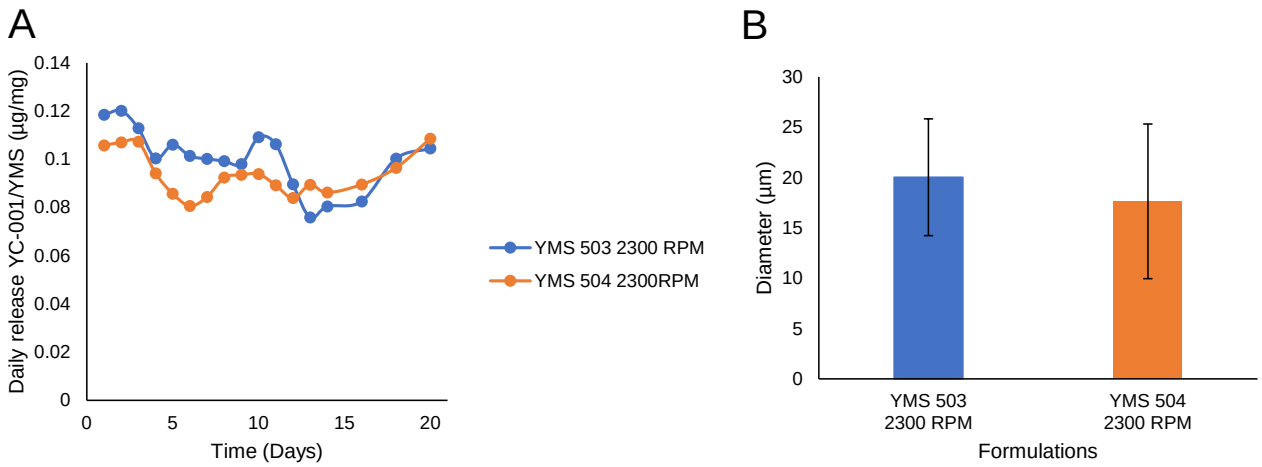

Figure 53 Release profile of YC-001 from YMS formulations (A) and YMS diameters (B). Data are presented as mean ± standard deviation.

Appendix B.4 Discussion

YC-001, an investigative small molecule for inherited retinal degeneration treatment, was successfully encapsulated in PLGA microspheres to improve the delivery of the drug when injected intravitreally. PLGA as a controlled release material for drug delivery to the posterior segment is a widely studied field [148, 256] with specific studies investigating retinal drug delivery of resveratrol from PLGA nanoparticles for age related macular degeneration [257] and tauroursodeoxycholic acid from PLGA microspheres for retinal degeneration in P23H rats [258]. While some studies explored the potential toxicity of microsphere starting materials (e.g. DCM, DMSO organic solvents) [259] and PLGA degradation products to retinal cells [260], there is substantial potential in tailoring candidate PLGA particle formulations for safe and efficacious treatment. As such, to improve the half-life of YC-001, we developed PLGA microspheres that release YC-001 over 20 days *in vitro*.

Based on the daily release of YC-001, there was no difference in magnitude of release and the release kinetics remained the same between 503 and 504 (Figure 53A). The magnitude of release was lower than our target drug release (0.12 µg/mg < 1.97 µg/mg), however we observed drug presentation for 20 days in *vitro*. Additionally, the size of microspheres at approximately 20 µm are compatible with the inner diameter of Hamilton needles (0.108 mm) and share similar sizes to intravitreally injected microspheres [258].

To improve upon preliminary YMS formulations, increasing the magnitude of drug release would support translation to a mouse model of retinal degeneration. Ongoing studies are investigating the fabrication of YMS at a homogenization speed of 7000 RPM to reduce the size of microspheres, thereby decreasing their surface area and potentially increasing the rate of PLGA degradation *in vitro*. Furthermore, *in vitro* release assays can harness the poor water solubility of YC-001 by including non-ionic surfactants (e.g sorbin oleate 80, polysorbate 80) in the release medium as performed for hydrophobic drug releases assays [261]. Ideally, the release profile from a candidate YMS formulation would be investigated in simulated vitreous humor [262] or within the proposed mouse model of P23H [263].

Appendix B.5 Conclusion and Future Directions

In summary, YC-001 was encapsulated in PLGA microspheres and tailored for compatibility with intravitreal injections in a mouse model of retinal degeneration. *In vitro* studies resulted in YMS formulations capable of releasing YC-001 over 20 days with a magnitude of drug release below our target drug levels. Thus, future work includes strategies to improve the magnitude of drug release *in vitro* and examining the ability to inject a candidate formulation into

a mouse model. Additionally, to test the therapeutic effect of YC-001 from YMS *in vivo,* mice injected with YMS would be observed over the course of drug release for a reduction in retinal degeneration with a combination of posterior segment imaging strategies including optical coherence tomography for retinal layer sizes [264] , fundus scope imaging for macula health [265], and electroretinography to evaluate visual activity [266].

Appendix C Integrating Public Health Topics in Drug Delivery Education

As part of continued training in the field of controlled drug delivery, Dr. DiLeo and I collaborated on a teaching-as-research project in an undergraduate course entitled “Controlled Drug Delivery”. This work was in fulfillment of the requirements for the Associate, Practitioner, and Scholar certification through the Center for Integrating Research, Teaching and Learning and the Engineering Education Research Center. Dr. April A. Dukes served as the scholarly teaching mentor of this project. In short, we utilized the experience of cystinosis therapies and lack of compatible therapies as a case study for inclusive teaching practices in the STEM classroom and evaluated student interest. We published our findings in the annual American Society of Engineering Education conference and can be found at Jimenez, J., & Dukes, A. A., & Fedorchak, M. V. (2021, July), Integrating Public Health Topics in Drug Delivery System Education Paper presented at 2021 ASEE Virtual Annual Conference Content Access, Virtual Conference.

Appendix C.1 Introduction

Health disparities (HD) are differences in health outcomes and their causes among groups of people. Often, HD are preventable, yet certain people have an extra burden of disease, injury, or violence [267]. Historically marginalized racial, ethnic, and other population groups (e.g., age, sex) experience differences in health outcomes and opportunities for optimal healthcare [267, 268], even when groups and their counterparts are controlled for socioeconomic status, education, and access [269, 270]. In the U.S., the federal Racial and Ethnic Health Disparities Initiative

documented HD in the following areas: infant mortality, cancer screening and management, diabetes, HIV/AIDS, and adult and child vaccinations [270]. Using vision health as an example, this is reflected in U.S. Latinx populations (Mexican-Americans) who have a prevalence of diabetic retinopathy that is 2 to 2.5 times greater than other U.S. population groups (Caucasian population), despite diabetic retinopathy arising as a complication of diabetes that can be managed and delayed with timely intervention [271, 272]. Furthermore, age is a known risk factor for primary open angle glaucoma increasing from 0.6% at ages 40-49 to 8.3% at age 80 or older, with African Americans being 4 to 5 times more likely to have glaucoma than European Americans [273-275]. The root cause of HD and health inequities are traditionally taught in the disciplines of humanities, public policy, public health, social sciences (e.g., anthropology, economics, sociology), and nursing [276]. Recently, inclusive teaching strategies in STEM education curriculum have incorporated HD topics with the motivation to bring awareness to and address long-standing HD using STEM principles and technology.

The disciplines of biology and biomedical engineering have attempted to increase the access of HD courses by integrating HD topics into undergraduate coursework, particularly at minority serving institutions. For example, at the historically Black college and universities University of the District of Columbia, an elective biology course for junior-level biology majors integrates the physiological determinants of health and social determinants of health (SDOH) via seminars with guest speakers who research HD [276]. At City College of New York, a Hispanic serving institute, their undergraduate biomedical engineering program engages students in HD challenges with established curricula on HD modules, undergraduate research initiatives in HD, and design projects focused on HD [277], [278]. Often, these two disciplines include students on a premedical track, which has also encouraged exposure to HD and SDOH in medical curriculum

[279] engaging potential medical students as socially responsible physicians that may mitigate health inequities in their future profession [280, 281]. As such, including HD and SDOH topics into established coursework where concepts of biology, engineering and medicine intersect, may pose an opportunity for engineering students to raise their awareness on HD and potentially innovate solutions towards reducing long-standing HD. A relevant topic in the field of engineering is the design of DDS to improve the safety and efficacy of medicine for human health and disease.

The field of DDS design using principles of controlled release is a well-established research and educational component to engineering programs. Engineers, guided by clinical collaborators [282], design DDS to improve the delivery of a drug (e.g., cell targeting, increased stability, reduced toxicity) by utilizing the engineering fundamentals of mass transfer, reaction kinetics, thermodynamics, and transport phenomena [283]. Using natural (animal or plant derived) and synthetic materials (polymers), engineers fabricate, characterize and evaluate novel DDS in research settings to maximize therapeutic efficacy and minimize side effects. This process is accomplished by impacting absorption, distribution, metabolism, and elimination (ADME) of a drug compound [283]. A main research focus is emphasized on the translation of DDS as therapies into society. This emphasis has led to partnerships across universities, medical systems, professional societies [284], and industry sectors [285]. Collaborations from these stakeholders support the translation of novel DDS from laboratory or "benchtop" research through commercialization, clinical trials and regulatory bodies and onto the patient, or "bedside" [286]. As a multidisciplinary field, researchers have contributed to engineering curriculum by developing drug delivery courses to engage engineering students with varied interest in medicine and the desire to pursue biomedical careers in pharmaceutical industries, research intensive institutions, and medical schools [287]. Historically, students enter this course with prior knowledge of

chemical engineering fundamentals, and are instructed by bioengineering and chemical engineering research faculty with experience in clinical translation

Appendix C.2 Methods

Appendix C.2.1 Institutional Review Board Approval and Study Design

The protocol for this work was evaluated and approved by the University of Pittsburgh Institutional Review Board under the protocol: STUDY200010154. An educational exemption was granted to evaluate student self-identified responses to surveys. Students (N=26) were surveyed prior to and after the implementation of HD and SDOH components within the course. Questionnaires captured student demographics, awareness of topics, and 5-point Likert scales evaluating students' familiarity, perceived importance, interest, and perceived relevance of HD and SDOH for drug delivery. For the purposes of the work presented in this appendix, the interest of lecture topics and case studies are presented and discussed in the results section.

An asynchronous online-lecture was developed by course instructors in which students were exposed to public health topics of HD and SDOH. Students were tasked to answer a pre-survey on their engineering social agency awareness and familiarity on HD and SDOH. An infographic of a research technology cycle [288], was used to outline biomedical advances, potential societal risks and future implications for health and medicine. This cycle explained DDS as biotechnology and biomedicine, their impact on impact on society (access, affordability, governance, regulation) with case studies supporting future implications (prevention, prediction, early detection, improving care delivery). As part of this cycle, HD and SDOH were introduced

following pedagogical frameworks in biomedical engineering curriculum [277, 278]. and public health [289]. The framework was utilized by instructors to examine peer-reviewed literature on agents of HD as case studies and relate them to clinical trials, genetic screening, engineering technology, health care policy and access, quality of care, and historical societal factors [278]. A list of SDOH) was developed from existing literature by instructors and introduced to students in the module. The SDOH list [290, 291], was the main topic used to align traditional course content as potential root cause factors to HD. Case studies were selected by instructors to align the traditional course content to SDOH with rationale.

Appendix C.2.2 Cystinosis Case Study

For each case, we discussed the purposes of reformulation into new DDS and aligned them to SDOH factors. During the discussion of the case studies, an emphasis was made on the impact the implementation of the new formulations had on their specific patient populations using supporting literature. The first case, cysteamine extended release, is a therapy for pediatric patients with Cystinosis. Cystinosis is rare disease defined as impacting less than 2000 people in the US [292, 293]. With a low population, rare disease communities often face additional psychosocial, morbidity, and disability burden resulting from disparities in access to affordable drugs, therapeutic discovery, clinical best practices and surveillance development [294]. For the second case, an abuse deterrent formulation was developed to reduce the likelihood of patients crushing a tablet formulation for snorting or injecting [295]. This example was further empathized with public data on disparities regarding prescription pain relief overdose deaths between men and women [296]. The focus for the third case was on women and birthing people from Black and Latinx communities. People from Black and Latinx communities face disparities in unplanned

pregnancies compared to White and Asian counterparts despite the availability and implementation of long-acting contraceptives [297]. After the new content was introduced, students were then surveyed after the HD and SDOH module and evaluate for their interest in topics.

Appendix C.3 Results

A total of 25 students responded to the surveys. As indicated by response counts, a few questions were skipped or omitted by students. Percentages are calculated based on response count (N). For surveys students were prompted to respond to "These are a few topics covered in the lecture, please indicate how you felt about them." using a 5-point Likert scale (1- very uninteresting, 2- somewhat uninteresting, 3- neutral, 4- somewhat interesting, 5-very interesting). Greater than 68% of students ($N \geq 17$, response count $N = 24$) found the following topics "very interesting" or "somewhat interesting": relationship of technology and society, social determinants of health, social barriers of delivery, and case studies (Figure 54). In reference to case studies, students were asked to respond to the prompt "Three case studies were presented, please rank which was the most interesting to you." The oxycontin extended-release case study was reported as the most interesting (52% response count $N = 23$), followed by long-acting reversible contraceptive, and cysteamine extended release (Figure 55).

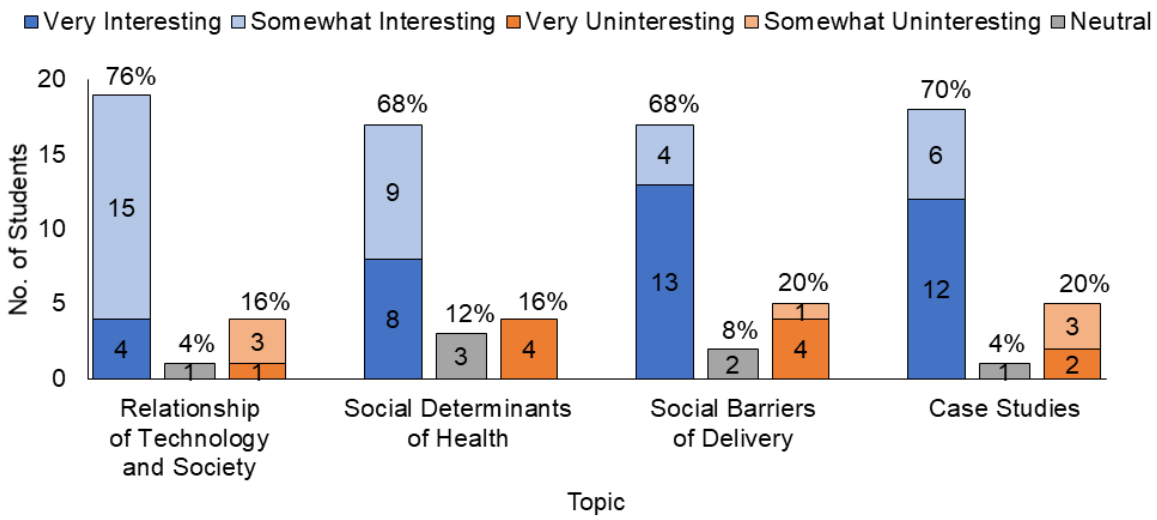

Figure 54 Student interest on public health topics. Percetanges were calculated based on the number of student responses (N=24).

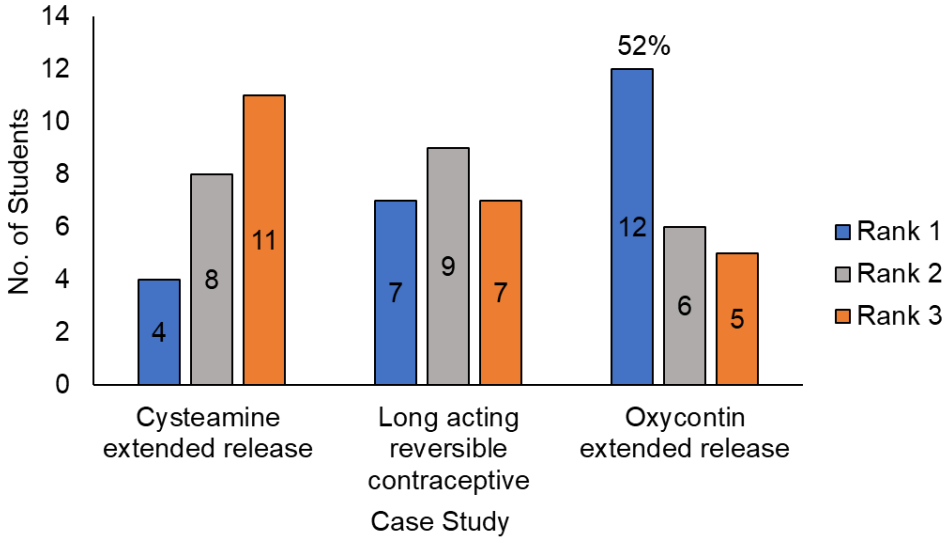

Figure 55 Case study ranking with Rank 1 as the most favorable of case studies presented. Percetange was calculated base on number of student responses (N=23)

Appendix C.4 Discussion

Authors from the National Academies of Sciences of the United States of America put forth a call to reimagine the role science has in the U.S. society and elevate the importance of inclusion within the scientific community [298]. The 2020 call describes the compounding effect the ongoing public health crisis has on STEM educational inequities. They further emphasize the need for broadening participation of historically marginalized people in STEM, and to provide experiential learning for all students, with an emphasis on creating scientific conversations with new perspectives that could lead to better health and social outcomes [298, 299]to Health Equity 2020]. Research has shown that inclusive teaching strategies, such as using examples that speak across gender, cultures, socioeconomic statuses, ages, and religions, may increases students' identity to course content [300, 301]. Because historically marginalized students in populations facing educational inequities also experience health inequities, creating inclusive teaching strategies that intersects public health content may engender students to course content. Research on STEM student motivation discuss utilizing content material and tasks that are personally meaningful and interesting to facilitate motivation in science [302]. In combination with motivation, research on student social agency and motivations of historically marginalized students in STEM argues that students from underrepresented groups (URGs) are underrepresented in STEM due to the lack of direct links to social justice, an area they find meaningful [303]. As a method for inclusive teaching, this qualitative study provided engineering students an additional HD and SDOH module to traditional controlled drug delivery content and evaluated their experience by survey collection.

The HD and SDOH module were stratified into the following components 1) research technology and society, 2) HD and SDOH, 3) Social barriers to drug delivery and 4) case studies.

These topics were received well by students as greater than the majority (68%) of students found the topics interesting (Figure 54). We also evaluated student's opinions on which case study they found most interesting. Diverse case studies included populations from rare disease communities (cysteamine extended release), Black and Latina women (long-acting reversible contraceptive implant), and those from communities experiencing violence and drug addiction (abuse deterrent pain relief hydrogel). These cases were then evaluated by students, of which 52% of the students (response count N=23) indicated the abuse deterrent pain relief hydrogel case study as the most interesting of the three cases (Figure 55). To our knowledge, there exists no such educational study that describes abuse deterrent pain relief delivery systems with a controlled release perspective. However, a study [304] describing the teaching of addiction to prescription pain relief drugs in pharmacy classrooms presented results from students that strongly agreed the course content helped them comprehend the science and practice to drugs of abuse and addiction. An assumption can be made to students are interested in talking about drug abuse and addiction.

The interests in these topics aligns with viewpoints from previous education studies in which engineering students were asked to gauge their understanding the role engineering has on society [305]. This study found that chemical-biological engineering students reported high understanding scores compared to students from other branches of engineering [305]. While we found similar trends in student interest and awareness of their role to society, our survey collection and design resulted in various response counts. Our study and survey collection occurred during a semester interrupted by the COVID-19 pandemic, which directly placed a spotlight on the importance of public health to the world. For safety, the class was moved to an online format midway through the course, which included the module on public health and survey, which may have added to the variability in response counts. Furthermore, a limitation to response data with

5-point Likert scales is the low sample size (N=25) and only obtained from one semester, and therefore not applicable for parametric statistical testing without group comparisons [306]. Despite these limitations, the survey results support interest public health perspectives of DDS impact to society.

Appendix C.5 Conclusion and Future Directions

The present study aimed to include a public health module in an undergraduate controlled drug delivery course, typically taken by bioengineering and chemical engineering students. Case studies on DDS and their impact on populations who face health inequities, were strategized to align course content to public health topics. Survey data indicated students were interested on the importance and relevance of health disparities and social determinants of health to their studies. As the field of engineering is becoming more interested in including people from historically marginalized populations, it is important to highlight the compounding effect health inequities may have on historically marginalized people within engineering curriculum. These methods may motivate historically marginalized students to identify with engineering design of DDS, and participate in developing solutions to reduce long-standing health disparities, and provide drug delivery educators with a novel strategy for inclusive teaching practices. To improve upon this work, implementing an active learning assessment requiring students to investigate society's response to acceptance of lipid nanoparticle delivery of mRNA -1273 against COVID-19 [307]. The technology for mRNA-1273 was developed by Moderna, Inc (Moderna Therapeutics), co-founded by a pioneer in the field of controlled drug delivery, Robert Langer [308]. To further align HD and SDOH topics into controlled drug delivery concepts, COVID-19 vaccine disparities in

acceptance [309] and access [310], may be integrated in future DDS coursework. Future improvements would include methods utilizing aforementioned COVID-19 vaccine development and a redesign of surveys used to collect student responses.

Bibliography

[1.] Jimenez, J., M. Sakthivel, K.K. Nischal, and M.V. Fedorchak. "Drug Delivery Systems and Novel Formulations to Improve Treatment of Rare Corneal Disease." *Drug Discovery Today* 24, no. 8 (2019): 1564–74. https://doi.org/10.1016/j.drudis.2019.03.005.

[2.] Jimenez, Jorge, Michael A. Washington, Jayde L. Resnick, Ken K. Nischal, and Morgan V. Fedorchak. "A Sustained Release Cysteamine Microsphere/Thermoresponsive Gel Eyedrop for Corneal Cystinosis Improves Drug Stability." *Drug Delivery and Translational Research*, February 4, 2021. https://doi.org/10.1007/s13346-020-00890-6.

[3.] Murteira, S., Z. Ghezaiel, S. Karray, and M. Lamure. "Drug Reformulations and Repositioning in Pharmaceutical Industry and Its Impact on Market Access: Reassessment of Nomenclature." *J Mark Access Health Policy* 1, no. 1 (2013).

[4.] Publishing, La Merie. "Competitor Analysis: Anti-VEGF and Anti-VEGF-R Biosimilars and Biosuperiors of Avastin, Cyramza, Eylea and Lucentis – a 2017 Update." Service. Market Research Reports® Inc. Market Research Reports® Inc., November 2, 2017. https://www.marketresearchreports.com/la-merie-publishing/competitor-analysis-anti-vegf-and-anti-vegf-r-biosimilars-and-biosuperiors.

[5.] Dear, J.W., P. Lilitkarntakul, and D.J. Webb. "Are Rare Diseases Still Orphans or Happily Adopted? The Challenges of Developing and Using Orphan Medicinal Products." *British Journal of Clinical Pharmacology* 62, no. 3 (2006): 264–71. https://doi.org/10.1111/j.1365-2125.2006.02654.x.

[6.] Xuan, Meng, Shurong Wang, Xin Liu, Yuxi He, Ying Li, and Yan Zhang. "Proteins of the Corneal Stroma: Importance in Visual Function." *Cell and Tissue Research* 364, no. 1 (April 1, 2016): 9–16. https://doi.org/10.1007/s00441-016-2372-3.

[7.] Zidan, Ghada, Ilva D. Rupenthal, Carol Greene, and Ali Seyfoddin. "Medicated Ocular Bandages and Corneal Health: Potential Excipients and Active Pharmaceutical Ingredients." *Pharmaceutical Development and Technology* 23, no. 3 (March 2018): 255–60. https://doi.org/10.1080/10837450.2017.1377232.

[8.] Ambrosone, Luigi, Germano Guerra, Mariapia Cinelli, Mariaelena Filippelli, Monica Mosca, Francesco Vizzarri, Dario Giorgio, and Ciro Costagliola. "Corneal Epithelial Wound Healing Promoted by Verbascoside-Based Liposomal Eyedrops." *BioMed Research International* 2014 (2014): 471642. https://doi.org/10.1155/2014/471642.

[9.] Ziaei, Mohammed, Ehsan Sharif-Paghaleh, and Bita Manzouri. "Pharmacotherapy of Corneal Transplantation." *Expert Opinion on Pharmacotherapy* 13, no. 6 (April 2012): 829–40. https://doi.org/10.1517/14656566.2012.673588.

[10.]Cholkar, K., S.P. Patel, A.D. Vadlapudi, and A.K. Mitra. "Novel Strategies for Anterior Segment Ocular Drug Delivery." *Journal of Ocular Pharmacology and Therapeutics* 29, no. 2 (2013): 106–23. https://doi.org/10.1089/jop.2012.0200.

[11.]Patel, A., K. Cholkar, V. Agrahari, and A.K. Mitra. "Ocular Drug Delivery Systems: An Overview." *World J. Pharmacol.* 2, no. 2 (2013): 47–64.

[12.]Mochizuki, H., M. Yamada, S. Hatou, and K. Tsubota. "Turnover Rate of Tear-Film Lipid Layer Determined by Fluorophotometry." *British Journal of Ophthalmology* 93, no. 11 (2009): 1535–38. https://doi.org/10.1136/bjo.2008.156828.

[13.]Huang, D., Y.-S. Chen, and I.D. Rupenthal. "Overcoming Ocular Drug Delivery Barriers through the Use of Physical Forces." *Advanced Drug Delivery Reviews* 126 (2018): 96–112. https://doi.org/10.1016/j.addr.2017.09.008.

[14.]Gaudana, R., J. Jwala, S.H.S. Boddu, and A.K. Mitra. "Recent Perspectives in Ocular Drug Delivery." *Pharmaceutical Research* 26, no. 5 (2009): 1197–1216. https://doi.org/10.1007/s11095-008-9694-0.

[15.]Gavhane, Y.N., and A.V. Yadav. "Loss of Orally Administered Drugs in GI Tract." *Saudi Pharmaceutical Journal* 20, no. 4 (2012): 331–44. https://doi.org/10.1016/j.jsps.2012.03.005.

[16.]Barar, J., A.R. Javadzadeh, and Y. Omidi. "Ocular Novel Drug Delivery: Impacts of Membranes and Barriers." *Expert Opinion on Drug Delivery* 5, no. 5 (2008): 567–81. https://doi.org/10.1517/17425247.5.5.567.

[17.]Gaudana, Ripal, Hari Krishna Ananthula, Ashwin Parenky, and Ashim K. Mitra. "Ocular Drug Delivery." *The AAPS Journal* 12, no. 3 (September 1, 2010): 348–60. https://doi.org/10.1208/s12248-010-9183-3.

[18.]Yellepeddi, V.K., and S. Palakurthi. "Recent Advances in Topical Ocular Drug Delivery." *Journal of Ocular Pharmacology and Therapeutics* 32, no. 2 (2016): 67–82. https://doi.org/10.1089/jop.2015.0047.

[19.]Deng, Zhengyu, and Shiyong Liu. "Controlled Drug Delivery with Nanoassemblies of Redox-Responsive Prodrug and Polyprodrug Amphiphiles." *Journal of Controlled Release: Official Journal of the Controlled Release Society* 326 (October 10, 2020): 276–96. https://doi.org/10.1016/j.jconrel.2020.07.010.

[20.]Ruman, Umme, Sharida Fakurazi, Mas Jaffri Masarudin, and Mohd Zobir Hussein. "Nanocarrier-Based Therapeutics and Theranostics Drug Delivery Systems for Next Generation of Liver Cancer Nanodrug Modalities." *International Journal of Nanomedicine* 15 (2020): 1437–56. https://doi.org/10.2147/IJN.S236927.

[21.]Badhani, Anjali, Prashant Dabral, Vinod Rana, and Kumud Upadhyaya. "Evaluation of Cyclodextrins for Enhancing Corneal Penetration of Natamycin Eye Drops." *Journal of Pharmacy & Bioallied Sciences* 4, no. Suppl 1 (March 2012): S29-30. https://doi.org/10.4103/0975-7406.94128.

[22.]Zhang, Yushi, Yao Chen, Xiaoxue Yu, Yangjia Qi, Yufeng Chen, Yuxi Liu, Yuntao Hu, and Zhihong Li. "A Flexible Device for Ocular Iontophoretic Drug Delivery." *Biomicrofluidics* 10, no. 1 (February 24, 2016): 011911. https://doi.org/10.1063/1.4942516.

[23.]Bhatnagar, Shubhmita, Amala Saju, Krishna Deepthi Cheerla, Sudeep Kumar Gade, Prashant Garg, and Venkata Vamsi Krishna Venuganti. "Corneal Delivery of Besifloxacin Using Rapidly Dissolving Polymeric Microneedles." *Drug Delivery and Translational Research* 8, no. 3 (June 2018): 473–83. https://doi.org/10.1007/s13346-017-0470-8.

[24.]Newman-Casey, P.A., A.L. Robin, T. Blachley, K. Farris, M. Heisler, K. Resnicow, and P.P. Lee. "The Most Common Barriers to Glaucoma Medication Adherence: A Cross-Sectional Survey." *Ophthalmology* 122, no. 7 (2015): 1308–16. https://doi.org/10.1016/j.ophtha.2015.03.026.

[25.]Park, Kinam. "Controlled Drug Delivery Systems: Past Forward and Future Back." *Journal of Controlled Release: Official Journal of the Controlled Release Society* 190 (September 28, 2014): 3–8. https://doi.org/10.1016/j.jconrel.2014.03.054.

[26.]N. Rothstein, Sam, and Steven R. Little. "A 'Tool Box' for Rational Design of Degradable Controlled Release Formulations." *Journal of Materials Chemistry* 21, no. 1 (2011): 29–39. https://doi.org/10.1039/C0JM01668C.

[27.]Rose, James B., Settimio Pacelli, Alicia J. El Haj, Harminder S. Dua, Andrew Hopkinson, Lisa J. White, and Felicity R. A. J. Rose. "Gelatin-Based Materials in Ocular Tissue Engineering." *Materials* 7, no. 4 (April 17, 2014): 3106–35. https://doi.org/10.3390/ma7043106.

[28.]"Diseases | Genetic and Rare Diseases Information Center (GARD) – an NCATS Program." Accessed November 29, 2018. https://rarediseases.info.nih.gov/diseases/.

[29.]NORD (National Organization for Rare Disorders). "Home." Accessed November 29, 2018. https://rarediseases.org/.

[30.]RESERVED, INSERM US14-- ALL RIGHTS. "Orphanet." Accessed November 29, 2018. http://www.orpha.net/consor/www/cgi-bin/index.php?lng=EN.

[31.]Mathews, P.M., K. Lindsley, A.J. Aldave, and E.K. Akpek. "Etiology of Global Corneal Blindness and Current Practices of Corneal Transplantation: A Focused Review." *Cornea* 37, no. 9 (2018): 1198–1203. https://doi.org/10.1097/ICO.0000000000001666.

[32.]Gain, P., R. Jullienne, Z. He, M. Aldossary, S. Acquart, F. Cognasse, and G. Thuret. "Global Survey of Corneal Transplantation and Eye Banking." *JAMA Ophthalmology* 134, no. 2 (2016): 167–73. https://doi.org/10.1001/jamaophthalmol.2015.4776.

[33.]Di Zazzo, A., A. Kheirkhah, T.B. Abud, S. Goyal, and R. Dana. "Management of High-Risk Corneal Transplantation." *Survey of Ophthalmology* 62, no. 6 (2017): 816–27. https://doi.org/10.1016/j.survophthal.2016.12.010.

[34.]Kusumesh, R., and M. Vanathi. "Graft Rejection in Pediatric Penetrating Keratoplasty: Clinical Features and Outcomes." *Oman Journal of Ophthalmology* 8, no. 1 (2015): 33–37. https://doi.org/10.4103/0974-620X.149862.

[35.]Krachmer, J.H. "Cornea: Fundamentals, Diagnosis and Management." *Am. Orthoptic J.* 61 (2011): 147.

[36.]Gower, N.J.D., R.J. Barry, M.R. Edmunds, L.C. Titcomb, and A.K. Denniston. "Drug Discovery in Ophthalmology: Past Success, Present Challenges, and Future Opportunities." *BMC Ophthalmology* 16, no. 1 (2016). https://doi.org/10.1186/s12886-016-0188-2.

[37.]Qazi, Y., and P. Hamrah. "Gene Therapy in Corneal Transplantation." *Seminars in Ophthalmology* 28, no. 5–6 (2013): 287–300. https://doi.org/10.3109/08820538.2013.825297.

[38.]Hsu, C.-C., C.-H. Peng, K.-H. Hung, Y.-Y. Lee, T.-C. Lin, S.-F. Jang, J.-H. Liu, et al. "Stem Cell Therapy for Corneal Regeneration Medicine and Contemporary Nanomedicine for Corneal Disorders." *Cell Transplantation* 24, no. 10 (2015): 1915–30. https://doi.org/10.3727/096368914X685744.

[39.]Moore, C.B.T., K.A. Christie, J. Marshall, and M.A. Nesbit. "Personalised Genome Editing – The Future for Corneal Dystrophies." *Progress in Retinal and Eye Research* 65 (2018): 147–65. https://doi.org/10.1016/j.preteyeres.2018.01.004.

[40.]Schiffmann, R., Y. Grishchuk, and E. Goldin. "Mucolipidosis IV." *GeneReviews*, 1993.

[41.]Smith, J.A., C.-C. Chan, E. Goldin, and R. Schiffmann. "Noninvasive Diagnosis and Ophthalmic Features of Mucolipidosis Type IV." *Ophthalmology* 109, no. 3 (2002): 588–94. https://doi.org/10.1016/S0161-6420(01)00968-X.

[42.]Bach, G. "Mucolipidosis Type IV." *Molecular Genetics and Metabolism* 73, no. 3 (2001): 197–203. https://doi.org/10.1006/mgme.2001.3195.

[43.]Newman, N.J., T. Starck, K.R. Kenyon, S. Lessell, I. Fish, and E.H. Kolodny. "Corneal Surface Irregularities and Episodic Pain in a Patient With Mucolipidosis IV." *Archives of Ophthalmology* 108, no. 2 (1990): 251–54. https://doi.org/10.1001/archopht.1990.01070040103041.

[44.]Boudewyn, L.C., and S.U. Walkley. "Current Concepts in the Neuropathogenesis of Mucolipidosis Type IV." *Journal of Neurochemistry* 148, no. 5 (2019): 669–89. https://doi.org/10.1111/jnc.14462.

[45.]Dangel, M.E., D.L. Bremer, and G.L. Rogers. "Treatment of Corneal Opacification in Mucolipidosis IV with Conjunctival Transplantation." *American Journal of Ophthalmology* 99, no. 2 (1985): 137–41. https://doi.org/10.1016/0002-9394(85)90221-1.

[46.]"The Natural History and Pathogenesis of Mucolipidosis Type IV - Full Text View - ClinicalTrials.Gov." Accessed November 28, 2018. https://clinicaltrials.gov/ct2/show/NCT00015782.

[47.]Huynh, J.M., H. Dang, I.A. Munoz-Tucker, M. O'Ketch, I.T. Liu, S. Perno, N. Bhuyan, A. Crain, I. Borbon, and H. Fares. "ESCRT-Dependent Cell Death in a Caenorhabditis Elegans Model of the Lysosomal Storage Disorder Mucolipidosis Type IV." *Genetics* 202, no. 2 (2016): 619–38. https://doi.org/10.1534/genetics.115.182485.

[48.]Li, H., W. Pei, S. Vergarajauregui, P.M. Zerfas, N. Raben, S.M. Burgess, and R. Puertollano. "Novel Degenerative and Developmental Defects in a Zebrafish Model of Mucolipidosis Type IV." *Human Molecular Genetics* 26, no. 14 (2017): 2701–18. https://doi.org/10.1093/hmg/ddx158.

[49.]Ko, A.-R., D.-K. Jin, S.Y. Cho, S.W. Park, M. Przybylska, N.S. Yew, S.H. Cheng, et al. "AAV8-Mediated Expression of N-Acetylglucosamine-1-Phosphate Transferase Attenuates Bone Loss in a Mouse Model of Mucolipidosis II." *Molecular Genetics and Metabolism* 117, no. 4 (2016): 447–55. https://doi.org/10.1016/j.ymgme.2016.02.001.

[50.]Mohan, R.R., A. Sharma, M.V. Netto, S. Sinha, and S.E. Wilson. "Gene Therapy in the Cornea." *Progress in Retinal and Eye Research* 24, no. 5 (2005): 537–59. https://doi.org/10.1016/j.preteyeres.2005.04.001.

[51.]Gupta, S., M.K. Fink, A. Ghosh, R. Tripathi, P.R. Sinha, A. Sharma, N.P. Hesemann, S.S. Chaurasia, E.A. Giuliano, and R.R. Mohan. "Novel Combination BMP7 and HGF Gene Therapy Instigates Selective Myofibroblast Apoptosis and Reduces Corneal Haze in Vivo." *Investigative Ophthalmology and Visual Science* 59, no. 2 (2018): 1045–57. https://doi.org/10.1167/iovs.17-23308.

[52.]Bach, G. "Mucolipin 1: Endocytosis and Cation Channel - A Review." *Pflugers Archiv European Journal of Physiology* 451, no. 1 (2005): 313–17. https://doi.org/10.1007/s00424-004-1361-7.

[53.]Weidle, E.G., and W. Lisch. "Corneal Opacification as an Indicating Sign of Familial Lecithin:Cholesterol Acyltransferase (LCAT) Deficiency. Case Report and Review of the Literature." *Klinische Monatsblatter Fur Augenheilkunde* 190, no. 3 (1987): 182–87. https://doi.org/10.1055/s-2008-1050353.

[54.]Cogan, D.G., H.S. Kruth, M.B. Datilis, and N. Martin. "Corneal Opacity in LCAT Disease." *Cornea* 11, no. 6 (1992): 595–99. https://doi.org/10.1097/00003226-199211000-00021.

[55.]Contacos, C., D.R. Sullivan, K.-A. Rye, H. Funke, and G. Assmann. "A New Molecular Defect in the Lecithin:Cholesterol Acyltransferase (LCAT) Gene Associated with Fish Eye Disease." *Journal of Lipid Research* 37, no. 1 (1996): 35–44.

[56.]McIntyre, N. "Familial LCAT Deficiency and Fish-Eye Disease." *Journal of Inherited Metabolic Disease* 11, no. 1 Supplement (1988): 45–56. https://doi.org/10.1007/BF01800570.

[57.]Viestenz, A., U. Schlötzer-Schrehardt, C. Hofmann-Rummelt, B. Seitz, and M. Küchle. "Histopathology of Corneal Changes in Lecithin-Cholesterol Acyltransferase Deficiency." *Cornea* 21, no. 8 (2002): 834–37. https://doi.org/10.1097/00003226-200211000-00022.

[58.]Lisch, W., and P. Saikia. “In Vivo Imaging of the Cornea in a Patient with Lecithin-Cholesterol Acyltransferase Deficiency.” *Cornea* 29, no. 10 (2010): 1207. https://doi.org/10.1097/ICO.0b013e3181d5291b.

[59.]Dimick, S.M., B. Sallee, B.F. Asztalos, P.H. Pritchard, J. Frohlich, and E.J. Schaefer. “A Kindred with Fish Eye Disease, Corneal Opacities, Marked High-Density Lipoprotein Deficiency, and Statin Therapy.” *Journal of Clinical Lipidology* 8, no. 2 (2014): 223–30. https://doi.org/10.1016/j.jacl.2013.11.005.

[60.]Aranda, P., P. Valdivielso, L. Pisciotta, J. Garcia, C. García-Arias, S. Bertolini, G. Martín-Reyes, P. González-Santos, and S. Calandra. “Therapeutic Management of a New Case of LCAT Deficiency with a Multifactorial Long-Term Approach Based on High Doses of Angiotensin II Receptor Blockers (ARBs).” *Clinical Nephrology* 69, no. 3 (2008): 213–18. https://doi.org/10.5414/CNP69213.

[61.]Shamburek, R.D., R. Bakker-Arkema, B.J. Auerbach, B.R. Krause, R. Homan, M.J. Amar, L.A. Freeman, and A.T. Remaley. “Familial Lecithin:Cholesterol Acyltransferase Deficiency: First-in-Human Treatment with Enzyme Replacement.” *Journal of Clinical Lipidology* 10, no. 2 (2016): 356–67. https://doi.org/10.1016/j.jacl.2015.12.007.

[62.]Shamburek, R.D., R. Bakker-Arkema, A.M. Shamburek, L.A. Freeman, M.J. Amar, B. Auerbach, B.R. Krause, et al. “Safety and Tolerability of ACP-501, a Recombinant Human Lecithin:Cholesterol Acyltransferase, in a Phase 1 Single-Dose Escalation Study.” *Circulation Research* 118, no. 1 (2016): 73–82. https://doi.org/10.1161/CIRCRESAHA.115.306223.

[63.]Wenger, D.A., T.J. Tarby, and C. Wharton. “Macular Cherry-Red Spots and Myoclonus with Dementia: Coexistent Neuraminidase and β-Galactosidase Deficiencies.” *Biochemical and Biophysical Research Communications* 82, no. 2 (1978): 589–95. https://doi.org/10.1016/0006-291X(78)90915-4.

[64.]Cimms, T. “Qualitative Research to Characterize Patients with Galactosialidosis.” *Mol. Genet Metab.* 123 (2018): S32–33.

[65.]Annunziata, I., and A. d’Azzo. “Galactosialidosis: Historic Aspects and Overview of Investigated and Emerging Treatment Options.” *Expert Opinion on Orphan Drugs* 5, no. 2 (2017): 131–41. https://doi.org/10.1080/21678707.2016.1266933.

[66.]Groener, J., P. Maaswinkel-Mooy, V. Smit, M.V.D. Hoeven, J. Bakker, Y. Campos, and A. D’Azzo. “New Mutations in Two Dutch Patients with Early Infantile Galactosialidosis.” *Molecular Genetics and Metabolism* 78, no. 3 (2003): 222–28. https://doi.org/10.1016/S1096-7192(03)00005-2.

[67.]Caciotti, A., S. Catarzi, R. Tonin, L. Lugli, C.R. Perez, H. Michelakakis, I. Mavridou, et al. “Galactosialidosis: Review and Analysis of CTSA Gene Mutations.” *Orphanet Journal of Rare Diseases* 8, no. 1 (2013). https://doi.org/10.1186/1750-1172-8-114.

[68.]Pedersen, I.S., P. Dervan, A. McGoldrick, M. Harrison, F. Ponchel, V. Speirs, J.D. Isaacs, T. Gorey, and A. McCann. “Systemic and Neurologic Abnormalities Distinguish the Lysosomal

Disorders Sialidosis and Galactosialidosis in Mice." *Human Molecular Genetics* 11, no. 12 (2002): XX1455-1464.

[69.]Leimig, T., L. Mann, M.D.P. Martin, E. Bonten, D. Persons, J. Knowles, J.A. Allay, et al. "Functional Amelioration of Murine Galactosialidosis by Genetically Modified Bone Marrow Hematopoietic Progenitor Cells." *Blood* 99, no. 9 (2002): 3169–78. https://doi.org/10.1182/blood.V99.9.3169.

[70.]Bonten, E.J., D. Wang, J.N. Toy, L. Mann, A. Mignardot, G. Yogalingam, and A. D'Azzo. "Targeting Macrophages with Baculovirus-Produced Lysosomal Enzymes: Implications for Enzyme Replacement Therapy of the Glycoprotein Storage Disorder Galactosialidosis." *FASEB Journal* 18, no. 9 (2004): 971–73. https://doi.org/10.1096/fj.03-0941fje.

[71.]Hu, H., E. Gomero, E. Bonten, J.T. Gray, J. Allay, Y. Wu, J. Wu, C. Calabrese, A. Nienhuis, and A. D'Azzo. "Preclinical Dose-Finding Study with a Liver-Tropic, Recombinant AAV-2/8 Vector in the Mouse Model of Galactosialidosis." *Molecular Therapy* 20, no. 2 (2012): 267–74. https://doi.org/10.1038/mt.2011.227.

[72.]Shaberman, B. "A Retinal Research Nonprofit Paves the Way for Commercializing Gene Therapies." *Human Gene Therapy* 28, no. 12 (2017): 1118–21. https://doi.org/10.1089/hum.2017.29058.bsh.

[73.]Clarke, L.A. "Mucopolysaccharidosis Type I." *GeneReviews*, 1993.

[74.]Wraith, J.E. "The Mucopolysaccharidoses: A Clinical Review and Guide to Management." *Archives of Disease in Childhood* 72, no. 3 (1995): 263–67. https://doi.org/10.1136/adc.72.3.263.

[75.]Cheema, H.A., H.S. Malik, M.A. Hashmi, Z. Fayyaz, I. Mushtaq, and N. Shahzadi. "Mucopolysaccharidoses - Clinical Spectrum and Frequency of Different Types." *Journal of the College of Physicians and Surgeons Pakistan* 27, no. 2 (2017): 80–83.

[76.]Javed, A., T. Aslam, S.A. Jones, and J. Ashworth. "Objective Quantification of Changes in Corneal Clouding over Time in Patients with Mucopolysaccharidosis." *Investigative Ophthalmology and Visual Science* 58, no. 2 (2017): 954–58. https://doi.org/10.1167/iovs.16-20647.

[77.]Harding, S.A., K.K. Nischal, A. Upponi-Patil, and D.J. Fowler. "Indications and Outcomes of Deep Anterior Lamellar Keratoplasty in Children." *Ophthalmology* 117, no. 11 (2010): 2191–95. https://doi.org/10.1016/j.ophtha.2010.03.025.

[78.]RESERVED, INSERM US14-- ALL RIGHTS. "Orphanet: ALDURAZYME." Accessed November 29, 2018. https://www.orpha.net/consor/cgi-bin/OC_Exp.php?lng=EN&Expert=42576.

[79.]Dornelles, A.D., O. Artigalás, A.A. Da Silva, D.L.V. Ardila, T. Alegra, T.V. Pereira, F.P. E Vairo, and I.V.D. Schwartz. "Efficacy and Safety of Intravenous Laronidase for

Mucopolysaccharidosis Type I: A Systematic Review and Meta-Analysis." *PLoS ONE* 12, no. 8 (2017). https://doi.org/10.1371/journal.pone.0184065.

[80.]Rodgers, N.J., A.M. Kaizer, W.P. Miller, K.D. Rudser, P.J. Orchard, and E.A. Braunlin. "Mortality after Hematopoietic Stem Cell Transplantation for Severe Mucopolysaccharidosis Type I: The 30-Year University of Minnesota Experience." *Journal of Inherited Metabolic Disease* 40, no. 2 (2017): 271–80. https://doi.org/10.1007/s10545-016-0006-2.

[81.]Aldenhoven, M., S.A. Jones, D. Bonney, R.E. Borrill, M. Coussons, J. Mercer, M.B. Bierings, et al. "Hematopoietic Cell Transplantation for Mucopolysaccharidosis Patients Is Safe and Effective: Results after Implementation of International Guidelines." *Biology of Blood and Marrow Transplantation* 21, no. 6 (2015): 1106–9. https://doi.org/10.1016/j.bbmt.2015.02.011.

[82.]Hinderer, C., P. Bell, B.L. Gurda, Q. Wang, J.-P. Louboutin, Y. Zhu, J. Bagel, et al. "Intrathecal Gene Therapy Corrects Cns Pathology in a Feline Model of Mucopolysaccharidosis i." *Molecular Therapy* 22, no. 12 (2014): 2018–27. https://doi.org/10.1038/mt.2014.135.

[83.]Wolf, D.A., A.W. Lenander, Z. Nan, L.R. Belur, C.B. Whitley, P. Gupta, W.C. Low, and R.S. McIvor. "Direct Gene Transfer to the CNS Prevents Emergence of Neurologic Disease in a Murine Model of Mucopolysaccharidosis Type I." *Neurobiology of Disease* 43, no. 1 (2011): 123–33. https://doi.org/10.1016/j.nbd.2011.02.015.

[84.]Sharma, A., J.C.K. Tovey, A. Ghosh, and R.R. Mohan. "AAV Serotype Influences Gene Transfer in Corneal Stroma in Vivo." *Experimental Eye Research* 91, no. 3 (2010): 440–48. https://doi.org/10.1016/j.exer.2010.06.020.

[85.]Igarashi, T., K. Miyake, N. Suzuki, K. Kato, H. Takahashi, K. Ohara, and T. Shimada. "New Strategy for in Vivo Transgene Expression in Corneal Epithelial Progenitor Cells." *Current Eye Research* 24, no. 1 (2002): 46–50. https://doi.org/10.1076/ceyr.24.1.46.5436.

[86.]Song, L., T. Llanga, L.M. Conatser, V. Zaric, B.C. Gilger, and M.L. Hirsch. "Serotype Survey of AAV Gene Delivery via Subconjunctival Injection in Mice." *Gene Therapy* 25, no. 6 (2018): 402–14. https://doi.org/10.1038/s41434-018-0035-6.

[87.]Vance, M., T. Llanga, W. Bennett, K. Woodard, G. Murlidharan, N. Chungfat, A. Asokan, et al. "AAV Gene Therapy for MPS1-Associated Corneal Blindness." *Scientific Reports* 6 (2016). https://doi.org/10.1038/srep22131.

[88.]Determan, A.S., J.H. Wilson, M.J. Kipper, M.J. Wannemuehler, and B. Narasimhan. "Protein Stability in the Presence of Polymer Degradation Products: Consequences for Controlled Release Formulations." *Biomaterials* 27, no. 17 (2006): 3312–20. https://doi.org/10.1016/j.biomaterials.2006.01.054.

[89.]Lopac, S.K., M.P. Torres, J.H. Wilson-Welder, M.J. Wannemuehler, and B. Narasimhan. "Effect of Polymer Chemistry and Fabrication Method on Protein Release and Stability from Polyanhydride Microspheres." *Journal of Biomedical Materials Research - Part B Applied Biomaterials* 91, no. 2 (2009): 938–47. https://doi.org/10.1002/jbm.b.31478.

[90.]Martins, A.M., V. D'Almeida, S.O. Kyosen, E.T. Takata, A.G. Delgado, A.M. Barbosa Ferreira Gonçalves, C.C. Benetti Filho, et al. "Guidelines to Diagnosis and Monitoring of Fabry Disease and Review of Treatment Experiences." *Journal of Pediatrics* 155, no. 4 SUPPL. (2009): S19–31. https://doi.org/10.1016/j.jpeds.2009.07.003.

[91.]Sodi, A., A. Ioannidis, and S. Pitz. "Ophthalmological Manifestations of Fabry Disease." *Fabry Disease: Perspectives from 5 Years of FOS*, 2006, 249–61.

[92.]Lanzl, I.M., and B.P. Leroy. "Ocular Features of Treatable Lysosomal Storage Disorders −Fabry Disease, Mucopolysaccharidoses I, II and VI and Gaucher Disease." *US Ophthalmic Rev.*, 2012.

[93.]Mehta, A., and D. Hughes. "Fabry Disease." *Gene Reviews*, 1993.

[94.]Frustaci, A., M.A. Russo, and C. Chimenti. "Paradoxical Response to Enzyme Replacement Therapy of Fabry Disease Cardiomyopathy." *Circulation: Cardiovascular Imaging* 9, no. 8 (2016). https://doi.org/10.1161/CIRCIMAGING.116.005078.

[95.]Schiffmann, R., J.B. Kopp, H.A. Austin, S. Sabnis, D.F. Moore, T. Weibel, J.E. Balow, and R.O. Brady. "Enzyme Replacement Therapy in Fabry Disease a Randomized Controlled Trial." *Journal of the American Medical Association* 285, no. 21 (2001): 2743–49. https://doi.org/10.1001/jama.285.21.2743.

[96.]Brady, R.O., G.J. Murray, D.F. Moore, and R. Schiffmann. "Enzyme Replacement Therapy in Fabry Disease." *Journal of Inherited Metabolic Disease* 24, no. SUPPL. 2 (2001): 18–24. https://doi.org/10.1023/A:1012451320105.

[97.]Pitz, S., G. Kalkum, L. Arash, N. Karabul, A. Sodi, S. Larroque, M. Beck, and A. Gal. "Ocular Signs Correlate Well with Disease Severity and Genotype in Fabry Disease." *PLoS ONE* 10, no. 3 (2015). https://doi.org/10.1371/journal.pone.0120814.

[98.]Tsilou, E., M. Zhou, W. Gahl, P.C. Sieving, and C.-C. Chan. "Ophthalmic Manifestations and Histopathology of Infantile Nephropathic Cystinosis: Report of a Case and Review of the Literature." *Survey of Ophthalmology* 52, no. 1 (2007): 97–105. https://doi.org/10.1016/j.survophthal.2006.10.006.

[99.]Gahl, W.A., E.M. Kuehl, F. Iwata, A. Lindblad, and M.I. Kaiser-Kupfer. "Corneal Crystals in Nephropathic Cystinosis: Natural History and Treatment with Cysteamine Eyedrops." *Molecular Genetics and Metabolism* 71, no. 1–2 (2000): 100–120. https://doi.org/10.1006/mgme.2000.3062.

[100.]Alsuhaibani, A.H., M.D. Wagoner, and A.O. Khan. "Confocal Microscopy of the Cornea in Nephropathic Cystinosis [3]." *British Journal of Ophthalmology* 89, no. 11 (2005): 1530–31. https://doi.org/10.1136/bjo.2005.074468.

[101.]Kaiser-Kupfer, M.I., L. Fujikawa, T. Kuwabara, S. Jain, and W.A. Gahl. "Removal of Corneal Crystals by Topical Cysteamine in Nephropathic Cystinosis." *New England Journal of Medicine* 316, no. 13 (1987): 775–79. https://doi.org/10.1056/NEJM198703263161304.

[102.]Huynh, N., W.A. Gahl, and R.J. Bishop. "Cysteamine Ophthalmic Solution 0.44% for the Treatment of Corneal Cystine Crystals in Cystinosis." *Expert Review of Ophthalmology* 8, no. 4 (2013): 341–45. https://doi.org/10.1586/17469899.2013.814885.

[103.] Luaces-Rodríguez, A., V. Díaz-Tomé, M. González-Barcia, J. Silva-Rodríguez, M. Herranz, M. Gil-Martínez, M.T. Rodríguez-Ares, et al. "Cysteamine Polysaccharide Hydrogels: Study of Extended Ocular Delivery and Biopermanence Time by PET Imaging." *International Journal of Pharmaceutics* 528, no. 1–2 (2017): 714–22. https://doi.org/10.1016/j.ijpharm.2017.06.060.

[104.]Buchan, B., G. Kay, A. Heneghan, K.H. Matthews, and D. Cairns. "Gel Formulations for Treatment of the Ophthalmic Complications in Cystinosis." *International Journal of Pharmaceutics* 392, no. 1–2 (2010): 192–97. https://doi.org/10.1016/j.ijpharm.2010.03.065.

[105.]Frost, L., P. Suryadevara, S.J. Cannell, P.W. Groundwater, P.A. Hambleton, and R.J. Anderson. "Synthesis of Diacylated Γ3-Glutamyl-Cysteamine Prodrugs, and in Vitro Evaluation of Their Cytotoxicity and Intracellular Delivery of Cysteamine." *European Journal of Medicinal Chemistry* 109 (2016): 206–15. https://doi.org/10.1016/j.ejmech.2015.12.027.

[106.]Hsu, K.-H., R.C. Fentzke, and A. Chauhan. "Feasibility of Corneal Drug Delivery of Cysteamine Using Vitamin e Modified Silicone Hydrogel Contact Lenses." *European Journal of Pharmaceutics and Biopharmaceutics* 85, no. 3 PART A (2013): 531–40. https://doi.org/10.1016/j.ejpb.2013.04.017.

[107.]Marcano, D.C., C.S. Shin, B. Lee, L.C. Isenhart, X. Liu, F. Li, J.V. Jester, S.C. Pflugfelder, J. Simpson, and G. Acharya. "Synergistic Cysteamine Delivery Nanowafer as an Efficacious Treatment Modality for Corneal Cystinosis." *Molecular Pharmaceutics* 13, no. 10 (2016): 3468–77. https://doi.org/10.1021/acs.molpharmaceut.6b00488.

[108.]Labbé, A., C. Baudouin, G. Deschênes, C. Loirat, M. Charbit, G. Guest, and P. Niaudet. "A New Gel Formulation of Topical Cysteamine for the Treatment of Corneal Cystine Crystals in Cystinosis: The Cystadrops OCT-1 Study." *Molecular Genetics and Metabolism* 111, no. 3 (2014): 314–20. https://doi.org/10.1016/j.ymgme.2013.12.298.

[109.]Liang, H., A. Labbé, J.L. Mouhaër, C. Plisson, and C. Baudouin. "A New Viscous Cysteamine Eye Drops Treatment for Ophthalmic Cystinosis: An Open-Label Randomized Comparative Phase III Pivotal Study." *Investigative Ophthalmology and Visual Science* 58, no. 4 (2017): 2275–83. https://doi.org/10.1167/iovs.16-21080.

[110.]Rocca, C.J., A. Kreymerman, S.N. Ur, K.E. Frizzi, S. Naphade, A. Lau, T. Tran, N.A. Calcutt, J.L. Goldberg, and S. Cherqui. "Treatment of Inherited Eye Defects by Systemic Hematopoietic Stem Cell Transplantation." *Investigative Ophthalmology and Visual Science* 56, no. 12 (2015): 7214–23. https://doi.org/10.1167/iovs.15-17107.

[111.]Elmonem, M.A., K. Veys, F. Oliveira Arcolino, M. Van Dyck, M.C. Benedetti, F. Diomedi-Camassei, G. De Hertogh, L.P. van den Heuvel, M. Renard, and E. Levtchenko. "Allogeneic HSCT Transfers Wild-Type Cystinosin to Nonhematological Epithelial Cells in Cystinosis: First

Human Report." *American Journal of Transplantation* 18, no. 11 (2018): 2823–28. https://doi.org/10.1111/ajt.15029.

[112.]Clemente-Tomás, R., D. Hernández-Pérez, P. Neira-Ibáñez, F. Farías-Rozas, R. Torrecillas-Picazo, V. Osorio-Alayo, and A.M. Duch-Samper. "Intracrystalline Ozurdex ® : Therapeutic Effect Maintained for 18 Months." *International Ophthalmology* 39, no. 1 (2019): 207–11. https://doi.org/10.1007/s10792-017-0780-3.

[113.]Walters, T., M. Endl, T.R. Elmer, J. Levenson, P. Majmudar, and S. Masket. "Sustained-Release Dexamethasone for the Treatment of Ocular Inflammation and Pain after Cataract Surgery." *Journal of Cataract and Refractive Surgery* 41, no. 10 (2015): 2049–59. https://doi.org/10.1016/j.jcrs.2015.11.005.

[114.]Balzus, B., F.F. Sahle, S. Hönzke, C. Gerecke, F. Schumacher, S. Hedtrich, B. Kleuser, and R. Bodmeier. "Formulation and Ex Vivo Evaluation of Polymeric Nanoparticles for Controlled Delivery of Corticosteroids to the Skin and the Corneal Epithelium." *European Journal of Pharmaceutics and Biopharmaceutics* 115 (2017): 122–30. https://doi.org/10.1016/j.ejpb.2017.02.001.

[115.]Rad, M.S., and S.A. Mohajeri. "Simultaneously Load and Extended Release of Betamethasone and Ciprofloxacin from Vitamin E-Loaded Silicone-Based Soft Contact Lenses." *Current Eye Research* 41, no. 9 (2016): 1185–91. https://doi.org/10.3109/02713683.2015.1107591.

[116.]García-Millán, E., S. Koprivnik, and F.J. Otero-Espinar. "Drug Loading Optimization and Extended Drug Delivery of Corticoids from PHEMA Based Soft Contact Lenses Hydrogels via Chemical and Microstructural Modifications." *International Journal of Pharmaceutics* 487, no. 1–2 (2015): 260–69. https://doi.org/10.1016/j.ijpharm.2015.04.037.

[117.]Bian, F., C.S. Shin, C. Wang, S.C. Pflugfelder, G. Acharya, and C.S. de Paiva. "Dexamethasone Drug Eluting Nanowafers Control Inflammation in Alkali-Burned Corneas Associated with Dry Eye." *Investigative Ophthalmology and Visual Science* 57, no. 7 (2016): 3222–30. https://doi.org/10.1167/iovs.16-19074.

[118.]Bonini, S., M. Coassin, S. Aronni, and A. Lambiase. "Vernal Keratoconjunctivitis." *Eye* 18, no. 4 (2004): 345–51. https://doi.org/10.1038/sj.eye.6700675.

[119.]Leonardi, A. "Management of Vernal Keratoconjunctivitis." *Ophthalmol Ther* 2, no. 2 (2013): 73–88.

[120.]Nebbioso, M., A. Iannaccone, M. Duse, M. Aventaggiato, A. Bruscolini, and A.M. Zicari. "Vascular Endothelial Growth Factor (VEGF) Serological and Lacrimal Signaling in Patients Affected by Vernal Keratoconjunctivitis (VKC)." *Journal of Ophthalmology* 2018 (2018). https://doi.org/10.1155/2018/3850172.

[121.]Leonardi, A., D. Lazzarini, A. La Gloria Valerio, T. Scalora, and I. Fregona. "Corneal Staining Patterns in Vernal Keratoconjunctivitis: The New VKC-CLEK Scoring Scale." *British Journal*

of Ophthalmology 102, no. 10 (2018): 1448–53. https://doi.org/10.1136/bjophthalmol-2017-311171.

[122.]Chan, T.C.Y., E.S. Wong, J.C.K. Chan, Y. Wang, M. Yu, N. Maeda, and V. Jhanji. "Corneal Backward Scattering and Higher-Order Aberrations in Children with Vernal Keratoconjunctivitis and Normal Topography." *Acta Ophthalmologica* 96, no. 3 (2018): e327–33. https://doi.org/10.1111/aos.13566.

[123.]Gupta, S., A.K. Khurana, B.K. Ahluwalia, and N.C. Gupta. "Topical Indomethacin for Vernal Keratoconjunctivitis." *Acta Ophthalmologica* 69, no. 1 (1991): 95–98. https://doi.org/10.1111/j.1755-3768.1991.tb02000.x.

[124.]Sharma, A., R. Gupta, J. Ram, and A. Gupta. "Topical Ketorolac 0.5% Solution for the Treatment of Vernal Keratoconjunctivitis." *Indian Journal of Ophthalmology* 45, no. 3 (1997): 177–80.

[125.]D'Angelo, G., A. Lambiase, M. Cortes, R. Sgrulletta, R. Pasqualetti, A. Lamagna, and S. Bonini. "Preservative-Free Diclofenac Sodium 0.1% for Vernal Keratoconjunctivitis." *Graefe's Archive for Clinical and Experimental Ophthalmology* 241, no. 3 (2003): 192–95. https://doi.org/10.1007/s00417-002-0612-6.

[126.]Lambiase, A., A. Leonardi, M. Sacchetti, V. Deligianni, S. Sposato, and S. Bonini. "Topical Cyclosporine Prevents Seasonal Recurrences of Vernal Keratoconjunctivitis in a Randomized, Double-Masked, Controlled 2-Year Study." *Journal of Allergy and Clinical Immunology* 128, no. 4 (2011): 896-897.e9. https://doi.org/10.1016/j.jaci.2011.07.004.

[127.]Pucci, N., E. Novembre, A. Cianferoni, E. Lombardi, R. Bernardini, R. Caputo, L. Campa, and A. Vierucci. "Efficacy and Safety of Cyclosporine Eyedrops in Vernal Keratoconjunctivitis." *Annals of Allergy, Asthma and Immunology* 89, no. 3 (2002): 298–303. https://doi.org/10.1016/S1081-1206(10)61958-8.

[128.]Gupta, P.C., and J. Ram. "Comparative Evaluation of Tacrolimus Versus Interferon Alpha-2b Eye Drops in the Treatment of Vernal Keratoconjunctivitis: A Randomized, Double-Masked Study." *Cornea* 37, no. 1 (2018): e1. https://doi.org/10.1097/ICO.0000000000001357.

[129.]Lallemand, F., P. Daull, S. Benita, R. Buggage, and J.S. Garrigue. "Successfully Improving Ocular Drug Delivery Using the Cationic Nanoemulsion, Novasorb." *J Drug Deliv* 2012 (2012).

[130.]Krachmer, J.H., M.J. Mannis, and E.J. Holland. "Cornea." *Cornea: Fundamentals, Diagnosis and Management*, 2005.

[131.]Weiss, J.S., H.U. Møller, A.J. Aldave, B. Seitz, C. Bredrup, T. Kivelä, F.L. Munier, et al. "IC3D Classification of Corneal Dystrophies-Edition 2." *Cornea* 34, no. 2 (2015): 117–59. https://doi.org/10.1097/ICO.0000000000000307.

[132.]Pellegrini, Graziella, Diego Ardigò, Giovanni Milazzo, Giorgio Iotti, Paolo Guatelli, Danilo Pelosi, and Michele De Luca. "Navigating Market Authorization: The Path Holoclar Took to

Become the First Stem Cell Product Approved in the European Union." *Stem Cells Translational Medicine* 7, no. 1 (January 2018): 146–54. https://doi.org/10.1002/sctm.17-0003.

[133.]Pellegrini, G., A. Lambiase, C. Macaluso, A. Pocobelli, S. Deng, G.M. Cavallini, R. Esteki, and P. Rama. "From Discovery to Approval of an Advanced Therapy Medicinal Product-Containing Stem Cells, in the EU." *Regenerative Medicine* 11, no. 4 (2016): 407–20. https://doi.org/10.2217/rme-2015-0051.

[134.]Ormonde, S., C.-Y. Chou, L. Goold, C. Petsoglou, R. Al-Taie, T. Sherwin, C.N.J. McGhee, and C.R. Green. "Regulation of Connexin43 Gap Junction Protein Triggers Vascular Recovery and Healing in Human Ocular Persistent Epithelial Defect Wounds." *Journal of Membrane Biology* 245, no. 7 (2012): 381–88. https://doi.org/10.1007/s00232-012-9460-4.

[135.]Becker, D.L., A.R. Phillips, B.J. Duft, Y. Kim, and C.R. Green. "Translating Connexin Biology into Therapeutics." *Seminars in Cell and Developmental Biology* 50 (2016): 49–58. https://doi.org/10.1016/j.semcdb.2015.12.009.

[136.]Dunaief, J.L., W.M. Eugene, and M.F. Goldberg. "Corneal Dystrophies of Epithelial Genesis: The Possible Therapeutic Use of Limbal Stem Cell Transplantation." *Archives of Ophthalmology* 119, no. 1 (2001): 120–22.

[137.]Mammen, A., E.G. Romanowski, M.V. Fedorchak, D.K. Dhaliwal, R.M. Shanks, and R.P. Kowalski. "Endophthalmitis Prophylaxis Using a Single Drop of Thermoresponsive Controlled-Release Microspheres Loaded with Moxifloxacin in a Rabbit Model." *Translational Vision Science and Technology* 5, no. 6 (2016). https://doi.org/10.1167/tvst.5.6.12.

[138.]Fedorchak, M.V., I.P. Conner, J.S. Schuman, A. Cugini, and S.R. Little. "Long Term Glaucoma Drug Delivery Using a Topically Retained Gel/Microsphere Eye Drop." *Scientific Reports* 7, no. 1 (2017). https://doi.org/10.1038/s41598-017-09379-8.

[139.]Pescina, Silvia, Federica Carra, Cristina Padula, Patrizia Santi, and Sara Nicoli. "Effect of PH and Penetration Enhancers on Cysteamine Stability and Trans-Corneal Transport." *European Journal of Pharmaceutics and Biopharmaceutics* 107 (October 1, 2016): 171–79. https://doi.org/10.1016/j.ejpb.2016.07.009.

[140.]Dixon, J M, and L Blackwood. "Thermal Variations of the Human Eye." *Transactions of the American Ophthalmological Society* 89 (1991): 183–93.

[141.]Kaiser-Kupfer, M. I., M. A. Gazzo, M. B. Datiles, R. C. Caruso, E. M. Kuehl, and W. A. Gahl. "A Randomized Placebo-Controlled Trial of Cysteamine Eye Drops in Nephropathic Cystinosis." *Archives of Ophthalmology (Chicago, Ill.: 1960)* 108, no. 5 (May 1990): 689–93. https://doi.org/10.1001/archopht.1990.01070070075038.

[142.]Bradbury, J. A., J. P. Danjoux, J. Voller, M. Spencer, and T. Brocklebank. "A Randomised Placebo-Controlled Trial of Topical Cysteamine Therapy in Patients with Nephropathic Cystinosis." *Eye (London, England)* 5 (Pt 6) (1991): 755–60. https://doi.org/10.1038/eye.1991.139.

[143.]Gahl, W.A., J.G. Thoene, and J.A. Schneider. "Medical Progress: Cystinosis." *New England Journal of Medicine* 347, no. 2 (2002): 111–21. https://doi.org/10.1056/NEJMra020552.

[144.]Nesterova, Galina, and William A. Gahl. "Cystinosis." In *GeneReviews*®, edited by Margaret P. Adam, Holly H. Ardinger, Roberta A. Pagon, Stephanie E. Wallace, Lora JH Bean, Karen Stephens, and Anne Amemiya. Seattle (WA): University of Washington, Seattle, 1993. http://www.ncbi.nlm.nih.gov/books/NBK1400/.

[145.]Kaiser Kupfer, M.I., R.C. Caruso, D.S. Minkler, and W.A. Gahl. "Long-Term Ocular Manifestations in Nephropathic Cystinosis." *Archives of Ophthalmology* 104, no. 5 (1986): 706–11. https://doi.org/10.1001/archopht.1986.01050170096030.

[146.]Gahl, W.A., J.Z. Balog, and R. Kleta. "Nephropathic Cystinosis in Adults: Natural History and Effects of Oral Cysteamine Therapy." *Annals of Internal Medicine* 147, no. 4 (2007): 242–50. https://doi.org/10.7326/0003-4819-147-4-200708210-00006.

[147.]Biswas, S., M. Gaviria, L. Malheiro, J.P. Marques, V. Giordano, and H. Liang. "Latest Clinical Approaches in the Ocular Management of Cystinosis: A Review of Current Practice and Opinion from the Ophthalmology Cystinosis Forum." *Ophthalmology and Therapy* 7, no. 2 (2018): 307–22. https://doi.org/10.1007/s40123-018-0146-6.

[148.]Kang-Mieler, J.J., C.R. Osswald, and W.F. Mieler. "Advances in Ocular Drug Delivery: Emphasis on the Posterior Segment." *Expert Opinion on Drug Delivery* 11, no. 10 (2014): 1647–60. https://doi.org/10.1517/17425247.2014.935338.

[149.]Kuśmierek, K., and E. Bald. "Measurement of Reduced and Total Mercaptamine in Urine Using Liquid Chromatography with Ultraviolet Detection." *Biomedical Chromatography* 22, no. 4 (2008): 441–45. https://doi.org/10.1002/bmc.959.

[150.]Bald, E., and R. Glowacki. "2-Chloro-1-Methylquinolinium Tetrafluoroborate as an Effective and Thiol Specific UV-Tagging Reagent for Liquid Chromatography." *Journal of Liquid Chromatography and Related Technologies* 24, no. 9 (2001): 1323–39. https://doi.org/10.1081/JLC-100103450.

[151.]Zhang, Q., N. Guo, Y. Sun, X. Li, and H. Yang. "Absolute Quantification of Poly(DL-Lactide-Co-Glycolide) in Microspheres Using Quantitative 1H NMR Spectroscopy." *Journal of Pharmaceutical and Biomedical Analysis* 146 (2017): 273–78. https://doi.org/10.1016/j.jpba.2017.08.046.

[152.]Eichenbaum, G., J. Zhou, A. De Smedt, S. De Jonghe, A. Looszova, T. Arien, F. Van Goethem, I. Vervoort, U. Shukla, and L. Lammens. "Methods to Evaluate and Improve the Injection Site Tolerability of Intravenous Formulations Prior to First-in-Human Testing." *Journal of Pharmacological and Toxicological Methods* 68, no. 3 (2013): 394–406. https://doi.org/10.1016/j.vascn.2013.08.002.

[153.]Abdelkader, H., S. Ismail, A. Hussein, Z. Wu, R. Al-Kassas, and R.G. Alany. "Conjunctival and Corneal Tolerability Assessment of Ocular Naltrexone Niosomes and Their Ingredients on the Hen's Egg Chorioallantoic Membrane and Excised Bovine Cornea Models." *International*

Journal of Pharmaceutics 432, no. 1–2 (2012): 1–10. https://doi.org/10.1016/j.ijpharm.2012.04.063.

[154.]OECD. "Test No. 437: Bovine Corneal Opacity and Permeability Test Method for Identifying i) Chemicals Inducing Serious Eye Damage and Ii) Chemicals Not Requiring Classification for Eye Irritation or Serious Eye Damage." *Test No. 438: Isolated Chicken Eye Test Method for Identifying i) Chemicals Inducing Serious Eye Damage and Ii) Chemicals Not Requiring Classification for Eye Irritation or Serious Eye Damage*, 2013.

[155.]Spinozzi, D., A. Miron, M. Bruinsma, J.T. Lie, I. Dapena, S. Oellerich, and G.R.J. Melles. "Improving the Success Rate of Human Corneal Endothelial Cell Cultures from Single Donor Corneas with Stabilization Medium." *Cell and Tissue Banking* 19, no. 1 (2018): 9–17. https://doi.org/10.1007/s10561-017-9665-y.

[156.]Armitage, W.J. "Preservation of Human Cornea." *Transfusion Medicine and Hemotherapy* 38, no. 2 (2011): 143–47. https://doi.org/10.1159/000326632.

[157.]"Cystaran_PI.Pdf." Accessed September 5, 2018. http://www.cystaran.com/Cystaran_PI.pdf.

[158.]Weterings, P.J.J.M., and Y.H.M. Van Erp. "Validation of the BECAM Assay - An Eye Irritancy Screening Test." *Alternative Methods in Toxicology* 5 (1987): 515–21.

[159.]McKenzie, B., G. Kay, K.H. Matthews, R. Knott, and D. Cairns. "Preformulation of Cysteamine Gels for Treatment of the Ophthalmic Complications in Cystinosis." *International Journal of Pharmaceutics* 515, no. 1–2 (2016): 575–82. https://doi.org/10.1016/j.ijpharm.2016.10.044.

[160.]Ramazani, F., W. Chen, C.F. Van Nostrum, G. Storm, F. Kiessling, T. Lammers, W.E. Hennink, and R.J. Kok. "Strategies for Encapsulation of Small Hydrophilic and Amphiphilic Drugs in PLGA Microspheres: State-of-the-Art and Challenges." *International Journal of Pharmaceutics* 499, no. 1–2 (2016): 358–67. https://doi.org/10.1016/j.ijpharm.2016.01.020.

[161.]Du, H., R. Wickramasinghe, and X. Qian. "Effects of Salt on the Lower Critical Solution Temperature of Poly (N-Isopropylacrylamide)." *Journal of Physical Chemistry B* 114, no. 49 (2010): 16594–604. https://doi.org/10.1021/jp105652c.

[162.]Zhang, Y., S. Furyk, L.B. Sagle, Y. Cho, D.E. Bergbreiter, and P.S. Cremer. "Effects of Hofmeister Anions on the LCST of PNIPAM as a Function of Molecular Weight." *Journal of Physical Chemistry C* 111, no. 25 (2007): 8916–24. https://doi.org/10.1021/jp0690603.

[163.]Meeus, J., M. Lenaerts, D.J. Scurr, K. Amssoms, M.C. Davies, C.J. Roberts, and G. Van Den Mooter. "The Influence of Spray-Drying Parameters on Phase Behavior, Drug Distribution, and in Vitro Release of Injectable Microspheres for Sustained Release." *Journal of Pharmaceutical Sciences* 104, no. 4 (2015): 1451–60. https://doi.org/10.1002/jps.24361.

[164.]Han, F.Y., K.J. Thurecht, A.K. Whittaker, and M.T. Smith. "Bioerodable PLGA-Based Microparticles for Producing Sustained-Release Drug Formulations and Strategies for

Improving Drug Loading." *Frontiers in Pharmacology* 7, no. JUN (2016). https://doi.org/10.3389/fphar.2016.00185.

[165.]Graf, M., and H.-O. Kalinowski. "1H-NMR Spectroscopic Evaluation of Cysteamine Eye Drops." *Klinische Monatsblatter Fur Augenheilkunde* 206, no. 4 (1995): 262–65. https://doi.org/10.1055/s-2008-1035436.

[166.]Cherqui, S., C. Sevin, G. Hamard, V. Kalatzis, M. Sich, M.O. Pequignot, K. Gogat, et al. "Intralysosomal Cystine Accumulation in Mice Lacking Cystinosin, the Protein Defective in Cystinosis." *Molecular and Cellular Biology* 22, no. 21 (2002): 7622–32. https://doi.org/10.1128/MCB.22.21.7622-7632.2002.

[167.]tunu, E.T., D.B. Granet, M.I. Kaiser-Kupfer, D. Thompson, A.S. Lindblad, G.F. Reed, B. Rubin, et al. "A Multicentre Randomised Double Masked Clinical Trial of a New Formulation of Topical Cysteamine for the Treatment of Corneal Cystine Crystals in Cystinosis." *British Journal of Ophthalmology* 87, no. 1 (2003): 28–31. https://doi.org/10.1136/bjo.87.1.28.

[168.]Ng, S.-F., J.J. Rouse, F.D. Sanderson, V. Meidan, and G.M. Eccleston. "Validation of a Static Franz Diffusion Cell System for in Vitro Permeation Studies." *AAPS PharmSciTech* 11, no. 3 (2010): 1432–41. https://doi.org/10.1208/s12249-010-9522-9.

[169.]Rahman, M.Q., K.-S. Chuah, E.C.A. MacDonald, J.P.M. Trusler, and K. Ramaesh. "The Effect of PH, Dilution, and Temperature on the Viscosity of Ocular Lubricants-Shift in Rheological Parameters and Potential Clinical Significance." *Eye (Basingstoke)* 26, no. 12 (2012): 1579–84. https://doi.org/10.1038/eye.2012.211.

[170.]Tauber, J. "Efficacy, Tolerability and Comfort of a 0.3% Hypromellose Gel Ophthalmic Lubricant in the Treatment of Patients with Moderate to Severe Dry Eye Syndrome." *Current Medical Research and Opinion* 23, no. 11 (2007): 2629–36. https://doi.org/10.1185/030079907X233197.

[171.]Dohil, R., B.L. Cabrera, J.A. Gangoiti, B.A. Barshop, and P. Rioux. "Pharmacokinetics of Cysteamine Bitartrate Following Intraduodenal Delivery." *Fundamental and Clinical Pharmacology* 28, no. 2 (2014): 136–43. https://doi.org/10.1111/fcp.12009.

[172.]Agrahari, Vibhuti, Abhirup Mandal, Vivek Agrahari, Hoang My Trinh, Mary Joseph, Animikh Ray, Hicheme Hadji, Ranjana Mitra, Dhananjay Pal, and Ashim K. Mitra. "A COMPREHENSIVE INSIGHT ON OCULAR PHARMACOKINETICS." *Drug Delivery and Translational Research* 6, no. 6 (December 2016): 735–54. https://doi.org/10.1007/s13346-016-0339-2.

[173.]Makoid, M. C., and J. R. Robinson. "Pharmacokinetics of Topically Applied Pilocarpine in the Albino Rabbit Eye." *Journal of Pharmaceutical Sciences* 68, no. 4 (April 1979): 435–43. https://doi.org/10.1002/jps.2600680411.

[174.]Horita, Shinya, Miwa Watanabe, Mai Katagiri, Hiroaki Nakamura, Hiroki Haniuda, Tomoyuki Nakazato, and Yoshiyuki Kagawa. "Species Differences in Ocular Pharmacokinetics and Pharmacological Activities of Regorafenib and Pazopanib Eye-Drops among Rats, Rabbits

and Monkeys." *Pharmacology Research & Perspectives* 7, no. 6 (2019): e00545. https://doi.org/10.1002/prp2.545.

[175.]Yu, Yu, Xingyan Lin, Qilin Wang, Mingguang He, and Ying Chau. "Long-term Therapeutic Effect in Nonhuman Primate Eye from a Single Injection of Anti-VEGF Controlled Release Hydrogel." *Bioengineering & Translational Medicine* 4, no. 2 (June 10, 2019): e10128. https://doi.org/10.1002/btm2.10128.

[176.]Nevo, Nathalie, Marie Chol, Anne Bailleux, Vasiliki Kalatzis, Ludivine Morisset, Olivier Devuyst, Marie-Claire Gubler, and Corinne Antignac. "Renal Phenotype of the Cystinosis Mouse Model Is Dependent upon Genetic Background." *Nephrology, Dialysis, Transplantation: Official Publication of the European Dialysis and Transplant Association - European Renal Association* 25, no. 4 (April 2010): 1059–66. https://doi.org/10.1093/ndt/gfp553.

[177.]Elmonem, Mohamed A., Ramzi Khalil, Ladan Khodaparast, Laleh Khodaparast, Fanny O. Arcolino, Joseph Morgan, Anna Pastore, et al. "Cystinosis (Ctns) Zebrafish Mutant Shows Pronephric Glomerular and Tubular Dysfunction." *Scientific Reports* 7, no. 1 (February 15, 2017): 42583. https://doi.org/10.1038/srep42583.

[178.]Hollywood, Jennifer A., Prasanna K. Kallingappa, Pang Yuk Cheung, Renita M. Martis, Sree Sreebhavan, Aparajita Chatterjee, Emma J. Buckels, Brya G. Mathews, Paula M. Lewis, and Alan J. Davidson. "Cystinosin Deficient Rats Recapitulate the Phenotype of Nephropathic Cystinosis," June 30, 2021. https://doi.org/10.1101/2021.06.29.450444.

[179.]Vareilles, Pierre, Philippe Conquet, and Jean-Claude Le Douarec. "A Method for the Routine Intraocular Pressure (IOP) Measurement in the Rabbit: Range of IOP Variations in This Species." *Experimental Eye Research* 24, no. 4 (April 1, 1977): 369–75. https://doi.org/10.1016/0014-4835(77)90149-X.

[180.]FRCSC, Mark B. Abelson, MD, CM. "The Secret World of Pharmacokinetics." Accessed September 29, 2021. https://www.reviewofophthalmology.com/article/the-secret-world-of-pharmacokinetics.

[181.]Larry, A. Meyer, Barney Nemiroff, L. Ubels John, Henry f. Edelhauser, and L. Dickerson Charlesworth. "Role of the Rabbit Nictitating Membrane in Ocular Irritancy Testing." *Journal of Toxicology: Cutaneous and Ocular Toxicology* 6, no. 1 (January 1, 1987): 43–56. https://doi.org/10.3109/15569528709052164.

[182.]Farkouh, Andre, Peter Frigo, and Martin Czejka. "Systemic Side Effects of Eye Drops: A Pharmacokinetic Perspective." *Clinical Ophthalmology (Auckland, N.Z.)* 10 (December 7, 2016): 2433–41. https://doi.org/10.2147/OPTH.S118409.

[183.]Vaajanen, Anu, and Heikki Vapaatalo. "A Single Drop in the Eye – Effects on the Whole Body?" *The Open Ophthalmology Journal* 11 (October 31, 2017): 305–14. https://doi.org/10.2174/1874364101711010305.

[184.]Prausnitz, Mark R., and Jeremy S. Noonan. “Permeability of Cornea, Sclera, and Conjunctiva: A Literature Analysis for Drug Delivery to the Eye.” *Journal of Pharmaceutical Sciences* 87, no. 12 (December 1, 1998): 1479–88. https://doi.org/10.1021/js9802594.

[185.]Luechtefeld, Thomas, Alexandra Maertens, Daniel P. Russo, Costanza Rovida, Hao Zhu, and Thomas Hartung. “Analysis of Draize Eye Irritation Testing and Its Prediction by Mining Publicly Available 2008–2014 REACH Data.” *ALTEX* 33, no. 2 (2016): 123–34. https://doi.org/10.14573/altex.1510053.

[186.]Hampshire, Victoria, and Sheilah Robertson. “Using the Facial Grimace Scale to Evaluate Rabbit Wellness in Post-Procedural Monitoring.” *Lab Animal* 44, no. 7 (July 2015): 259–60. https://doi.org/10.1038/laban.806.

[187.]“Test No. 405: Acute Eye Irritation/Corrosion.” Text. Accessed June 13, 2021. https://www.oecd-ilibrary.org/environment/test-no-405-acute-eye-irritation-corrosion_9789264185333-en.

[188.]Varga, Molly. *The Rabbit-Friendly Practice. BSAVA Manual of Rabbit Medicine*. BSAVA Library, 2014. https://doi.org/10.22233/9781910443217.6.

[189.]Iwata, F., E. M. Kuehl, G. F. Reed, L. M. McCain, W. A. Gahl, and M. I. Kaiser-Kupfer. “A Randomized Clinical Trial of Topical Cysteamine Disulfide (Cystamine) versus Free Thiol (Cysteamine) in the Treatment of Corneal Cystine Crystals in Cystinosis.” *Molecular Genetics and Metabolism* 64, no. 4 (August 1998): 237–42. https://doi.org/10.1006/mgme.1998.2725.

[190.]Lyseng-Williamson, Katherine A. “Cystadrops® (Cysteamine Hydrochloride 0.55% Viscous Eye-Drops Solution) in Treating Corneal Cystine Crystal Deposits in Patients with Cystinosis: A Profile of Its Use.” *Drugs & Therapy Perspectives* 33, no. 5 (May 1, 2017): 195–201. https://doi.org/10.1007/s40267-017-0398-6.

[191.]Inc, Recordati Rare Diseases. “U.S. FDA Approves CYSTADROPS® (Cysteamine Ophthalmic Solution) 0.37%, A New Practical Treatment Option for the Ocular Manifestations of Cystinosis.” Accessed June 13, 2021. https://www.prnewswire.com/news-releases/us-fda-approves-cystadrops-cysteamine-ophthalmic-solution-0-37-a-new-practical-treatment-option-for-the-ocular-manifestations-of-cystinosis-301118026.html.

[192.]Dohil, R., B.L. Cabrera, J.A. Gangoiti, B.A. Barshop, and P. Rioux. “Pharmacokinetics of Cysteamine Bitartrate Following Intraduodenal Delivery.” *Fundamental and Clinical Pharmacology* 28, no. 2 (2014): 136–43. https://doi.org/10.1111/fcp.12009.

[193.]Gertsman, Ilya, Wynonna S. Johnson, Connor Nishikawa, Jon A. Gangoiti, Bonnie Holmes, and Bruce A. Barshop. “Diagnosis and Monitoring of Cystinosis Using Immunomagnetically Purified Granulocytes.” *Clinical Chemistry* 62, no. 5 (May 2016): 766–72. https://doi.org/10.1373/clinchem.2015.252494.

[194.]Lin, Junli, Jingjing Sun, Yandong Wang, Yan Ma, Wenpei Chen, Ziyang Zhang, Gang Gui, and Baoqin Lin. "Ocular Pharmacokinetics of Naringenin Eye Drops Following Topical Administration to Rabbits." *Journal of Ocular Pharmacology and Therapeutics* 31, no. 1 (February 1, 2015): 51–56. https://doi.org/10.1089/jop.2014.0047.

[195.]Liang, Hong, Christophe Baudouin, Rachid Tahiri Joutei Hassani, Françoise Brignole-Baudouin, and Antoine Labbe. "Photophobia and Corneal Crystal Density in Nephropathic Cystinosis: An In Vivo Confocal Microscopy and Anterior-Segment Optical Coherence Tomography Study." *Investigative Ophthalmology & Visual Science* 56, no. 5 (May 1, 2015): 3218–25. https://doi.org/10.1167/iovs.15-16499.

[196.]Lim, K. Sheng, Sanjeewa S. Wickremasinghe, M. Francesca Cordeiro, Catey Bunce, and Peng T. Khaw. "Accuracy of Intraocular Pressure Measurements in New Zealand White Rabbits." *Investigative Ophthalmology & Visual Science* 46, no. 7 (July 1, 2005): 2419–23. https://doi.org/10.1167/iovs.04-0610.

[197.]Vareilles, Pierre, Philippe Conquet, and Jean-Claude Le Douarec. "A Method for the Routine Intraocular Pressure (IOP) Measurement in the Rabbit: Range of IOP Variations in This Species." *Experimental Eye Research* 24, no. 4 (April 1, 1977): 369–75. https://doi.org/10.1016/0014-4835(77)90149-X.

[198.]Atallah, Carla, Catherine Charcosset, and Hélène Greige-Gerges. "Challenges for Cysteamine Stabilization, Quantification, and Biological Effects Improvement." *Journal of Pharmaceutical Analysis* 10, no. 6 (December 1, 2020): 499–516. https://doi.org/10.1016/j.jpha.2020.03.007.

[199.]Tuntland, Tove, Brian Ethell, Takatoshi Kosaka, Francesca Blasco, Richard Xu Zang, Monish Jain, Ty Gould, and Keith Hoffmaster. "Implementation of Pharmacokinetic and Pharmacodynamic Strategies in Early Research Phases of Drug Discovery and Development at Novartis Institute of Biomedical Research." *Frontiers in Pharmacology* 5 (2014): 174. https://doi.org/10.3389/fphar.2014.00174.

[200.]Simpson, Jennifer, Chyong Jy Nien, Kevin Flynn, Brian Jester, Stephanie Cherqui, and James Jester. "Quantitative in Vivo and Ex Vivo Confocal Microscopy Analysis of Corneal Cystine Crystals in the Ctns Knockout Mouse." *Molecular Vision* 17 (2011): 2212–20.

[201.]Simpson, Jennifer L., Chyong Jy Nien, Kevin J. Flynn, and James V. Jester. "Evaluation of Topical Cysteamine Therapy in the CTNS−/− Knockout Mouse Using in Vivo Confocal Microscopy." *Molecular Vision* 17 (2011): 2649.

[202.]Rocca, Celine J., Alexander Kreymerman, Sarah N. Ur, Katie E. Frizzi, Swati Naphade, Athena Lau, Tammy Tran, Nigel A. Calcutt, Jeffrey L. Goldberg, and Stephanie Cherqui. "Treatment of Inherited Eye Defects by Systemic Hematopoietic Stem Cell Transplantation." *Investigative Ophthalmology & Visual Science* 56, no. 12 (November 2015): 7214–23. https://doi.org/10.1167/iovs.15-17107.

[203.]Aumann, Silke, Sabine Donner, Jörg Fischer, and Frank Müller. "Optical Coherence Tomography (OCT): Principle and Technical Realization." In *High Resolution Imaging in*

Microscopy and Ophthalmology: New Frontiers in Biomedical Optics, edited by Josef F. Bille. Cham (CH): Springer, 2019. http://www.ncbi.nlm.nih.gov/books/NBK554044/.

[204.]Csorba, Anita, Erika Maka, Otto Alexander Maneschg, Attila Szabó, Nóra Szentmáry, Mária Csidey, Miklós Resch, László Imre, Krisztina Knézy, and Zoltán Zsolt Nagy. "Examination of Corneal Deposits in Nephropathic Cystinosis Using in Vivo Confocal Microscopy and Anterior Segment Optical Coherence Tomography: An Age-Dependent Cross Sectional Study." *BMC Ophthalmology* 20 (February 26, 2020). https://doi.org/10.1186/s12886-020-01336-w.

[205.]Keidel, Leonie, Katharina Hohenfellner, Benedikt Schworm, Siegfried Priglinger, Nikolaus Luft, and Claudia Priglinger. "Spectral Domain Optical Coherence Tomography-Based Retinochoroidal Cystine Crystal Score: A Window into Infantile Nephropathic Cystinosis." *British Journal of Ophthalmology*, September 16, 2021. https://doi.org/10.1136/bjophthalmol-2021-319612.

[206.]Kozak, Igor, J. Fernando Arevalo, and Samir S. Shoughy. "Intraretinal Crystals in Nephopathic Cystinosis and Fanconi Syndrome." *JAMA Ophthalmology* 135, no. 3 (March 9, 2017): e165169. https://doi.org/10.1001/jamaophthalmol.2016.5169.

[207.]Schindelin, Johannes, Ignacio Arganda-Carreras, Erwin Frise, Verena Kaynig, Mark Longair, Tobias Pietzsch, Stephan Preibisch, et al. "Fiji: An Open-Source Platform for Biological-Image Analysis." *Nature Methods* 9, no. 7 (July 2012): 676–82. https://doi.org/10.1038/nmeth.2019

[208.]Machholz, Elton, Guy Mulder, Casimira Ruiz, Brian F. Corning, and Kathleen R. Pritchett-Corning. "Manual Restraint and Common Compound Administration Routes in Mice and Rats." *Journal of Visualized Experiments : JoVE*, no. 67 (September 26, 2012): 2771. https://doi.org/10.3791/2771.

[209.]Kalueff, Allan V., Adam Michael Stewart, Cai Song, Kent C. Berridge, Ann M. Graybiel, and John C. Fentress. "Neurobiology of Rodent Self-Grooming and Its Value for Translational Neuroscience." *Nature Reviews Neuroscience* 17, no. 1 (January 2016): 45–59. https://doi.org/10.1038/nrn.2015.8.

[210.]Lewis, Craig, and Elias I. Traboulsi. "Use of Tegaderm™ for Postoperative Eye Dressing in Children." *Journal of American Association for Pediatric Ophthalmology and Strabismus* 12, no. 4 (August 1, 2008): 420. https://doi.org/10.1016/j.jaapos.2008.01.014.

[211.]Brown, Cyndi. "Restraint Collars. Part I: Elizabethan Collars and Other Types of Restraint Collars." *Lab Animal* 35, no. 2 (February 2006): 23–25. https://doi.org/10.1038/laban0206-23.

[212.]Boote, Craig, Yiqin Du, Sian Morgan, Jonathan Harris, Christina S. Kamma-Lorger, Sally Hayes, Kira L. Lathrop, et al. "Quantitative Assessment of Ultrastructure and Light Scatter in Mouse Corneal Debridement Wounds." *Investigative Ophthalmology & Visual Science* 53, no. 6 (May 1, 2012): 2786–95. https://doi.org/10.1167/iovs.11-9305.

[213.]Tahara, Kohei, Keiichi Karasawa, Risako Onodera, and Hirofumi Takeuchi. “Feasibility of Drug Delivery to the Eye’s Posterior Segment by Topical Instillation of PLGA Nanoparticles.” *Asian Journal of Pharmaceutical Sciences* 12, no. 4 (July 1, 2017): 394–99. https://doi.org/10.1016/j.ajps.2017.03.002.

[214.]Swetledge, Sean, Renee Carter, Rhett Stout, Carlos E. Astete, Jangwook P. Jung, and Cristina M. Sabliov. “Stability and Ocular Biodistribution of Topically Administered PLGA Nanoparticles.” *Scientific Reports* 11, no. 1 (June 10, 2021): 12270. https://doi.org/10.1038/s41598-021-90792-5.

[215.]Gupta, Himanshu, Mohammed Aqil, Roop K. Khar, Asgar Ali, Aseem Bhatnagar, and Gaurav Mittal. “Sparfloxacin-Loaded PLGA Nanoparticles for Sustained Ocular Drug Delivery.” *Nanomedicine: Nanotechnology, Biology, and Medicine* 6, no. 2 (April 2010): 324–33. https://doi.org/10.1016/j.nano.2009.10.004.

[216.]Caro, Adam C, F Claire Hankenson, and James O Marx. “Comparison of Thermoregulatory Devices Used during Anesthesia of C57BL/6 Mice and Correlations between Body Temperature and Physiologic Parameters.” *Journal of the American Association for Laboratory Animal Science : JAALAS* 52, no. 5 (September 2013): 577–83.

[217.]Vogel, Benjamin, Heike Wagner, Johanna Gmoser, Anja Wörner, Anna Löschberger, Laura Peters, Anna Frey, Ulrich Hofmann, and Stefan Frantz. “Touch-Free Measurement of Body Temperature Using Close-up Thermography of the Ocular Surface.” *MethodsX* 3 (January 1, 2016): 407–16. https://doi.org/10.1016/j.mex.2016.05.002.

[218.]Li, Qiao, Cheng Qian, and Feng-Quan Zhou. “Investigating Mammalian Axon Regeneration: In Vivo Electroporation of Adult Mouse Dorsal Root Ganglion.” *Journal of Visualized Experiments : JoVE*, no. 139 (September 1, 2018): 58171. https://doi.org/10.3791/58171.

[219.]Marschner, Julian A., Hannah Schäfer, Alexander Holderied, and Hans-Joachim Anders. “Optimizing Mouse Surgery with Online Rectal Temperature Monitoring and Preoperative Heat Supply. Effects on Post-Ischemic Acute Kidney Injury.” *PLOS ONE* 11, no. 2 (February 18, 2016): e0149489. https://doi.org/10.1371/journal.pone.0149489.

[220.]Gargiulo, Sara, Adelaide Greco, Matteo Gramanzini, Silvia Esposito, Andrea Affuso, Arturo Brunetti, and Giancarlo Vesce. “Mice Anesthesia, Analgesia, and Care, Part I: Anesthetic Considerations in Preclinical Research.” *ILAR Journal* 53, no. 1 (2012): E55-69. https://doi.org/10.1093/ilar.53.1.55.

[221.]Wang, Guoliang, Yuhua Xue, Yanzi Wang, Fei Dong, Mei Shen, Rongrong Zong, Zuguo Liu, and Cheng Li. “The Role of Autophagy in the Pathogenesis of Exposure Keratitis.” *Journal of Cellular and Molecular Medicine* 23, no. 6 (2019): 4217–28. https://doi.org/10.1111/jcmm.14310.

[222.]Lennikov, Anton, Nobuyoshi Kitaichi, Satoru Kase, Kousuke Noda, Yukihiro Horie, Akira Nakai, Shigeaki Ohno, and Susumu Ishida. “Induction of Heat Shock Protein 70 Ameliorates

Ultraviolet-Induced Photokeratitis in Mice." *International Journal of Molecular Sciences* 14, no. 1 (January 2013): 2175–89. https://doi.org/10.3390/ijms14012175.

[223.]Burkholder, Tanya, Charmaine Foltz, Eleanor Karlsson, C Garry Linton, and Joanne M Smith. "Health Evaluation of Experimental Laboratory Mice." *Current Protocols in Mouse Biology* 2 (June 2012): 145–65. https://doi.org/10.1002/9780470942390.mo110217.

[224.]Brown, C. Restraint collars. Part II: specific issues with restraint collars. Lab Anim. (NY) 35(3), 25–27 (2006). https://doi.org/10.1038/laban0306-25.

[225.]Lanzl, I.M. "Ocular Features of Treatable Lysosomal Storage Disorders – Fabry Disease, Mucopolysaccharidoses I, II and VI and Gaucher Disease." *European Ophthalmic Review*, February 15, 2011. http://www.touchophthalmology.com/anterior-segment/journal-articles/ocular-features-of-treatable-lysosomal-storage-disorders-fabry-disease-mucopolysaccharidoses-i-ii-and-vi-and-gaucher-disease/.

[226.]Fenzl, Carlton R., Kyla Teramoto, and Majid Moshirfar. "Ocular Manifestations and Management Recommendations of Lysosomal Storage Disorders I: Mucopolysaccharidoses." *Clinical Ophthalmology* 9 (September 7, 2015): 1633–44. https://doi.org/10.2147/OPTH.S78368.

[227.]Biswas, Jyotirmay, Krishnendu Nandi, Sudharshan Sridharan, and Prabhat Ranjan. "Ocular Manifestation of Storage Diseases." *Current Opinion in Ophthalmology* 19, no. 6 (November 2008): 507–11. https://doi.org/10.1097/ICU.0b013e32831215c3.

[228.]Barabino, Stefano, Linling Shen, Lu Chen, Saadia Rashid, Maurizio Rolando, and M. Reza Dana. "The Controlled-Environment Chamber: A New Mouse Model of Dry Eye." *Investigative Ophthalmology & Visual Science* 46, no. 8 (August 2005): 2766–71. https://doi.org/10.1167/iovs.04-1326.

[229.]Shen, Jun, Qin Wang, YuXia Zhang, Xuan Wang, and Peng Shi. "Combination of Warming Blanket and Prewarmed Intravenous Infusion Is Effective for Rewarming in Infants with Postoperative Hypothermia in China." *Paediatric Anaesthesia* 25, no. 11 (November 2015): 1139–43. https://doi.org/10.1111/pan.12733.

[230.]Rajak, Saul, Juliette Rajak, and Dinesh Selva. "Performing a Tarsorrhaphy." *Community Eye Health* 28, no. 89 (2015): 10–11.

[231.]Panda, A., N. Pushker, and L. M. Bageshwar. "Lateral Tarsorrhaphy: Is It Preferable to Patching?" *Cornea* 18, no. 3 (May 1999): 299–301. https://doi.org/10.1097/00003226-199905000-00010.

[232.]Shetty, Nivedita, Heejun Park, Dmitry Zemlyanov, Sharad Mangal, Sonal Bhujbal, and Qi (Tony) Zhou. "Influence of Excipients on Physical and Aerosolization Stability of Spray Dried High-Dose Powder Formulations for Inhalation." *International Journal of Pharmaceutics* 544, no. 1 (June 10, 2018): 222–34. https://doi.org/10.1016/j.ijpharm.2018.04.034.

[233.]Esparza, Yussef, Tri-Dung Ngo, Carole Fraschini, and Yaman Boluk. "Aggregate Morphology and Aqueous Dispersibility of Spray-Dried Powders of Cellulose Nanocrystals." *Industrial & Engineering Chemistry Research* 58, no. 43 (October 30, 2019): 19926–36. https://doi.org/10.1021/acs.iecr.9b03951.

[234.]Benet, L. Z. "Pharmacokinetic Parameters: Which Are Necessary to Define a Drug Substance?" *European Journal of Respiratory Diseases. Supplement* 134 (1984): 45–61.

[235.]Santos, Valentin Aranha dos, Leopold Schmetterer, Hannes Stegmann, Martin Pfister, Alina Messner, Gerald Schmidinger, Gerhard Garhofer, and René M. Werkmeister. "CorneaNet: Fast Segmentation of Cornea OCT Scans of Healthy and Keratoconic Eyes Using Deep Learning." *Biomedical Optics Express* 10, no. 2 (January 17, 2019): 622–41. https://doi.org/10.1364/BOE.10.000622.

[236.]Ouyang, Jiahong, Jiahong Ouyang, Jiahong Ouyang, Tejas Sudharshan Mathai, Tejas Sudharshan Mathai, Tejas Sudharshan Mathai, Kira Lathrop, et al. "Accurate Tissue Interface Segmentation via Adversarial Pre-Segmentation of Anterior Segment OCT Images." *Biomedical Optics Express* 10, no. 10 (October 1, 2019): 5291–5324. https://doi.org/10.1364/BOE.10.005291.

[237.]Wolf, Michael S., Jennifer King, Elizabeth A. H. Wilson, Laura M. Curtis, Stacy Cooper Bailey, James Duhig, Allison Russell, et al. "Usability of FDA-Approved Medication Guides." *Journal of General Internal Medicine* 27, no. 12 (December 2012): 1714–20. https://doi.org/10.1007/s11606-012-2068-7.

[238.]Sykes, Sean, Eva Chou, Robert A. Mazzoli, Joseph Pasternak, Denise Ryan, Rose Sia, and Marcus Colyer. "Comparison of Simulation-Based versus Live Tissue–Based Ocular Trauma Training on Novice Ophthalmologists: Repair of Marginal Eyelid Laceration Model." *Journal of Academic Ophthalmology* 10, no. 1 (January 2018): e61–68. https://doi.org/10.1055/s-0038-1653972.

[239.]Kashiwagi, Kenji. "Wide Variation of Squeezing Force and Dispensing Time Interval among Eyedropper Bottles." *Journal of Ophthalmology* 2019 (April 16, 2019): 7250563. https://doi.org/10.1155/2019/7250563.

[240.]Nordmann, Jean-Philippe, Philippe Denis, Marc Vigneux, Elyse Trudeau, Isabelle Guillemin, and Gilles Berdeaux. "Development of the Conceptual Framework for the Eye-Drop Satisfaction Questionnaire (EDSQ©) in Glaucoma Using a Qualitative Study." *BMC Health Services Research* 7, no. 1 (August 6, 2007): 124. https://doi.org/10.1186/1472-6963-7-124.

[241.]Law, Gloria C., Alpaslan Bülbül, Christina J. Jones, and Helen Smith. "'The Mean Mummy Way' – Experiences of Parents Instilling Eye Drops to Their Young Children as Described in Online Forums and Blogs." *BMC Pediatrics* 20, no. 1 (December 2020): 1–8. https://doi.org/10.1186/s12887-020-02410-4.

[242.]Charrier, Cedric, Catherine Rodger, Jennifer Robertson, Aleksandra Kowalczuk, Nicola Shand, Douglas Fraser-Pitt, Derry Mercer, and Deborah O'Neil. "Cysteamine (Lynovex®), a

Novel Mucoactive Antimicrobial & Antibiofilm Agent for the Treatment of Cystic Fibrosis." *Orphanet Journal of Rare Diseases* 9, no. 1 (November 30, 2014): 189. https://doi.org/10.1186/s13023-014-0189-2.

[243.]Paul, Bindu D., and Solomon H. Snyder. "Therapeutic Applications of Cysteamine and Cystamine in Neurodegenerative and Neuropsychiatric Diseases." *Frontiers in Neurology* 10 (December 12, 2019): 1315. https://doi.org/10.3389/fneur.2019.01315.

[244.]Khanna, Kritika, Wilfred Raymond, Annabelle R. Charbit, Jing Jin, Irina Gitlin, Monica Tang, Hannah S. Sperber, et al. "Binding of SARS-CoV-2 Spike Protein to ACE2 Is Disabled by Thiol-Based Drugs; Evidence from in Vitro SARS-CoV-2 Infection Studies." *BioRxiv: The Preprint Server for Biology*, December 8, 2020, 2020.12.08.415505. https://doi.org/10.1101/2020.12.08.415505.

[245.]Thoene, Jess, Robert F. Gavin, Aaron Towne, Lauren Wattay, Maria Grazia Ferrari, and Ranajit Pal. "In Vitro Activity of Cysteamine Against SARS-CoV-2 Variants Alpha, Beta,Gamma and Delta," October 4, 2021. https://doi.org/10.1101/2021.10.02.462862.

[246.]Devereux, Graham, Danielle Wrolstad, Stephen J. Bourke, Cori L. Daines, Simon Doe, Ryan Dougherty, Rose Franco, et al. "Oral Cysteamine as an Adjunct Treatment in Cystic Fibrosis Pulmonary Exacerbations: An Exploratory Randomized Clinical Trial." *PloS One* 15, no. 12 (2020): e0242945. https://doi.org/10.1371/journal.pone.0242945.

[247.]Verny, Christophe, Anne-Catherine Bachoud-Lévi, Alexandra Durr, Cyril Goizet, Jean-Philippe Azulay, Clémence Simonin, Christine Tranchant, et al. "A Randomized, Double-Blind, Placebo-Controlled Trial Evaluating Cysteamine in Huntington's Disease." *Movement Disorders: Official Journal of the Movement Disorder Society* 32, no. 6 (June 2017): 932–36. https://doi.org/10.1002/mds.27010.

[248.]Faraj, Janine, Manish Bodas, Garrett Pehote, Doug Swanson, Ajit Sharma, and Neeraj Vij. "Novel Cystamine-Core Dendrimer-Formulation Rescues ΔF508-CFTR and Inhibits Pseudomonas Aeruginosa Infection by Augmenting Autophagy." *Expert Opinion on Drug Delivery* 16, no. 2 (February 2019): 177–86. https://doi.org/10.1080/17425247.2019.1575807.

[249.]Zhi, Kaining, Babatunde Raji, Anantha R. Nookala, Mohammad Moshahid Khan, Xuyen H. Nguyen, Swarna Sakshi, Tayebeh Pourmotabbed, et al. "PLGA Nanoparticle-Based Formulations to Cross the Blood–Brain Barrier for Drug Delivery: From R&D to CGMP." *Pharmaceutics* 13, no. 4 (April 6, 2021): 500. https://doi.org/10.3390/pharmaceutics13040500.

[250.]Bruk, Liza A., Katherine E. Dunkelberger, Pawjai Khampang, Wenzhou Hong, Srivatsun Sadagopan, Cuneyt M. Alper, and Morgan V. Fedorchak. "Controlled Release of Ciprofloxacin and Ceftriaxone from a Single Ototopical Administration of Antibiotic-Loaded Polymer Microspheres and Thermoresponsive Gel." *PLOS ONE* 15, no. 10 (October 12, 2020): e0240535. https://doi.org/10.1371/journal.pone.0240535.

[251.]Schilling, Andrea L., Yalcin Kulahci, John Moore, Eric W. Wang, Stella E. Lee, and Steven R. Little. "A Thermoresponsive Hydrogel System for Long-Acting Corticosteroid Delivery

into the Paranasal Sinuses." *Journal of Controlled Release: Official Journal of the Controlled Release Society* 330 (February 10, 2021): 889–97. https://doi.org/10.1016/j.jconrel.2020.10.062.

[252.]Chen, Yuanyuan, Yu Chen, Beata Jastrzebska, Marcin Golczak, Sahil Gulati, Hong Tang, William Seibel, et al. "A Novel Small Molecule Chaperone of Rod Opsin and Its Potential Therapy for Retinal Degeneration." *Nature Communications* 9, no. 1 (May 17, 2018): 1976. https://doi.org/10.1038/s41467-018-04261-1.

[253.]Dryja, Thaddeus P., Terri L. McGee, Lauri B. Hahn, Glenn S. Cowley, Jane E. Olsson, Elias Reichel, Michael A. Sandberg, and Eliot L. Berson. "Mutations within the Rhodopsin Gene in Patients with Autosomal Dominant Retinitis Pigmentosa." *New England Journal of Medicine* 323, no. 19 (November 8, 1990): 1302–7. https://doi.org/10.1056/NEJM199011083231903.

[254.]Rivera, Andrea, Karen White, Heidi Stöhr, Klaus Steiner, Nadine Hemmrich, Timo Grimm, Bernhard Jurklies, et al. "A Comprehensive Survey of Sequence Variation in the ABCA4 (ABCR) Gene in Stargardt Disease and Age-Related Macular Degeneration." *The American Journal of Human Genetics* 67, no. 4 (October 1, 2000): 800–813. https://doi.org/10.1086/303090.

[255.]Morimura, Hiroyuki, Gerald A. Fishman, Sandeep A. Grover, Anne B. Fulton, Eliot L. Berson, and Thaddeus P. Dryja. "Mutations in the RPE65 Gene in Patients with Autosomal Recessive Retinitis Pigmentosa or Leber Congenital Amaurosis." *Proceedings of the National Academy of Sciences* 95, no. 6 (March 17, 1998): 3088–93. https://doi.org/10.1073/pnas.95.6.3088.

[256.]Herrero-Vanrell, Rocio, and Miguel F Refojo. "Biodegradable Microspheres for Vitreoretinal Drug Delivery." *Advanced Drug Delivery Reviews*, Drug Delivery to the Posterior Segments of the Eye, 52, no. 1 (October 31, 2001): 5–16. https://doi.org/10.1016/S0169-409X(01)00200-9.

[257.]Bhatt, Priyanka, Gulimirerouzi Fnu, Deepak Bhatia, Amna Shahid, and Vijaykumar Sutariya. "Nanodelivery of Resveratrol-Loaded PLGA Nanoparticles for Age-Related Macular Degeneration." *AAPS PharmSciTech* 21, no. 8 (October 21, 2020): 291. https://doi.org/10.1208/s12249-020-01836-4.

[258.]Fernández-Sánchez, Laura, Irene Bravo-Osuna, Pedro Lax, Alicia Arranz-Romera, Victoria Maneu, Sergio Esteban-Pérez, Isabel Pinilla, María del Mar Puebla-González, Rocío Herrero-Vanrell, and Nicolás Cuenca. "Controlled Delivery of Tauroursodeoxycholic Acid from Biodegradable Microspheres Slows Retinal Degeneration and Vision Loss in P23H Rats." *PLOS ONE* 12, no. 5 (May 25, 2017): e0177998. https://doi.org/10.1371/journal.pone.0177998.

[259.]Jin, Qiu-xia, Xin-ran Dong, Jing-meng Chen, Ke Yao, and Ya-lin Wu. "Effects of Organic Solvents on Two Retinal Pigment Epithelial Lipofuscin Fluorophores, A2E and All-Trans-Retinal Dimer." *Journal of Zhejiang University. Science. B* 15, no. 7 (July 2014): 661–69. https://doi.org/10.1631/jzus.B1300194.

[260.]Lin, Haijiang, Yueran Yue, Daniel E. Maidana, Peggy Bouzika, Alp Atik, Hidetaka Matsumoto, Joan W. Miller, and Demetrios G. Vavvas. "Drug Delivery Nanoparticles: Toxicity Comparison in Retinal Pigment Epithelium and Retinal Vascular Endothelial Cells." *Seminars in Ophthalmology* 31, no. 1–2 (2016): 1–9. https://doi.org/10.3109/08820538.2015.1114865.

[261.]Abouelmagd, Sara A., Bo Sun, Alice C. Chang, Youn Jin Ku, and Yoon Yeo. "Release Kinetics Study of Poorly Water-Soluble Drugs from Nanoparticles: Are We Doing It Right?" *Molecular Pharmaceutics* 12, no. 3 (March 2, 2015): 997–1003. https://doi.org/10.1021/mp500817h.

[262.]Awwad, Sahar, Alastair Lockwood, Steve Brocchini, and Peng T. Khaw. "The PK-Eye: A Novel In Vitro Ocular Flow Model for Use in Preclinical Drug Development." *Journal of Pharmaceutical Sciences* 104, no. 10 (2015): 3330–42. https://doi.org/10.1002/jps.24480.

[263.]Sakami, Sanae, Alexander V. Kolesnikov, Vladimir J. Kefalov, and Krzysztof Palczewski. "P23H Opsin Knock-in Mice Reveal a Novel Step in Retinal Rod Disc Morphogenesis." *Human Molecular Genetics* 23, no. 7 (April 1, 2014): 1723–41. https://doi.org/10.1093/hmg/ddt561.

[264.]Huber, Gesine, Susanne C. Beck, Christian Grimm, Ayse Sahaboglu-Tekgoz, Francois Paquet-Durand, Andreas Wenzel, Peter Humphries, T. Michael Redmond, Mathias W. Seeliger, and M. Dominik Fischer. "Spectral Domain Optical Coherence Tomography in Mouse Models of Retinal Degeneration." *Investigative Ophthalmology & Visual Science* 50, no. 12 (December 2009): 5888–95. https://doi.org/10.1167/iovs.09-3724.

[265.]Butler, Mark C., and Jack M. Sullivan. "A Novel, Real-Time, In Vivo Mouse Retinal Imaging System." *Investigative Ophthalmology & Visual Science* 56, no. 12 (November 9, 2015): 7159–68. https://doi.org/10.1167/iovs.14-16370.

[266.]Benchorin, Gillie, Melissa A. Calton, Marielle O. Beaulieu, and Douglas Vollrath. "Assessment of Murine Retinal Function by Electroretinography." *Bio-Protocol* 7, no. 7 (April 5, 2017): e2218. https://doi.org/10.21769/BioProtoc.2218.

[267.]Centers for Disease Control and Prevention (2013). CDC health disparities and inequalities report—United States, 2013. MMWR Surveill Summ 62 (suppl 3), 1–187

[268.]Health, Institute of Medicine (US) Committee on Capitalizing on Social Science and Behavioral Research to Improve the Public's, Brian D. Smedley, and S. Leonard Syme. *Understanding and Reducing Socioeconomic and Racial/Ethnic Disparities in Health*. *Promoting Health: Intervention Strategies from Social and Behavioral Research*. National Academies Press (US), 2000. https://www.ncbi.nlm.nih.gov/books/NBK222826/.

[269.]Nelson, Alan. "Unequal Treatment: Confronting Racial and Ethnic Disparities in Health Care." *Journal of the National Medical Association* 94, no. 8 (August 2002): 666–68.

[270.]Chokshi, Dave A. "Teaching About Health Disparities Using a Social Determinants Framework." *Journal of General Internal Medicine* 25, no. 2 (May 1, 2010): 182–85. https://doi.org/10.1007/s11606-009-1230-3.

[271.]West, S. K., R. Klein, J. Rodriguez, B. Muñoz, A. T. Broman, R. Sanchez, R. Snyder, and Proyecto VER. "Diabetes and Diabetic Retinopathy in a Mexican-American Population: Proyecto VER." *Diabetes Care* 24, no. 7 (July 2001): 1204–9. https://doi.org/10.2337/diacare.24.7.1204.

[272.]Harris, M. I., R. Klein, C. C. Cowie, M. Rowland, and D. D. Byrd-Holt. "Is the Risk of Diabetic Retinopathy Greater in Non-Hispanic Blacks and Mexican Americans than in Non-Hispanic Whites with Type 2 Diabetes? A U.S. Population Study." *Diabetes Care* 21, no. 8 (August 1998): 1230–35. https://doi.org/10.2337/diacare.21.8.1230.

[273.]Khachatryan, Naira, Maxwell Pistilli, Maureen G. Maguire, Rebecca J. Salowe, Raymond M. Fertig, Tanisha Moore, Harini V. Gudiseva, et al. "Primary Open-Angle African American Glaucoma Genetics (POAAGG) Study: Gender and Risk of POAG in African Americans." *PLOS ONE* 14, no. 8 (August 1, 2019): e0218804. https://doi.org/10.1371/journal.pone.0218804.

[274.]Tielsch, James M., Alfred Sommer, Joanne Katz, Richard M. Royall, Harry A. Quigley, and Jonathan Javitt. "Racial Variations in the Prevalence of Primary Open-Angle Glaucoma: The Baltimore Eye Survey." *JAMA* 266, no. 3 (July 17, 1991): 369–74. https://doi.org/10.1001/jama.1991.03470030069026.

[275.]Gupta, Priya, Di Zhao, Eliseo Guallar, Fang Ko, Michael V. Boland, and David S. Friedman. "Prevalence of Glaucoma in the United States: The 2005–2008 National Health and Nutrition Examination Survey." *Investigative Ophthalmology & Visual Science* 57, no. 6 (May 1, 2016): 2905–13. https://doi.org/10.1167/iovs.15-18469.

[276.]Benabentos, Rocio, Payal Ray, and Deepak Kumar. "Addressing Health Disparities in the Undergraduate Curriculum: An Approach to Develop a Knowledgeable Biomedical Workforce." *CBE Life Sciences Education* 13, no. 4 (2014): 636–40. https://doi.org/10.1187/cbe.14-06-0101.

[277.]Vazquez, Maribel. "Engaging Biomedical Engineering in Health Disparities Challenges." *Journal of Community Medicine & Health Education* 8, no. 2 (2018). https://doi.org/10.4172/2161-0711.1000595.

[278.]Vazquez, Maribel, Otto Marte, Joseph Barba, and Karen Hubbard. "An Approach to Integrating Health Disparities within Undergraduate Biomedical Engineering Education." *Annals of Biomedical Engineering* 45, no. 11 (November 2017): 2703–15. https://doi.org/10.1007/s10439-017-1903-8.

[279.]Sharma, Malika, Andrew D. Pinto, and Arno K. Kumagai. "Teaching the Social Determinants of Health: A Path to Equity or a Road to Nowhere?" *Acad Med* 93, no. 1 (2018): 25–30. https://doi.org/10.1097/ACM.0000000000001689.

[280.]Raddatz, Michael A. "Getting Our Priorities Right: Social Determinants of Health in Medical Education." *Academic Medicine* 94, no. 5 (May 2019): 615–16. https://doi.org/10.1097/ACM.0000000000002608.

[281.]Siegel, Jennifer, David Coleman, and Thea James. “Integrating Social Determinants of Health Into Graduate Medical Education: A Call for Action.” *Academic Medicine* 93, no. 2 (February 2018): 159–62. https://doi.org/10.1097/ACM.0000000000002054.

[282.]Wen, Hong, Huijeong Jung, and Xuhong Li. “Drug Delivery Approaches in Addressing Clinical Pharmacology-Related Issues: Opportunities and Challenges.” *The AAPS Journal* 17, no. 6 (August 15, 2015): 1327–40. https://doi.org/10.1208/s12248-015-9814-9.

[283.]Siepmann, Juergen, Ronald A. Siegel, and Michael J. Rathbone, eds. *Fundamentals and Applications of Controlled Release Drug Delivery*. Advances in Delivery Science and Technology. Springer US, 2012. https://doi.org/10.1007/978-1-4614-0881-9.

[284.]Little, Steven R. “The Current Status and Future Directions of CRS Focus Groups.” *Journal of Controlled Release* 300 (April 28, 2019): 46–51. https://doi.org/10.1016/j.jconrel.2019.02.020.

[285.]Collins, David S., Manuel Sánchez-Félix, Advait V. Badkar, and Randall Mrsny. “Accelerating the Development of Novel Technologies and Tools for the Subcutaneous Delivery of Biotherapeutics.” *Journal of Controlled Release* 321 (May 10, 2020): 475–82. https://doi.org/10.1016/j.jconrel.2020.02.036.

[286.]Havel, Henry, Gregory Finch, Pamela Strode, Marc Wolfgang, Stephen Zale, Iulian Bobe, Hagop Youssoufian, Matthew Peterson, and Maggie Liu. “Nanomedicines: From Bench to Bedside and Beyond.” *The AAPS Journal* 18, no. 6 (November 2016): 1373–78. https://doi.org/10.1208/s12248-016-9961-7.

[287.]Nance, Elizabeth. “Careers in Nanomedicine and Drug Delivery.” *Advanced Drug Delivery Reviews*, NanoDDS 2018: Engineering the next wave of nanomedicine and drug delivery systems, 144 (April 1, 2019): 180–89. https://doi.org/10.1016/j.addr.2019.06.009.

[288.]Dzau, Victor J., and Celynne A. Balatbat. “Health and Societal Implications of Medical and Technological Advances.” *Science Translational Medicine* 10, no. 463 (October 17, 2018). https://doi.org/10.1126/scitranslmed.aau4778.

[289.]Njoku, Anuli. “Teaching Health Disparities Awareness in Undergraduate Public Health Courses.” *International Journal for the Scholarship of Teaching and Learning* 12, no. 2 (July 24, 2018). https://doi.org/10.20429/ijsotl.2018.120215.

[290.]Social Determinants of Health (SDOH).” *Catalyst Carryover* 3, no. 6 (2017). https://doi.org/10.1056/CAT.17.0312.

[291.]Dingake, O. B. K. “The Rule of Law as a Social Determinant of Health.” *Health and Human Rights* 19, no. 2 (December 2017): 295–98.

[292.]*Pharmacoeconomic Review Report: Cysteamine Delayed-Release Capsules (Procysbi): Horizon Pharma Ireland Ltd. Indication: For the Treatment of Nephropathic Cystinosis*. CADTH Common Drug Reviews. Ottawa (ON): Canadian Agency for Drugs and Technologies in Health, 2018. http://www.ncbi.nlm.nih.gov/books/NBK534498/.

[293.]Hancock, Emily Kopp, Jay. "The High Cost Of Hope: When The Parallel Interests Of Pharma And Families Collide." *Kaiser Health News* (blog), September 7, 2018. https://khn.org/news/the-high-cost-of-hope-when-the-parallel-interests-of-pharma-and-families-collide/.

[294.]Holtzclaw Williams, Pamela. "Policy Framework for Rare Disease Health Disparities." *Policy, Politics & Nursing Practice* 12, no. 2 (May 2011): 114–18. https://doi.org/10.1177/1527154411404243.

[295.]Severtson, Stevan Geoffrey, Matthew S. Ellis, Steven P. Kurtz, Andrew Rosenblum, Theodore J. Cicero, Mark W. Parrino, Michael K. Gilbert, et al. "Sustained Reduction of Diversion and Abuse after Introduction of an Abuse Deterrent Formulation of Extended Release Oxycodone." *Drug and Alcohol Dependence* 168 (November 1, 2016): 219–29. https://doi.org/10.1016/j.drugalcdep.2016.09.018.

[296.]Center for Disease Control and Prevention. (2013). Prescription Painkiller Overdoses: A Growing Epidemic, Especially Among Women. Atlanta, GA: Centers for Disease Control and Prevention. https://www.cdc.gov/vitalsigns/prescriptionpainkilleroverdoses/index.html#anchor_1490283089

[297.]Parks, Caitlin, and Jeffrey F. Peipert. "Eliminating Health Disparities in Unintended Pregnancy with Long-Acting Reversible Contraception (LARC)." *American Journal of Obstetrics and Gynecology* 214, no. 6 (June 2016): 681–88.

[298.]Hrabowski, Freeman A., J. Kathleen Tracy, and Peter H. Henderson. "Opinion: At a Crossroads: Reimagining Science, Engineering, and Medicine—and Its Practitioners." *Proceedings of the National Academy of Sciences* 117, no. 31 (August 4, 2020): 18137–41. https://doi.org/10.1073/pnas.2013588117.

[299.]National Academies of Sciences, Engineering, and Medicine. 2017. *"Communities in Action: Pathways to Health Equity" at NAP.Edu*. Accessed February 20, 2021. https://doi.org/10.17226/24624.

[300.]Moriña, Anabel. "Inclusive Education in Higher Education: Challenges and Opportunities." *European Journal of Special Needs Education* 32, no. 1 (January 2, 2017): 3–17. https://doi.org/10.1080/08856257.2016.1254964.

[301.]Mitchell, David, and Dean Sutherland. *What Really Works in Special and Inclusive Education: Using Evidence-Based Teaching Strategies*. Routledge, 2020.

[302.]Pintrich, Paul R. "A Motivational Science Perspective on the Role of Student Motivation in Learning and Teaching Contexts." *Journal of Educational Psychology* 95, no. 4 (2003): 667–86. https://doi.org/10.1037/0022-0663.95.4.667.

[303.]Garibay, Juan C. "STEM Students' Social Agency and Views on Working for Social Change: Are STEM Disciplines Developing Socially and Civically Responsible Students?" *Journal of Research in Science Teaching* 52, no. 5 (2015): 610–32. https://doi.org/10.1002/tea.21203.

[304.]Miller, Lindsey N., and Susan L. Mercer. “Drugs of Abuse and Addiction: An Integrated Approach to Teaching.” *Currents in Pharmacy Teaching and Learning* 9, no. 3 (May 1, 2017): 405–14. https://doi.org/10.1016/j.cptl.2017.01.003.

[305.]Canney, N. E., & Bielefeldt, A. R. (2012, June), Engineering Students' Views of the Role of Engineering in Society Paper presented at 2012 ASEE Annual Conference & Exposition, San Antonio, Texas. 10.18260/1-2—21315

[306.]Barnette, J. Jackson. “Effects of Stem and Likert Response Option Reversals on Survey Internal Consistency: If You Feel the Need, There Is a Better Alternative to Using Those Negatively Worded Stems.” Educational and Psychological Measurement 60, no. 3 (June 1, 2000): 361–70. https://doi.org/10.1177/00131640021970592.

[307.]World Health Organization. (2021). Background document on the mRNA-1273 vaccine (Moderna) against COVID-19: background document to the WHO Interim recommendations for use of the mRNA-1273 vaccine (Moderna), 3 February 2021. World Health Organization. https://apps.who.int/iris/handle/10665/339218. License: CC BY-NC-SA 3.0 IGO

[308.]R, Langer. “Drug Delivery and Targeting.” *Nature* 392, no. 6679 Suppl (April 1, 1998): 5–10.

[309.]Callaghan, Timothy, Ali Moghtaderi, Jennifer A. Lueck, Peter J. Hotez, Ulrich Strych, Avi Dor, Erika Franklin Fowler, and Matt Motta. “Correlates and Disparities of COVID-19 Vaccine Hesitancy.” SSRN Scholarly Paper. Rochester, NY: Social Science Research Network, August 5, 2020. https://doi.org/10.2139/ssrn.3667971.

[310.]Persad, Govind, Monica E. Peek, and Ezekiel J. Emanuel. “Fairly Prioritizing Groups for Access to COVID-19 Vaccines.” *JAMA* 324, no. 16 (October 27, 2020): 1601–2. https://doi.org/10.1001/jama.2020.18513.